Theme V: Application of high-strength steels including weathering steels to high-rise and long-span structures

V

Emploi des aciers à haute résistance et à protection naturelle pour les structures hautes ou à grande portée

Anwendung hochfester Stähle, inklusive wetterfester Stähle, für hohe und weitgespannte Tragwerke

Application of high-strength Steels including weathering Steels to high-rise and long-span Structures

Va

Comportement sous charges en incluant les constructions hybrides

Tragverhalten, einschliesslich hybride Tragwerke

Structural Behaviour including Hybrid Construction

Vb

Problèmes de conception

Entwurfsprobleme

Design Problems

Vc

Problèmes de fabrication et de montage

Herstellungs- und Montageprobleme

Fabrication and Erection Problems

Leere Seite
Blank page
Page vide

Comments by the Author of the Introductory Report

Remarques de l'auteur du rapport introductif

Bemerkungen des Verfassers des Einführungsberichtes

BEN KATO
Prof. Dr.-Eng.
University of Tokyo
Tokyo, Japan

Structural Behavior Including Hybrid Construction

The state-of-the-art on the structural behavior of members and structures made of high-strength steels is outlined in this report according to sub-items listed in Table 1. Characteristics of the structural behavior of those made of high-strength steels are discussed in relation to those made of mild steel in order to provide the information by which a designer can decide whether a grade of high-strength steel should or should not be used in a particular part or in a particular structure in association with the imposed loading conditions.

1.MATERIAL	← BEEDLE et.al.
2.TENSION MEMBERS	
3.BEAMS & BEAM-COLUMNS -In Plane Behavior-	← FISHER et.al. (composite beam)
4.STABILITY	
4.1.COLUMN BUCKLING	
4.2.LOCAL BUCKLING	← FUKUCHI et.al.
4.3.LATERAL-TORSIONAL BUCKLING	← FUKUMOTO SUZUKI et.al.
4.4.ROTATION CAPACITY	← BEEDLE et.al.
5.FRAMES	
6.PLATE & BOX GIRDERS	← KUNIHIRO et.al. MAEDA et.al. YAMASAKI et.al.
7.FRACTURE & FATIGUE	

Table.1 Outline of the Theme and Contributors

In this table,authors and topics which were contributed to the preliminary report are identified,and the synthesis of these contributions will be made in the following together with the key points of the introductory report.

Structural steels can be grouped into three classes as shown in Fig.1. Of which C-class steels are called as "extra high-strength steel",and mechanical properties of these steels in plastic region such as strain at initial strain hardening,strain hardening modulus and the yield ratio of material are considerably small compared with those of mild steel.

Dr.Beedle and his colleagues had studied a new type steel,designated as A572,Grade 65. This steel is a low-alloy columbium-vanadium steel and mechanical properties are in between of B and C-class steels as shown in Fig.2.

The poor capacities of deformation and energy absorbtion of tension members,beams, beam-columns and frames made of C-class steels are attributed to these characteristics of mechanical properties.

A-class: CARBON STEEL(MILD STEEL)
B-class: HIGH STRENGTH LOW-ALLOY STEEL
C-class: HEAT-TREATED CONSTRUCTIONAL ALLOY STEEL

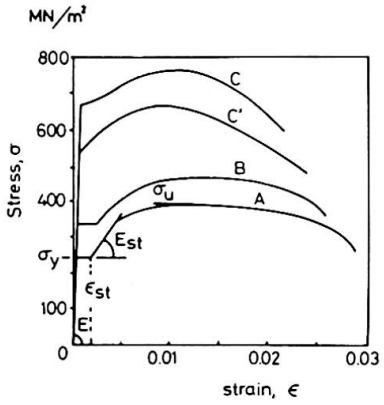

CHARACTERISTIC VALUES IN PLASTIC RANGE
ϵ_{st} : Strain at Initial Strain Hardening
E_{st} : Strain Hardening Modulus
σ_y/σ_u : Yield Ratio of Materials

Fig.1 Classification of Structural Steels

The buckling behavior of members can be discussed by categorizing them into three groups according to their slenderness.
Since all compression elements have the same Eulerian strength regardless of the yield strength of the material,there will be no merit to use high-strength steels for slender members. For compression members with intermediate slenderness,the secondary factors such as

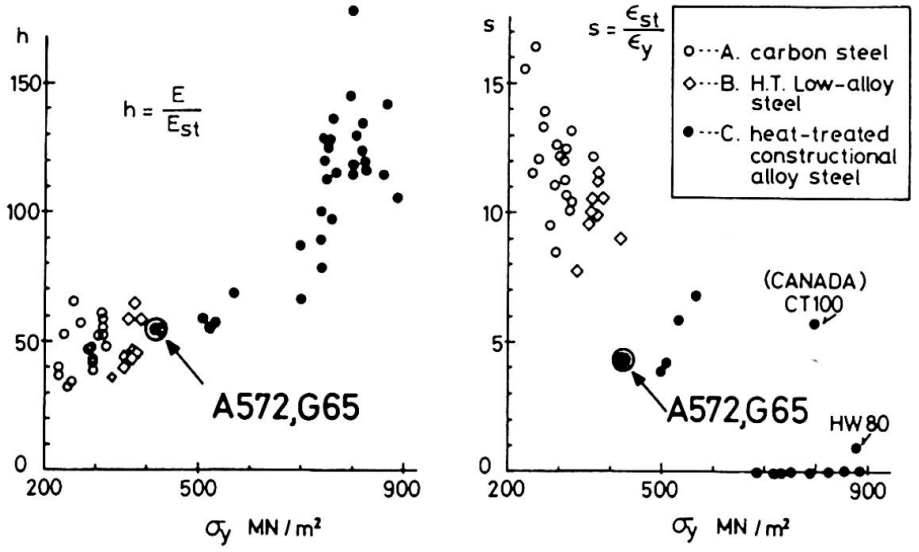

Fig.2 Characteristic Values in Plastic Region

residual stress,initial curvature and eccentricity have the greatest effect on tneir buckling strength. It is known that the effect of residual stress is less pronounced for higher strength steels than it is for mild steel,thus as the yield stress increases,initial curvature and eccentricity take on increasing importance in relation to residual stress. Dr.Fukumoto had carried out the lateral buckling tests of beams made of B and C-class steels with intermediate slenderness. A total 36 beam-type and 7 girder-type members was tested under uniform moment and moment gradient,and test results were compared with theoretical prediction. Fog.4 shows a non-dimensional presentation of the critical moment to slenderness relationship, and a comparison is made between the annealed beams and the as-weld beams having the same sizes for the residual stress effect. It has been concluded that the welding residual stress distributions may reduce the buckling strength for about 11% for B-class steel,and 6% for C-class steel against the beams without residual stress, and that initial lateral deflection of 0.1% of the beam length may explain the lower bound estimate against the plotted test results.

The deformability and ultimate strength of members or member elements with very small slenderness are the topics of increasing interest in relation to the development of plastic design and of earthquake resistant design. Because the behavior is determined almost entirely by the plastic properties of the material in such a short and stocky members,characteristic behavior of extra high-strength steels or C-class steels will be paramount in this range. Fig.5 shows the relationship between the rotation capacity and the slenderness of beams which subject to lateral buckling under uniform moment. Shown by the double circle is the Beedle's test

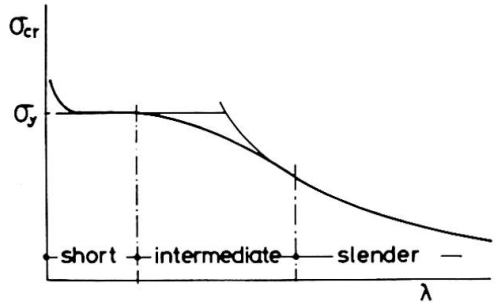

Fig.3 Categories of Slenderness of Compression Elements

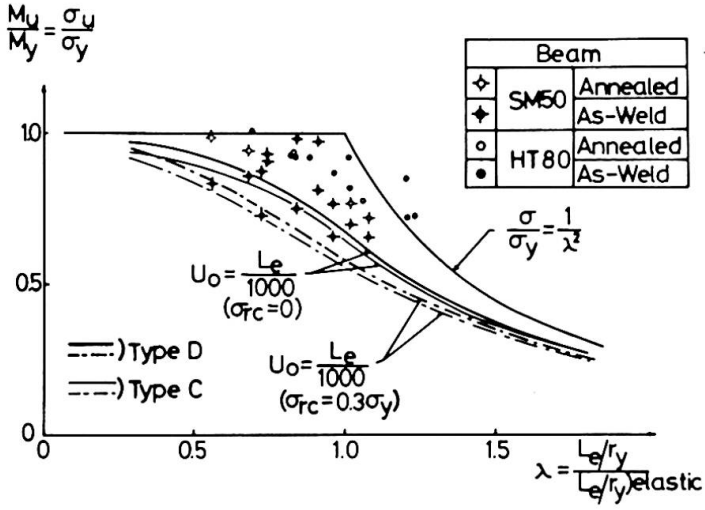

Fig.4 Test results and Theoretical Predictions

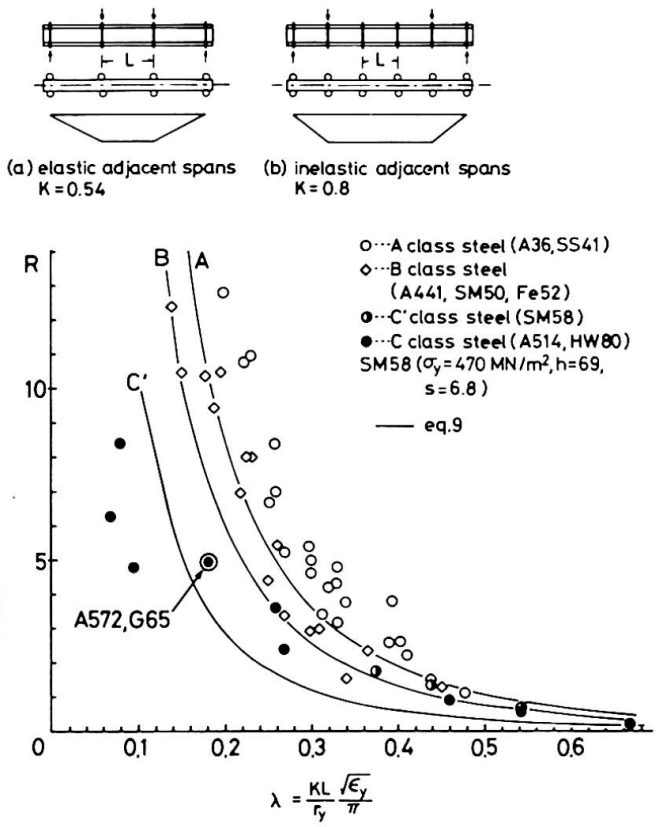

Fig.5 Rotation Capacity under Uniform Moment

result of which the beam is made of columbium-vanadium steel as refered previously. Rotation capacity falls in between those of B and C-class steels as is expected from mechanical properties of this steel.
Dr.Suzuli and Mr.Ono had carried out lateral buckling tests of beams and beam-columns with short slenderness. Steels used are of A,B and C-class. Fig.6 shows the relationship between the axial load and the slenderness of beam-columns. Theoretical prediction by Suzuki that assures the rotation capacity of 3 are shown by bold solid lines,and test results rotation of which were less than 3 are checked by x-mark. On the other hand,a suggested axial load limitation given by eq.(12) in the introductory report is shown by the fine solid lines. It seems that eq.(12) be not satisfactory for C-class steel. Considering the fact that the information on the rotation capacity of beam-columns is insufficient as yet,this contribution is very important. Test results on beams reported by Suzuki were already refered in the introductory report.

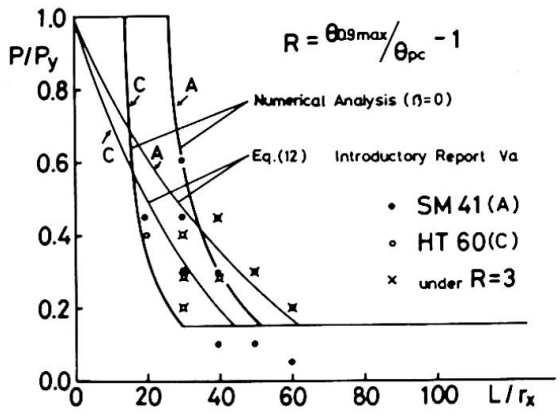

Fig.6 Rotation Capacity of Beam-Columns

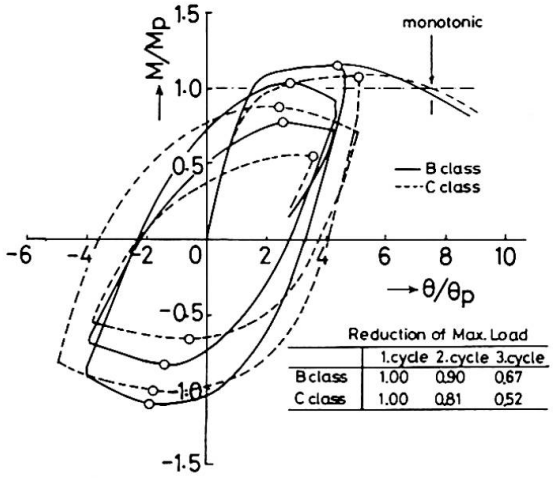

Fig.7 Cyclic Behavior of Beams

Behavior of beams under cyclic loading were investigated by Dr.Fukuchi and his colleagues. Fig.7 shows cyclic behavior of beams which subject to lateral and local buckling in their course of loading. Beams made of B-class and C-class steels which have almost the same rotation capacity when subjected to monotonic loading were tested and compared in this figure. Reduction of maximum load at each cycle is shown in the table,and it can be said that the rotation capacity of higher strength steel beams under cyclic loading will be more severely impaired than that expected from the monotonic test.

Hybrid beams are fabricated beams and girders which use a stronger steel in the flanges than in the web. The design of hybrid beams is based on the shakedown phenomenon, which ensures that the members will behave elastically after local yielding of the web. It seems that high-strength steels can be most efficiently utilized in this field of application as far as static loading is concerned. However this concept can not be applied to the fatigue design off hand,since metallurgical discontinuity and local stress condition around the welded joints will affect the fatigue strength considerably.

Typical patterns of fatigue cracks which will occur in hybrid girders are shown in Fig.8.

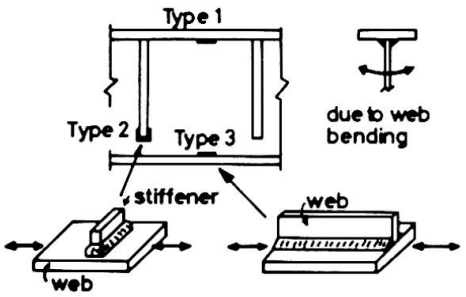

Fug.8 Typical Patterns of Fatigue Cracks

Type 1 crack will be caused by web breathing due to initial bending of the web, Type 2 crack initiated at the toe of vertical stiffener-to-web fillet weld can be compared to that of a transverse non-load carrying fillet welded joint,and Type 3 crack initiated at tension flange-to-web fillet weld can be compared to that of a longitudinal fillet welded joint as shown in the figure.

Three papers were contributed to this topic. Dr.Maeda and his colleagues had studied Type 1 and Type 2 fatigue phenomena and found out that Type 1 crack can be prevented up to 2 million cycles of loading by limiting out of plane movement of web plate, depending on web slenderness and rigidity of a horizontal stiffener, and also found out that Type 2 crack can be prevented by controlling a tensile web stress bellow the fatigue strength of transverse non-load carrying fillet welded joints.
Dr.Kunihiro's group and Dr.Yamasaki 's group had investigated the fatigue strength of Type 3.
Solid circles in Fig.9 represent the test results for hybrid specimens and open circles are for homogeneous specimens. As seen in this figure,test points are somewhat scattered and no statistical difference was found between fatigue strengthes of homogeneous and hybrid specimens. This might mean that the influence of geometrical and metallurgical imperfections of welded joints is large enough to cover up the characteristics of hybrid joints. In any case,the results of these two groups had supported the conclusion of Joint ASCE-AASHO Committee that "hybrid beams can generally be designed for fatigue as if they were made entirely of the grade of steel used in the flanges". In addition to these fatigue studies,Dr.Maeda and Dr.Kunihiro had discussed on the static behavior and economy of hybrid girders, and Dr.Yamasaki had analysed the problem of fatigue crack propagation by applying a theory of fracture mechanics.

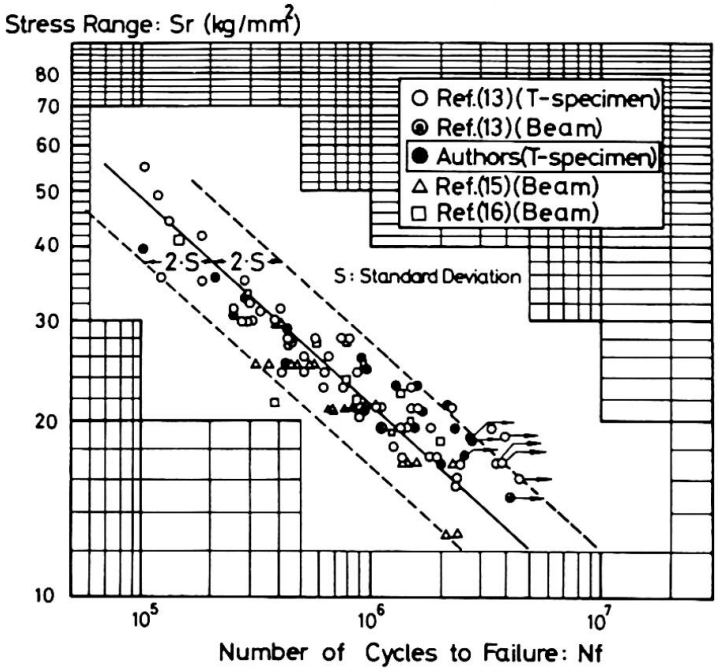

Fig.9 S-N Diagram of Hybrid Specimens

Finally,the design problem of composite beams were discussed by Dr.Fisher and his colleagues. With respect to the composite beam in which a concrete floor slab with formed steel deck and a steel beam made of mild steel are connected by means of shear connectors,a design formula based on the ultimate strength concept has been already proposed by Fisher himself. At present study,Dr.Fisher and his colleagues had examined the possibility of extensive application of high strength steel beams to this composite beam system by a series of tests,and concluded that "the flexural capacity of a composite beam utilizing high-strength steel is not adversely affected by the increased slab force and can be predicted provided that the connector capacity is known".

As reviewed herewith,the problems of fracture and fatigue in their proper sense were not contributed to the preliminary report,and the author hopes these problems would be discussed in prepared and free discussions.

Leere Seite
Blank page
Page vide

Bemerkungen des Verfassers des Einführungsberichtes

Comments by the Author of the Introductory Report

Remarques de l'auteur du rapport introductif

OTTO JUNGBLUTH
Prof. Dr.-Ing.
Technische Hochschule Darmstadt
Darmstadt, BR Deutschland

Entwurfsprobleme

Die Berücksichtigung hochfester Stähle beim Entwurf von Ingenieurbauwerken kann nur dann erfolgreich sein, wenn deren besondere Eigenschaften im Hinblick auf das Tragverhalten sowie auf die speziellen Herstellungs- und Montageprobleme beachten werden.

Aus diesen gegenseitigen Rückwirkungen ergibt sich, daß die Probleme der drei Unterthemen ineinandergreifen und ihre Grenzen fließend sind, wie auch die Beiträge der verschiedenen Autoren gezeigt haben.

Das unterschiedliche elastisch-plastische Verhalten der normalen und der hochfesten Baustähle wird von AKYAMA vorteilhaft für den erdbebensicheren Entwurf von Hochhäusern herausgestellt. Das über die Plastizierungsgrenze der normalen Stähle hinauswirkende elastische Verhalten der hochfesten Stähle verteilt die Erdbebeneinwirkungen über die Höhe des Gebäudes und vermeidet dadurch Beanspruchungskonzentrationen in den einzelnen Stockwerken. Deshalb schlägt der Verfasser Hybridkonstruktionen vor (Vorbericht Seite 445) mit vertikalen Korsettstäben aus hochfesten Stahlgliedern in der Mitte oder an den Außenseiten des Hochhauses, damit die Schwingungsenergie durch eine kombinierte plastische Deformation der normalen und elastische Verformung der hochfesten Stahlglieder abgebaut werden kann. Wie Vergleichsuntersuchungen ergeben haben, genügt bereits ein Anteil von 10 % bis 15 % hochfester Stahlstützensysteme im Verbund, um die Energiekonzentration um 50 % zu vermindern. Die Berechnung solcher hybrider Tragwerke für den Entwurf erdbebensicherer Bauten nach AKYAMA zeigt gute Übereinstimmung mit Modellversuchen.

Daß hochfeste Stähle nicht nur im Verbund mit normalen Baustählen, sondern als Stützen auch im Verbund mit Unterzügen und Decken aus Stahlbeton vorteilhaft verwendet werden können, zeigt der Beitrag von GRAVERT. Während für den erdbebensicheren Entwurf von Hochhäusern die hochfesten Stahlglieder lastverteilend wirken, ermöglichen sie hier durch Lastkonzentration auf wenige geschweißte Stahlstützen mit Blechdicken bis zu 100 mm einen erheblichen Nutzflächengewinn (Vorbericht S. 451) gegenüber Stahlbetonstützen, die fast die vierfache Fläche benötigt hätten. Die geschoßweise horizontale Stabilisierung der Stahlstützen durch die Stahlbetondeckenscheiben läßt eine Bemessung auf Knicken nicht maßgebend werden. Die wegen ihrer größeren Lastaufnahmefähigkeit relativ größeren Stauchungsmaße der hochfesten Stahlstützen gegenüber den dehnsteiferen Stahlbetonkernen werden durch Auflagerüberhöhung der Geschoßdecken im Rohbauzustand weitgehend ausgeglichen. Der Beitrag von GRAVERT zeigt, daß der Einsatz von hochfesten Baustählen beim Entwurf von Ingenieurtragwerken nicht nur vom Standpunkt der kostengünstigeren Konstruktion, sondern auch von der wirtschaftlicheren Nutzung her zu beurteilen ist.

Das bekannte Problem der Mitwirkung der Längsträger bei der Hauptträgerbeanspruchung von Fachwerkeisenbahnbrücken mit offener Fahrbahn ist, wie von STRELETZKIJ erläutert wird, beim Einsatz hochfester Stähle für die Hauptträgergurte infolge deren relativ größeren Dehnungsnachgiebigkeit in noch stärkerem Maße zu beachten. Eine genaue computerisierte Berechnung unter Berücksichtigung des räumlichen Zusammenwirkens aller Tragwerksteile (Vorbericht S. 469) und besondere konstruktive Maßnahmen bei den Verbindungen senken dank der Verwendung hochfester Stähle für die Gurte den Stahlverbrauch für diese hybriden Eisenbahnbrücken um 5 % und verbessern darüber hinaus nach STRELETZKIJ auch die Betriebssicherheit und die sonstigen Nutzungseigenschaften. Insbesondere wird ein Freivorbau ohne Montageverstärkungen ermöglicht.

BOLSCHAKOW und POTAPKIN berichten über die Anwendung hochfester Baustähle in weitgespannten Straßen- und Eisenbahnbrücken. Die Festigkeitsuntersuchungen erfolgten durch die Autoren unter Berücksichtigung einer maximalen plastischen Restdehnung auf der Basis der Plastizitätstheorie. Für den Dauerfestigkeitsnachweis wurden Abminderungsfaktoren sowohl für den hochfesten Grundwerkstoff als auch für die hochfesten Verbindungen ermittelt. Die Abminderungsfaktoren für den Knicknachweis geschweißter und gewalzter Breitflanschprofile wurden unter Berücksichtigung von Eigenspannungen berechnet. Auch für längsversteifte Platten in Druckgurten von Kastenträgern im überkritischen Bereich und für kombinierte Verformungen von Trägern im elastisch-plastischen Bereich werden Beziehungen angegeben.

Um die Effizienz hochfester Stähle mit 50 und 60 kp/mm^2 Streckgrenze zu untersuchen, wurden 3 Stahlbrückentypen entworfen. Bei einer Fachwerkeisenbahnbrücke wurden mögliche Gewichtseinsparungen von 2 bis 6 %, bei einer Kastenträgerautobahnbrücke mit orthotroper Stahlfahrbahn von 5 bis 6 %, aber mit Stahlbetonfahrbahn von 20 % ermittelt. An ausgeführten Brücken (Vorbericht S. 463) wird berichtet über eine Autobahn-Bogenbrücke aus hochfestem Stahl mit 50 kp/mm^2 Streckgrenze, über eine vollgeschweißte Autobahnrahmenträgerbrücke aus hochfestem Baustahl mit einer Streckgrenze von 60 kp/mm^2 und eine Verbundbrücke mit zwei Hohlkästen, die ursprünglich aus Stahl mit Streckgrenze 40 kp/mm^2 ausgeführt werden sollte, für die das Stahlwerk aber hochfesten Stahl S 60 geliefert hat. Nach Auffassung von BOLSCHAKOW und POTAPKIN haben die hochfesten Stähle S 50 und S 60 bisher nicht die erwarteten Vorteile gebracht, insbesondere wegen der im Verhältnis zur Streckgrenzenerhöhung nicht mitwachsenden Dauerfestigkeit. Hervorgehoben wird ihre Widerstandsfähigkeit gegen niedrige Temperaturen.

Kriterien für die Dauerfestigkeitsnachweise der Honschu-Schikoku-Hängebrücken, die als kombinierte Autobahn-Eisenbahnbrücken mit hochfesten Baustählen der Festigkeitsklassen HT 60 bis HT 80 geplant sind, geben TAJIMA, OKUKAWA und TANAKA an. Versuche an Schweißverbindungen erlaubten die Festlegung von zulässigen Dauerfestigkeitsspannungen unter Berücksichtigung von 7 Kerbgruppen für Normal- und Schubspannungen (Vorbericht S. 479). Für jede dieser Kerbgruppen wurden Dauerfestigkeitsgrundwerte ermittelt. Zur Berücksichtigung des Mittelspannungseinflusses sind einfache Beziehungen in Abhängigkeit vom Spannungsverhältnis k angegeben, die unabhängig von der Kerbgruppe und für die Festigkeitsklassen 60 kp/mm^2 bis 80 kp/mm^2 gleich sind. Bei Schweißverbindungen aus hochfesten Stählen kann durch verschiedene Nachbehandlungsverfahren eine deutliche Erhöhung der Dauerfestigkeit bewirkt werden, wodurch eine Einstufung in die nächst höhere Kerbgruppe zulässig wird. Hervorzuheben ist, daß TAJIMA, OKUKAWA und TANAKA durch eine Schadensakkumulationsrechnung (cumulative damage) auf der Basis der Miner-Regel für die in 100 Jahren auftretenden Belastungswechsel Verbessungsfaktoren für die Dauerfestigkeitswerte ermitteln. Die bei der Miner-Rechnung zu Grunde gelegte normierte Wöhlerlinie (S-N-Curve) verläuft etwas flacher als die in Deutschland verwendete, d.h. bei gleicher Dauerfestigkeit wird die Zeitfestigkeit für die hochfesten Stähle in Japan etwas niedriger eingeschätzt. In gewisser Übereinstimmung mit den japanischen Untersuchungen ergaben auch deutsche Versuche, daß bei Bauteilen mit geringen Kerbfaktoren, Beanspruchungen mit hohen Mittellasten, Belastungen mit geringer Lastspielzahl und Betriebslastkollektive- mit geringem Völligkeitsgrad, die hochfesten Stähle

auch bei schwingender Beanspruchung den niedriger festen Stählen überlegen sind.

HAJDIN berichtet, daß hochfeste Stahldrähte als Paralleldrahtbündel auch unter der schwingenden Beanspruchung einer Schrägseil-Eisenbahnbrücke vorteilhaft eingesetzt werden können, insbesondere, wenn bei günstigem Lastkollektiv das Spannungsverhältnis $\varkappa$ (Vorbericht S. 475) angehoben werden kann. Eine Vergleichsuntersuchung ergab eine Gewichtsersparnis von 25 % zugunsten des Paralleldrahtbündels gegenüber dem verschlossenen Seil. HAJDIN befürwortet auf Grund von Schwingfestigkeitsversuchen eine Erhöhung der zulässigen Schwingbreiten um 25 % für das Paralleldrahtbündel, dessen Korrosionsbeständigkeit ein umhüllendes Polyäthylenrohr, in das Injektionsmörtel eingepreßt wird, gewährleistet.

In Ergänzung zu meinem Einführungsbericht kann ich noch mitteilen, daß in einer kürzlich am Institut für Statik und Stahlbau der Technischen Hochschule Darmstadt abgeschlossenen Forschungsarbeit [1] die Andwendbarkeit des vereinfachten Traglastverfahrens mit Fließgelenkhypothese für hochfeste Baustähle am Beispiel des Rahmenträgers überprüft wurde. Experimentelle Untersuchungen haben gezeigt, daß der Bereich Verfestigungsdehnung ε_{St} minus Fließdehnung ε_F und der Verfestigungsmodul E_{St} auch für hochfeste Stähle hinreichend groß sind, um in allen Fällen zu einer ausgeprägten Fließgelenkwirkung zu führen.

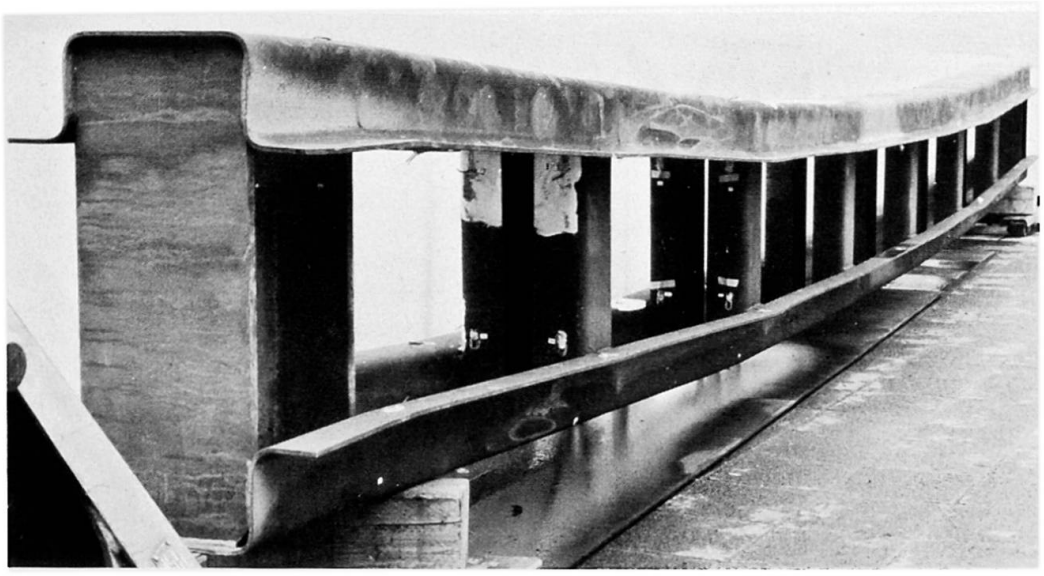

Bild 1

Im Versuch (Bild 1) geprüft wurden wirklichkeitsnahe Rahmenträger mit 8,40 m Spannweite aus abgekanteten Blechprofilen der 4 genormten Festigkeitsklassen mit Regelstreckgrenzen σ_F = 24, 36, 47 und 70 kp/mm^2 (Bild 2).

①	②	③	④	⑤
Stahl	Streckgrenze [kp/mm²]	$P_u / P_{gr,F}^{pl,N}$	$P_u / P_{gr,R}^{pl}$	$P_u / P_{gr,F}^{el}$
St 37	$\sigma_F = 24$	1,16	1,12	1,53
St 52	$\sigma_F = 36$	1,11	1,06	1,53
StE 47	$\sigma_F = 47$	1,05	1,01	1,40
StE 70	$\sigma_F = 70$	1,09	1,04	1,59

Vergleich der elastischen und plastischen Grenzlasten bei Rahmenträgern aus 4 Festigkeitsklassen.

Bild 2

Die Gegenüberstellung der im Versuch erreichten höchsten experimentellen Traglast P_u mit den theoretischen Grenzlasten, bei denen aber die konstruktiv bedingten Anschlußsteifigkeiten an den Knotenpunkten berücksichtigt wurden, ergibt folgendes: Für alle 4 Baustahlfestigkeitsklassen liegt die plastische Grenzlast $P_{gr,F}^{pl,N}$ mit Berücksichtigung des Normalkrafteinflusses und der tatsächlichen Streckgrenze σ_F mit 5 bis 16 % auf der sicheren Seite (Spalte 3). In unseren Untersuchungen hat sich ferner gezeigt, daß die gute Übereinstimmung mit den Versuchswerten immer noch auf der sicheren Seite lag, wenn man (Spalte 4) den rechentechnisch aufwendigen aber grenzlastmindernden Normalkrafteinfluß mit der gegenüber den tatsächlichen Lieferwerten statistisch niedriger liegenden normenmäßigen Regelstreckgrenze kompensiert. Eine Berechnung nach der elastischen Grenzlast bei unbeschränkter Gültigkeit des Hook'schen Gesetzes (nach Spalte 5) würde aber die Tragfähigkeit des Rahmenträgers um ca. 40 bis 60 % unterschätzen. Diese Versuche bestätigen, daß die plastische Grenzlastbemessung auch für hochfeste Baustähle anwendbar ist.

Meine Damen und Herren,
zusammenfassend läßt sich feststellen, daß beim Entwurf von Hoch- und Brückenbauten hochfeste Baustähle in vielen Fällen vorteilhaft berücksichtigt werden können, insbesondere bei Hybrid- und Verbundkonstruktionen. Wenn auch ihre Dauerfestigkeit wegen der gleichen Naturkerbigkeit nicht höher liegt als die der niedriger festen Stähle, so ist im Zeitfestigkeitsbereich und bei günstigen Lastkollektiven ihre höhere Festigkeit auch bei dynamisch beanspruchten Tragwerken ausnutzbar.

Insbesondere auf den Gebieten der Stabilität und der schwingenden Beanspruchung sind aber noch weitere Forschungsergebnisse erforderlich, um alle notwendigen Entwurfsparameter verfügbar zu haben.

[1] O. Jungbluth und H. Bahernejad:

" Zur Traglastbemessung bei Verwendung der hochfesten Baustähle StE 47 und StE 70 ",

Deutscher Ausschuß für Stahlbau, Forschung und Entwicklung im Stahlbau, 1977.

Comments by the Author of the Introductory Report

Remarques de l'auteur du rapport introductif

Bemerkungen des Verfassers des Einführungsberichtes

TOSHIE OKUMURA
Emeritus Professor
University of Tokyo
Tokyo, Japan

Fabrication and Erection Problems

Session Vc is intended for discussions on fabrication and erection problems of long-span bridges for the application of high-strength steels. Since long-span bridge projects are going to be planned in the world, the subject will bring forward the most realistic and important problems for bridge engineers.

Although the introductory report on the present subject was not presented to our regret, we have three Preliminary Reports. Now, the author is going to discuss some problems together with the summary of the Preliminary Reports.

One of the Reports treated Saint-Nazaire Bridge in France which is the world-longest cable-stayed girder bridge with a center span of 404 m. The second report covered the choice of high-strength steels at Osaka Port Bridge in Japan, and at the third report the use of high-strength steels was discussed for support forces of steel bridge girders during their launching. It is thought that each of the reports is characteristics from the point of the present subject.

The author believes that it is the determination of an erection method to influence most on the safety and economy of long-span bridges. Four bridges accidents during their erection have been reported very recently, and the Merrison Committee Report was published and also at the Session VII, Professor Massonnet and Dr. Henderson will make some proposals on erection at their General Reports. It is advisable to consider fully such suggestions or recommendations at the design of future bridges.

Now, the author would like to emphasize that it might be dangerous to apply directly the engineering experience obtained from mild steels to the use of high-strength steels. Generally, uniform elongation of high-strngth steels will decrease with an increase of strength, and particularly, at quenched and tempered high-strength steels over 60 kg/mm^2, their yielding ratio will be increased and their stress-strain curve will be different from mild steels.

For example, judging from fatigue tests of steel plates with a notch, mild steels are a kind of stiff-type steel, but heat-treated high-strength steels become a kind of soft-type steel. From buckling, high-strength steels seem to be advantageous at the effect of residual stresses due to welding, but there are no sufficient test data to verify the effect. Therefore, careful considerations will be required at the design of details of a structure.

On the other hand, as welding problems, crack sensitivity due to welding will be higher at high-strength steels and particularly, brittleness of weld bond parts will be unavoidable in relation to weld heat input at heat-treated high-strength steels.

It will be concluded that a thorough study on the structural behavior of welded structures will be required and at the same time, material properties of high-strength steels and especially, weldability in relation to fracture mechanism have to be understood well at the further study.

Recenly, large-block erection methods have been applied to long-span bridges to satisfy environmental conditions, as seen in erection works of Saint-Nazaire Bridge and Osaka Port Bridge.

At the erection of Saint-Nazaire Bridge, the side spans were erected by a large-en bloc lifting-up method without any staging, and yet the main span was erected by a cantilever method. Since a uniform section of box gorders was used on account of easy works of fabrication and erection, working stresses induced during the erection forced the side spans to be made of steels more than 42 kg/mm^2 in yielding point. It is reported that such steels satisfied the required KCV-20°C in the direction of rolling and the perpendicular direction to it at the pre-and post welding.

At the erection and fabrication of Osaka Port Bridge, it is reported as follows:

1) The suspended truss span (span length is 186 m and steel weight including floor is approximately 4500 tons) was fabricated at a shop and towed to the site by a deck barge in 15,000 tons. Finally, it was lifted using a lifting equipment composed of wires and winches to the ends of the cantilever spans to the height of approximately 50 m above the sea level.

2) Out of the total steel weight 40,000 tons, 4197 tons and 1075 tons of high-strength steels of 80 kg/mm^2 and 70 kg/mm^2 grades, respectively, were used. Furthermore, the maximum plate thickness were 75 mm for the web plate of the chord and 100 mm for the bottom plate of the tower base.

3) To improve the weldability of members and elements, lamellar tear tests, restrained cracking tests, tests on the performance of corner weld joints, and tests to study on the various characteristics of the actual members using full scale models, were conducted prior to the fabrication.

It will be highly evaluated that with such well-prepared tests, the fabrication of the whole bridge structure was completed without any trouble.

It will be recognized at any rate that the use of high-strength steels at long-span bridges is somewhat advantageous because it can reduce their own weight at the erection. Fig. 1 illustrates the relation between allowable stress and cost ratio based on the cost of various steels in Japan. Although there are social and environmental requirements for bridges and all problems cannot be solved by one factor as shown in Fig. 1, it seems that the figure will give you a certain index to choose the material.

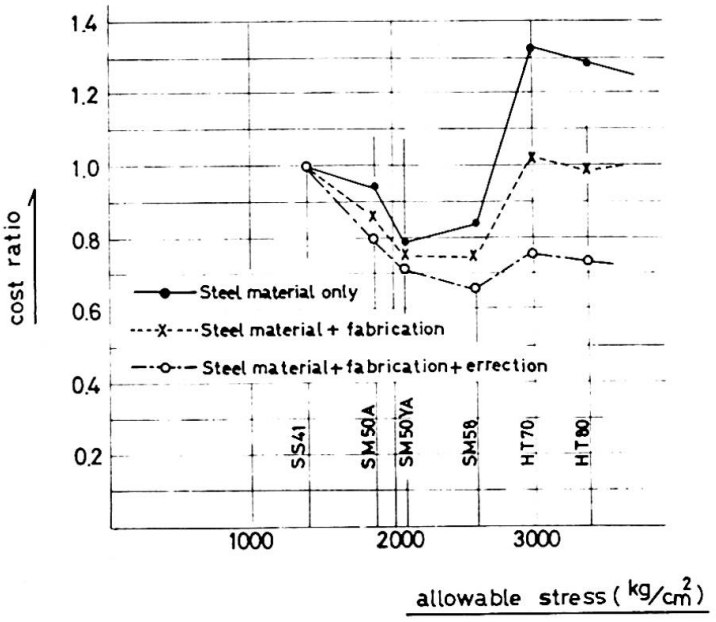

Fig. 1 Relation between allowable stress and cost ratio

At the paper presented by Prof. Bergfelt and Mr. Wilson, when a bridge was erected by launchimg, they observed experimentally girder behaviors due to local yielding, buckling and their combined action, and they concluded the use of high-strength steels would be advantageous to avoid damages of a structure due to concentrated loadings.

It is the author's opinion that the improvement of material properties in the direction of plate thickness is required from the point of stress transmission, when member sections of bridges are going to be larger and higher-strength steels are required for detailed design of welded sections. At 80 kg/mm^2 grade steels in Osaka Port Bridge, the improvement of manufacturing

steels was tried to reduce the impurity of steels, so that the contents of S and P were kept around or within 0.01 %. Then, HT80 steels could be satisfactorily applied to this bridge, as seen in Table 2, in comparison with 60 kg/mm^2 steels in Table 1.

Fig. 2 shows the relationship among sulphur content, elongation in the direction transverse to the plate, and non-metal inclusion. Fig. 3 gives the relationship between elongation in the direction transverse to the plate and crack-growth rate by Cranfield Test which is a representative test of lamellar tear due to welding.

Finally, the author suggests that, since it is very important to pay close attention to the improvement of material properties in the direction of plate thickness at the use of high-strength steels, fabrication and erection of long-span bridges have to be done in cooperation with manufacturers of steels.

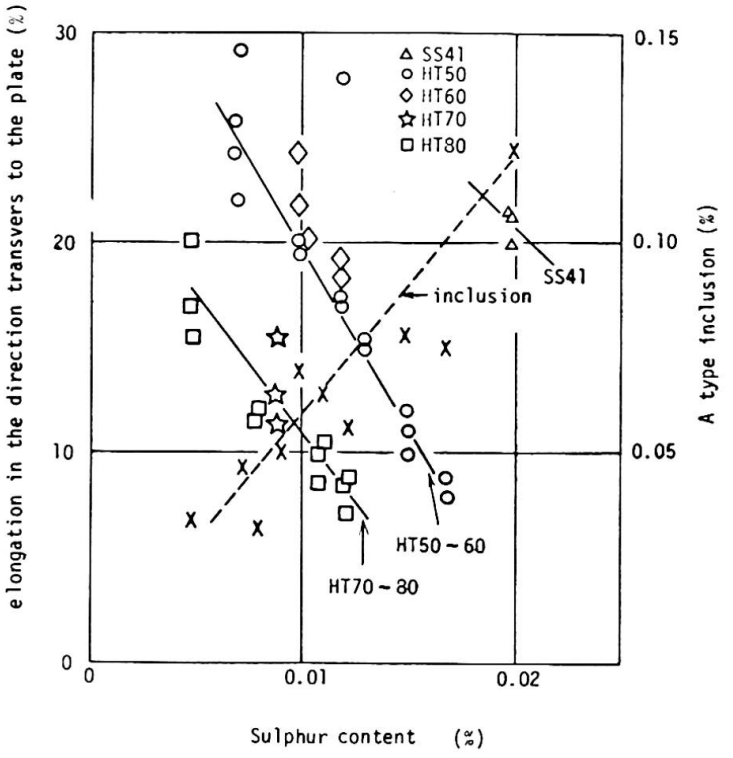

Fig. 2 Relationship among sulphur content, elongation in the direction transverse to the plate and non-metal inclusion

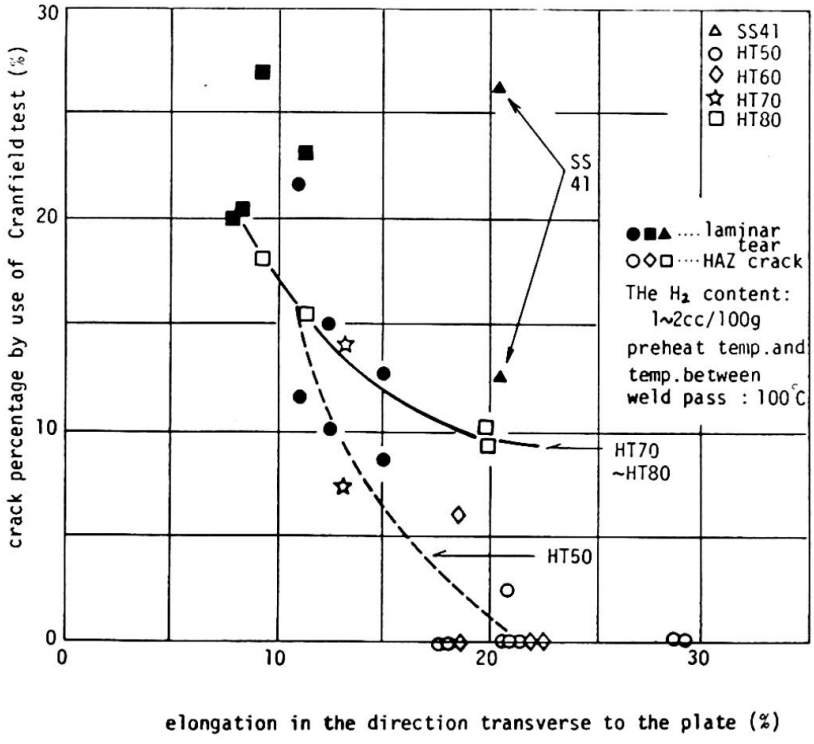

Fig. 3 Relationship between elongation in the direction transverse to the plate and Cranfield crack-growth rate

Table 1 Properties of 60 kg/mm^2 high-tensile steel plate

T*	Chemical composition											Properties in longitudinal and cross direction (JIS 4)								Properties in direction of thickness						Remarks
mm	C	Si	Mn	P	S	Cu	Cr	Ni	Mo	V	Ceq	P*	D*	Y.P.	T.S.	El.	R.A.	vEo	vTs	vTe	Y.P.	T.S.	El.	R.A.	vEo	vTs	
75	13	26	132	10	6	20	15	38	14	4	438	t/4	L	57.1	67.4	27.3	75.7	29.3	-63	-66	55.9	65.6	21.9	-	3.4	+15	D=14mm
													C	56.2	67.2	25.3	69.0	19.8	-42	-42							
85	15	30	137	18	10	3	3	2	24	6	461		L	59.2	68.7	21.8	-	VE-5 23.4	-30	-34	56.5	65.9	20.7	-	VE-5 1.5	+20	GL=50mm
													C	59.6	68.9	19.5	-	VE-5 6.6	+5	- 8							

Table 2 Properties of 80 kg/mm^2 high-tensile steel plate

T*	Chemical composition												Properties in longitudinal and cross direction (JIS 4)								Properties in direction of thickness						Remarks
mm	C	Si	Mn	P	S	Cu	Cr	Ni	Mo	V	B	Ceq	P*	D*	Y.P.	T.S.	El.	R.A.	vEo	vTs	vTe	Y.P.	T.S.	El.	R.A.	vEo	vTs	
33	12	27	87	11	7	27	47	99	45	3	15	500	t/4	L	80.4	85.0	25.6	69	19.4	-110	-99	76.6	82.3	15.0	33	-	-	
														C	81.7	85.3	21.1	55	6.4	-81	-92							
44.5	12	28	95	10	8	27	48	106	47	3	13	531		L	82.8	87.3	22.7	67	19.0	-91	-91	77.4	82.6	15.9	35	-	-	D=8.5mm GL=30mm
														C	83.7	87.8	20.8	58	6.8	-80	-97							
50	11	27	100	10	9	26	49	108	47	4	12	533		L	77.3	83.6	24.7	68	17.0	-50	-59	71.6	79.4	17.8	52	-	-	
														C	73.7	80.3	19.7	64	11.0	-60	-76							
50	10	31	90	7	5	26	47	103	47	3	12	502		L	81.7	86.0	23.6	72	20.9	-93	-92	79.8	83.1	11.5	33	7.2	-66	D=14mm GL=50mm
														C	81.6	85.8	22.6	66	132	-72	-66							
63.5	12	27	87	11	7	27	47	99	45	3	15	500		L	81.9	86.9	23.3	66	19.0	-90	-90	77.9	83.2	16.5	39	-	-	D=8.5mm GL=30mm
														C	80.5	85.4	23.6	60	9.2	-74	-77							
78	13	28	86	8	6	23	47	129	47	4	13	530		L	80.7	85.9	23.6	67	20.8	-96	-93	79.8	84.4	17.8	39	21.2	-122	D=14mm
														C	80.1	84.8	23.1	62	13.8	-76	-71							
100	12	27	89	8	5	24	52	143	48	3	18	542		L	77.1	84.2	25.2	71	23.4	-105	-93	74.8	81.5	22.0	-	11.9	-32	GL=50mm
														C	77.0	83.5	24.4	68	19.4	-95	-90							

C, Si, Mn, Cu, Cr, Ni, Mo, V : (10^{-2})
P, S, Ceq. : (10^{-3})
B : (10^{-4})

Y.P., T.S. : (kg/mm^2) , vTs, vTc : (C)
El., R.A. : (%)
vEo : (kg-m)

T*=thickness
P*=position
D*=direction of test

Leere Seite
Blank page
Page vide

Versuchsergebnisse vorgespannter Stahlträger im elastischen und elastoplastischen Zustand

Results of Tests of Prestressed Steel Beams in Elastic and Elastoplastic State

Résultats d'essais sur des poutres en acier précontraintes, à l'état élastique et élastoplastique

PAVEL FERJENCIK
Dozent, Dipl.-Ing., CSc
Fakultät für Bauwesen der Slowakischen Technischen Hochschule
Bratislava, CSSR

MILOSLAV TOCHACEK
Dipl.-Ing. CSc
Bauinstitut der Tschechischen TU Praha
Praha, CSSR

Ziel der Prüfungen sechs vorgespannter Walzträger war die Ermittlung der wirklichen Wirkung dieser Träger, im elastischen wie auch im elastoplastischen Zustand und der Vergleich der Ergebnisse mit der Theorie /1/. Es waren grundsätzlich diese Gründe für die Wahl der Walzträger: Überprüfung der Theorie an herstellungsmässig einfachen Elementen, die geringe Anschaffungskosten haben, und Überprüfung der Verstärkungsmöglichkeit so wie auch der Tragfähigkeitserhöhung der Walzträger durch vorgespannte hochfeste Zugbänder.

Verwendet wurden Walzträger I PE 30 aus Stahl 11 373 mit 3800 mm Spannweite. Auf der ganzen Spannweitelänge waren die Träger mit einem hochfestem Zugband aus patentierten Drähten 20 Ø P 4,5 mm vorgespannt; das Zugband lief unter dem Trägeruntergurtflansch, parallel mit diesem, Bild 1. Die Träger N 1 bis N 6

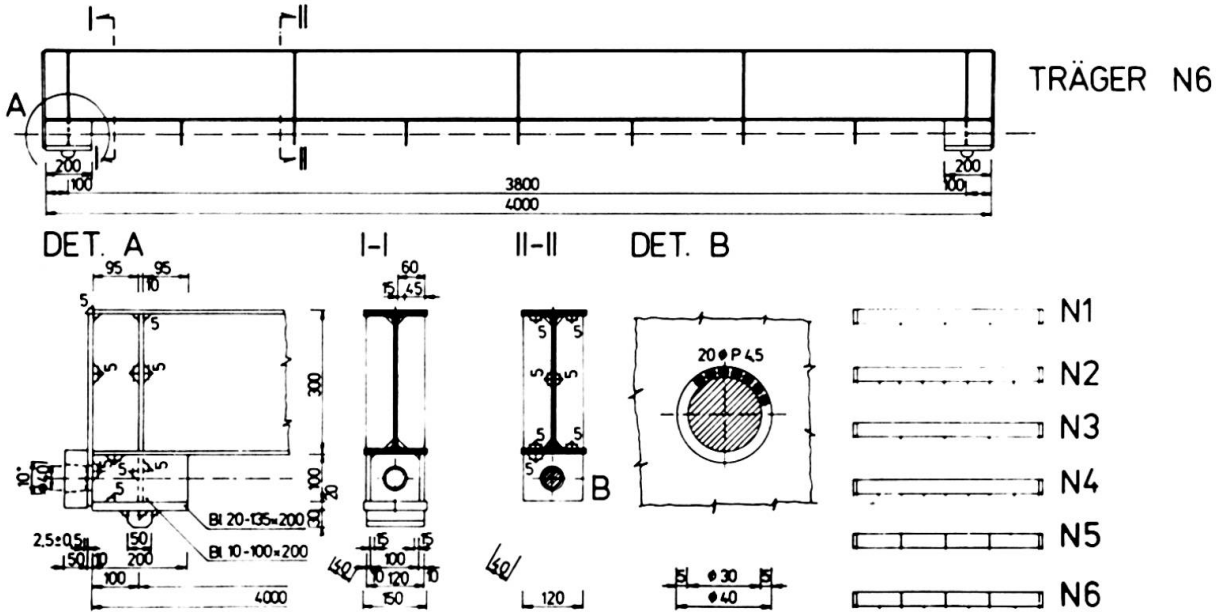

Bild 1. Prüfträger N 1 bis N 6

hatten unterschiedliche Zahlen der Stegdiafragmen, stabilisierenden Diafragmen unter dem Trägeruntergurtflansch und Einlagen im Zugbandinneren.

Die Ansicht der Gesamtanordnung der Prüfung ist am Bild 2 zu sehen. Oben sieht man den stützenden Hilfsträger, unten ist der Prüfträger, zwischen beiden Trägern sind drei Belastungspressen. Die Vorrichtung am Bild 2 rechts sichert die Stabilität der geprüften Konstruktion. Am Bild 3 ist das Zugband vom Ringquerschnitt an der Stelle des stabilisierenden Diafragma mit /Bild 3a/ und ohne /Bild 3b/ der pressenden Einlagen. Die Vorspannpistole /Bild 4/ stützte sich auf den ringförmigen Dynamometer, mit dem die Zugbandkraft kontrolliert wurde.

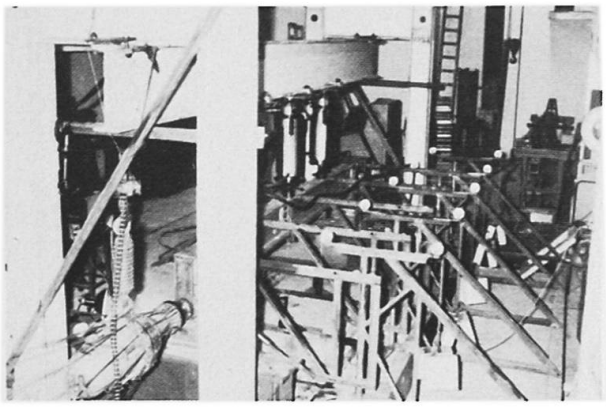

Bild 2.

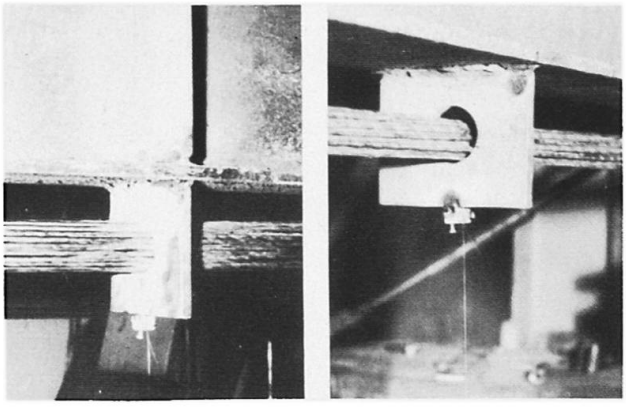

a/ b/

Bild 3.

Die Spannungen im Träger wurden mit 16 Widerstandstensometern gemessen, die 10 cm von der Spannweitemitte des Trägers angeordnet waren. Die Durchbiegungen wurden mittels Durchbiegungsmessern an den Viertelpunkten der Spannweite /unter den Lasten/ gemessen, Bild 5.

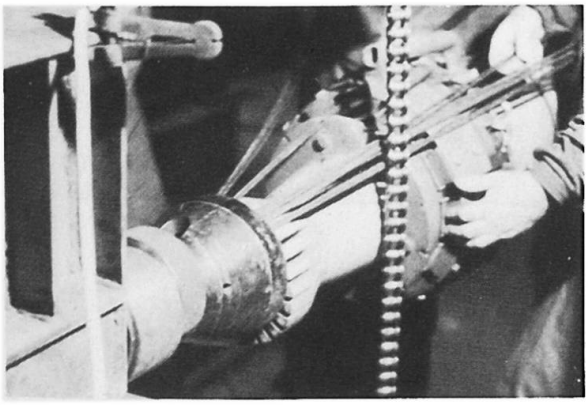

Bild 4.

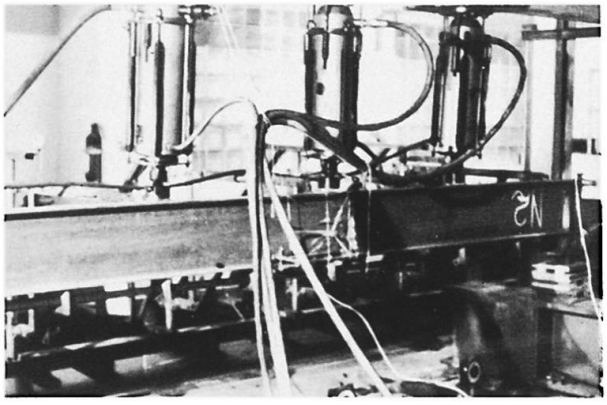

Bild 5.

Kontrolliert wurde auch die Stützensenkung. Bei zwei Trägern wurde die Trägerstabilität mit einer Ergänzungsprüfung gemessen, und zwar bei der Belastung nur durch die Vorspannkraft V: in einem Falle nach Beseitigung aller stabilisierenden Diafragmen /Bild 6/, in zweitem Fall beim Belassen dieser in der Spannweitemitte des Trägers.

Bei den Trägerprüfungen kamen folgende Belastungsstufen zur Geltung: Vorspannkraft V = 0-50-100-150-250-300 kN; lotrechte Lasten P = 0-20-5-40-5-60-5-80-5-90-5-100-110 kN, usw. bis zum Bruch der Konstruktion.

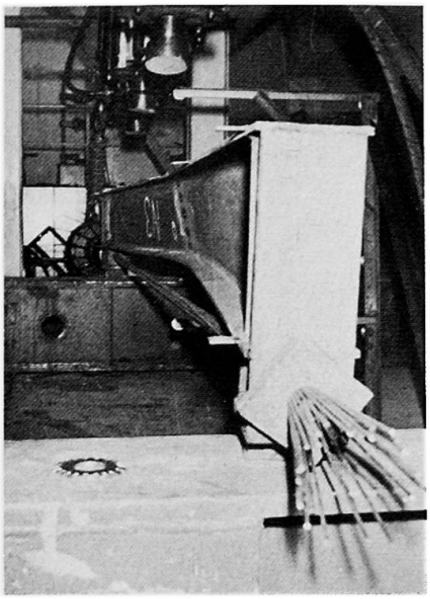

Bild 6. Stabilitätsverlust des Trägers, bei dem die stabilisierenden Diafragmen beseitigt wurden

Die Messergebnisse sind zu Diagrammen verarbeitet, von welchen je eines die Bilder 7 und 8 zeigen. Die erste Diagrammgruppe, die im Bild 7 gezeigt wird, stellt den Verlauf der Normalspannungen in der Trägermitte dar. Der Diagrammtyp im Bild 8 stellt das Anwachsen der verhältnismässigen Verformungen dar /lotrecht aufgetragen/, nachdem sie durch den Elastizitätsmodul multipliziert wurden /im elastischen Bereich also der Normalspannungen σ /in Abhängigkeit vom Anwachsen der Vorspannkraft V /horizontal nach rechts/ und der Belastung P /zurück in der Linksrichtung/. Ähnlich wurden die Messergebnisse der Durchbiegung y verarbeitet, Bild 9.

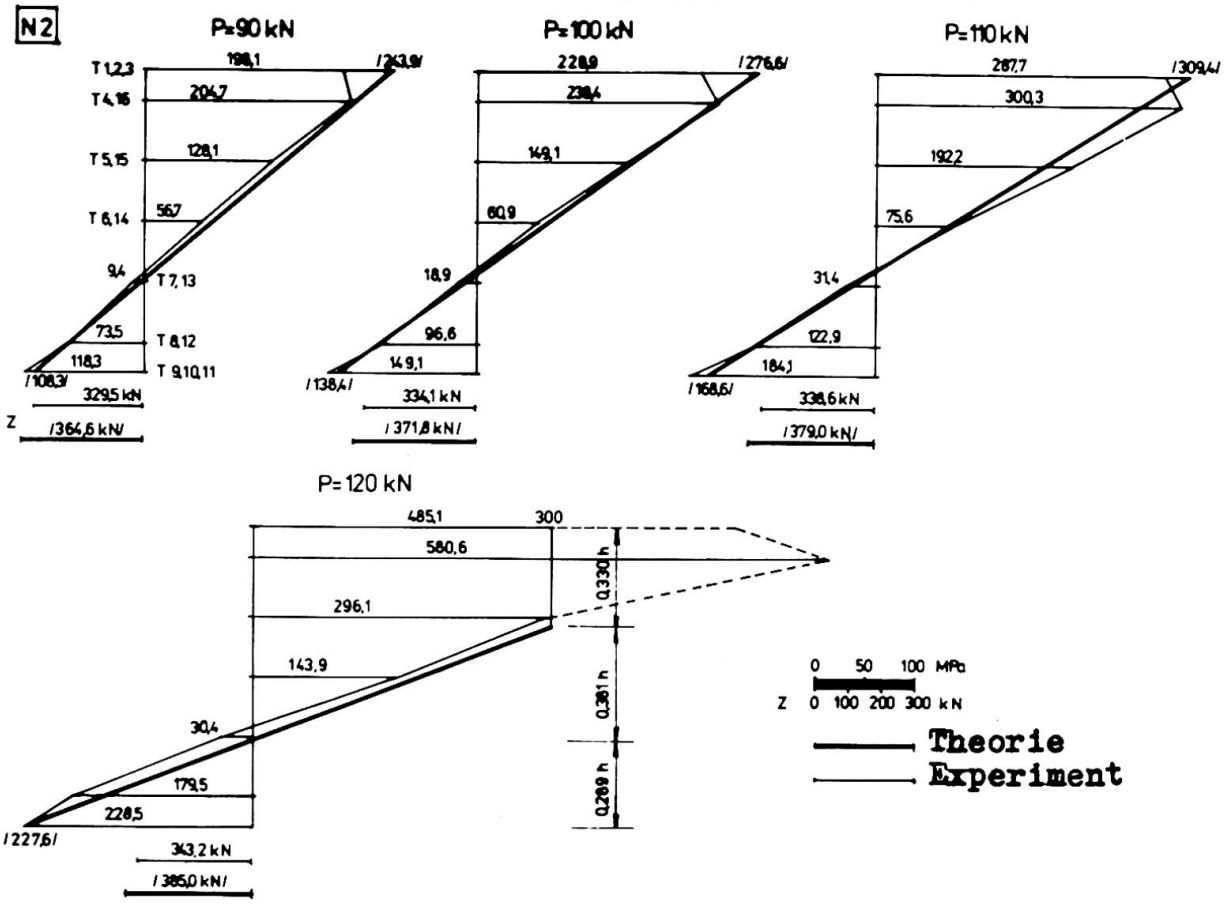

Bild 7. Träger N 2: Normalspannungen in der Mitte der Spannweite bei verschiedener Belastungsgrösse 3xP

Die Prüfungen brachten folgende Erkenntnisse:

Die erwartete Tragfähigkeit vorgespannter Träger im elastischen Zustand /bei der Normfliessgrenze σ_{fl} = 240 MPa grösser als Berechnungsbeanspruchung R = 210 MPa/ war 3x90 kN. Durch den Einfluss noch höherer wirklicher Fliessgrenze $\sigma_{fl} \doteq$ 300 MPa, stieg die theoretische elastische Tragfähigkeit auf cca 3x110 kN. Nach der Norm /2/ berech-

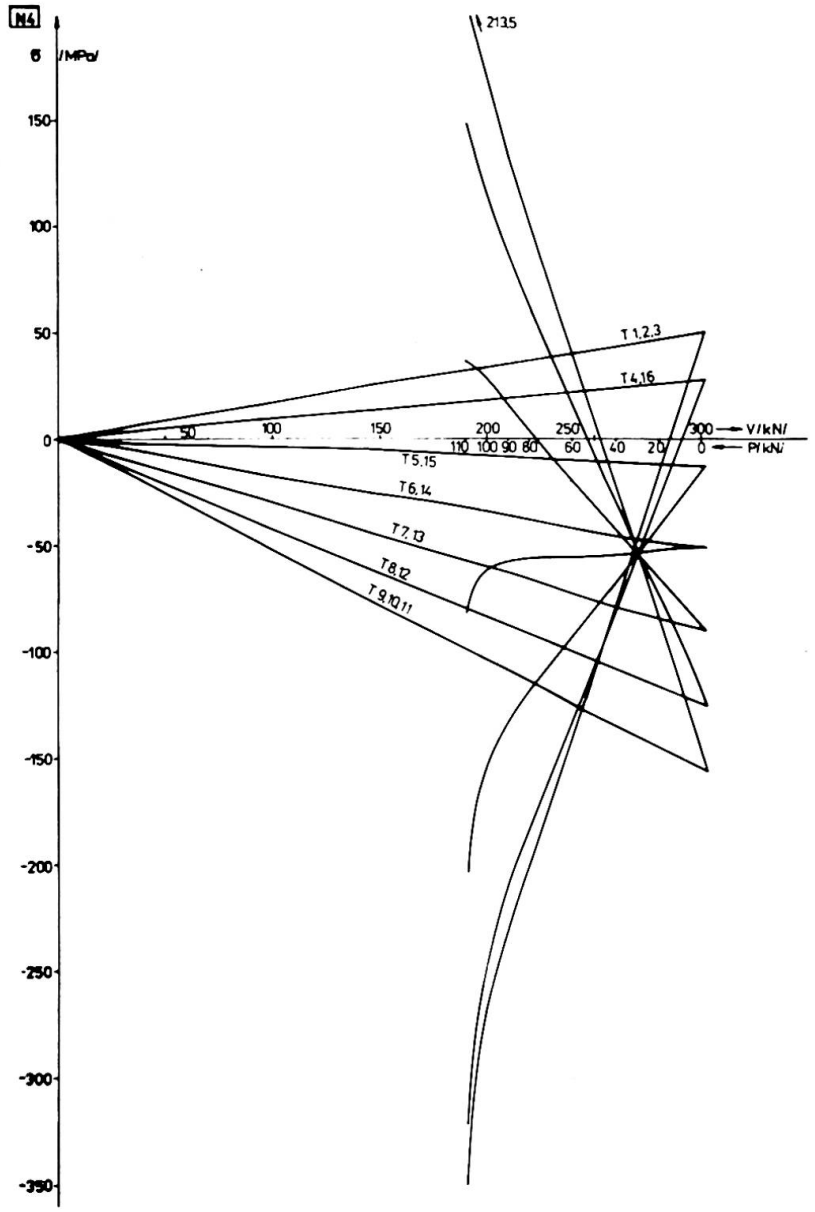

Bild 8. Träger N 4: Spannungsverlauf in Abhängigkeit von der Vorspannung V und Belastung P

net sich bei R = 210 MPa die tragende Last eines nicht vorgespannten Trägers I PE 30 mit 3x61,6 kN. In den ersten vier Trägern wurde eine hohe Tragfähigkeit erreicht, cca die doppelte des nach /2/ berechneten nicht vorgespannten Trägers. Bei den letzten zwei Trägern kam es zur Verringerung der Tragfähigkeit infolge Kippens; die Stützvorrichtung konnte den Obergurt nicht halten - auch so erreichte man eine um die Hälfte grössere Tragfähigkeit als beim nicht vorgespannten, nach /2/ berechneten, Träger.

Tensometrische Messungen zeigten eine sehr gute bis gute Übereinstimmung der Theorie und der Experimente. Es zeigte sich, dass mit den Vorkehrungen, die die Stabilität der Trägerdruckteile sichern, plastische Bereiche hervorgerufen werden können.

Die Durchbiegungsmessungen brachten folgende Erkenntnisse:

- Solange nur die Vorspannkraft wirkte, bestand eine sehr gute Übereinstimmung der theoretischen und gemessenen Durchbiegungen.

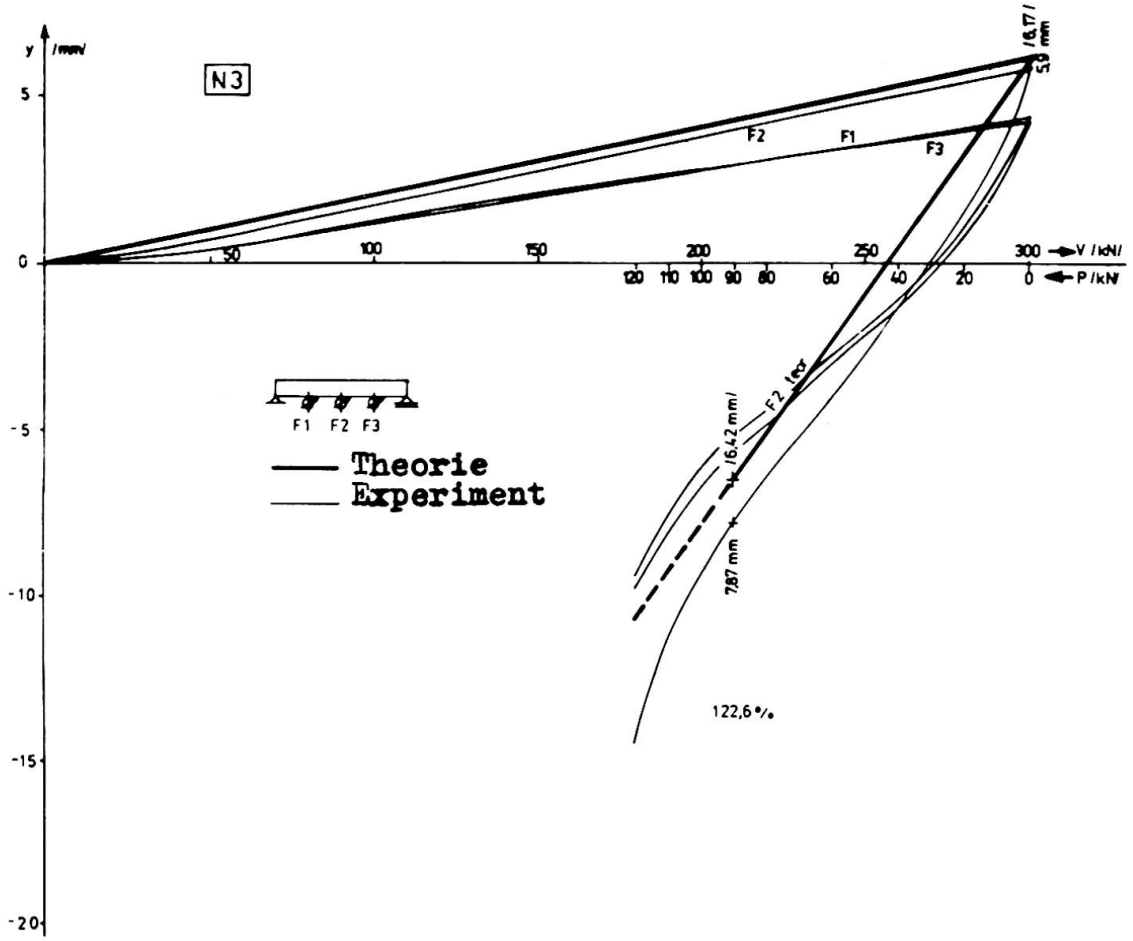

Bild 9. Durchbiegungen y des Trägers N 3 in Abhängigkeit von der Vorspannung V und Belastung P

In den Diagrammen, von denen eines am Bild 9 gezeigt wird, sind numerisch Kontrollwerte bei der Vorspannkraft V = 300 kN angegeben. Die theoretische Durchbiegung ist 6,17 mm /100%/; der durchschnittliche Wert aus den gemessenen Durchbiegungen ist 5,71 mm /92,5%/, also nur wenig geringer als berechnet. In den meisten Fällen wuchs die Durchbiegung linear.

- Wenn ausser der Vorspannung noch eine vertikale Belastung wirkte, waren die maximalen Durchbiegungen im Durchschnitt um 37% grösser als berechnet. Die Durchbiegungen waren grundsätzlich in guter Übereinstimmung mit den Spannungen, die gleichfalls höher waren als die berechneten.

Die Verschiedenheit der konstruktiven Lösung hat sich auf die Trägertragfähigkeit nicht ausgewirkt: Der Walzträger I PE hat einen genügend dicken Steg, so dass er hohe Einzellasten überträgt ohne dass der nicht ausgesteifte Steg lokal ausbeulte /I PE 30 überträgt verlässlich die Lasten 3x126 kN/. Der starke Untergurt braucht keine dichte Anordung der stabilisierenden Diafragmen. Auch ein Träger ohne stabilisierende Diafragmen übertrug eine Vorspannkraft von 400 kN /also um 100 kN mehr als der verlangte Wert/.

Die Prüfungen haben bestätigt, dass durch Vorspannung mittels eines hochfesten Zugbandes die Tragfähigkeit der Walzträger bedeutend erhöht werden kann, besonders im elastischen Bereich. Die Tragfähigkeit wächst weiter, wenn die plastische Reserve des Stahles

genützt wird. Die Ausnutzung der plastischen Reserve stösst auf Probleme der Stabilität. Infolge der Vorspannung, Nutzung der plastischen Reserve des Materials und bedeutend hoher Fliessgrenze des verwendeten Stahls erreichte man in 2/3 der Fälle der angeführten Experimente eine doppelte Tragfähigkeit gegenüber der, die die Berechnung des nicht vorgespannten Trägers /2/ ergibt.

Literatur:

/1/ Ferjenčík, P. - Tocháček, M.: Skúšky predpätých oceľových nosníkov v pružnom a pružnoplastickom stave. Druhá dielčia etapa úlohy P 12-124-003-02/2,e Predpäté kovové a lanové konštrukcie. Bratislava, KKDK SvF SVŠT, 1975.

/2/ ČSN 73 1401 Navrhování ocelových konstrukcí. Praha ÚNM /Gültigkeit ab 1. 1. 1968/.

Behaviour of Hybrid Beam-Columns under Cyclic Loading

Comportement de montants hybrides soumis à des flexions cycliques

Verhalten von hybriden Stahlstützen unter zyklischer Biegebeanspruchung

M. YAMADA Prof.
B. TSUJI Prof.
Faculty of Engineering, Kobe University
Kobe, Japan

1. INTRODUCTION

The cyclic bending deformation behavior of the wide flange section was discussed by the senior auther(1),(2), and it was clarified that the cyclic bending moment-curvature relationship under the constant axial force asymptotes to the relationship of the pure bending due to the strain hardening effect. The cyclic bending behavior of the hybrid member is discussed here.

2.ANALYSIS

2.1. Analytical Model

A wide flange section is simplified into a three points model(2) such as shown in Fig.1. The area of the web is k times the one of the flange. The yield stress σ_{yw} of the web is ρ times the yield stress σ_{yf} of the flange. The stress-strain relationship of the material is tri-linear type such as shown in Fig.2. In general, with the increase of the yield stress σ_y, the yield ratio $\zeta=\sigma_y/\sigma_{max}$ increases and the strain hardening coefficient $\mu=E_{st}/E$ decreases. Fig.3 shows the relationship between the yield ratio ζ or the strain hardening coefficient μ and the yield stress σ_y. Indicating the stresses of each point as $\bar{\sigma}_i=\sigma_i/\sigma_{iy}(i=1,2,3)$, the axial force $N=nN_y$ and the bending moment $M=mM_y$ are obtained as follows:

$$n=\frac{\bar{\sigma}_1+\bar{\sigma}_3+\rho k\bar{\sigma}_2}{2+\rho k}$$

$$m=\frac{\bar{\sigma}_1-\bar{\sigma}_3}{2}$$

The stresses of each point are obtained by summation of the elastic stress and the residual stress such as shown in Fig.4, and are represented as follows:

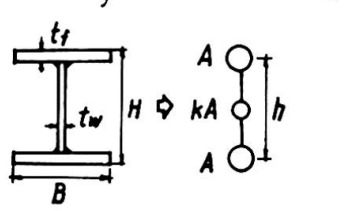

Fig.1 Three Points Model

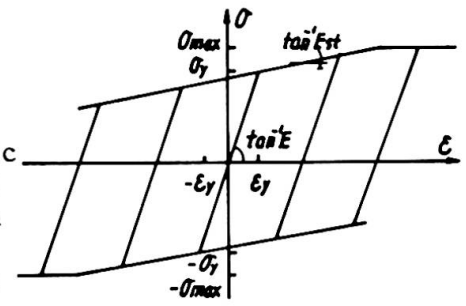

Fig.2 σ - ε Relationship

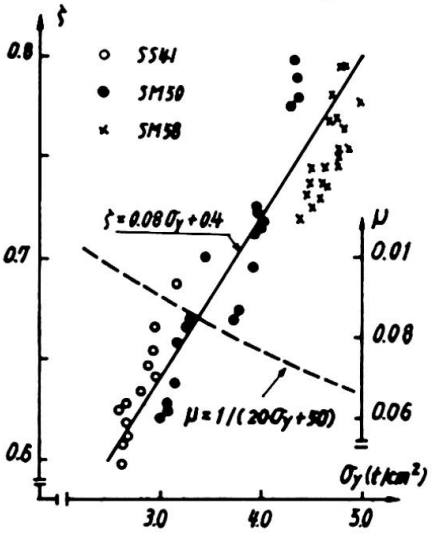

Fig.3 Yield Ratio ζ and Strain Hard. Coeff. μ

$$\bar{\sigma}_1=(2+\rho k)/(2+k)n+m+\xi$$

$$\bar{\sigma}_2=(2+\rho k)/\rho(2+k)n-2\xi/\rho k$$

$$\bar{\sigma}_3=(2+\rho k)/(2+k)n-m+\xi$$

where ξ is a parameter indicating the magnitude of the residual stress. The yield conditions of each point are as follows:

$$\alpha_i-2\leq\bar{\sigma}_i\leq\alpha_i$$

$$-1/\zeta_i\leq\bar{\sigma}_i\leq 1/\zeta_i$$

where α_i shows the subsequent yield stress. Fig.5 shows the yield polygon. The broken line shows the envelope of the yield polygon and a stress point can not go out of this range.

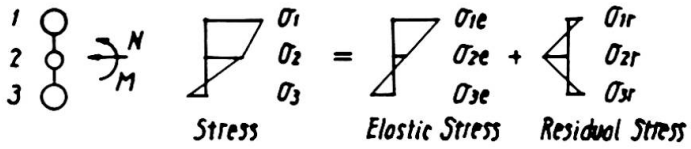

Fig.4 Stress Distribution

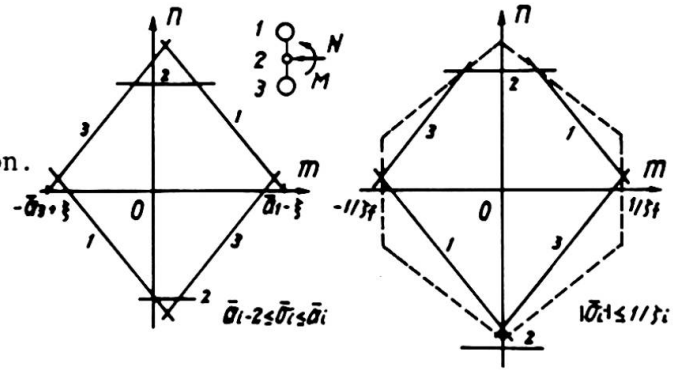

Fig.5 Yield Conditions

2.2. Bending Moment-Curvature Relationship

Fig.6 shows the bending moment-curvature relationship under the constant axial force of $N=0.5N_y$. Four types of the cross section computed are shown in Table 1. Figs.(a) and (b) correspond to the homogeneous members using a mild steel and a high strength steel, and Figs.(c) and (d) to the hybrid member using a high strength steel as the flange and the web, respectively. In each case, the relationships converge to the steady state loop at the three or four cycles. In the case of type A and D, the relationships converge to those of the pure bending due to the strain hardening effect, whereas in the case of type B and C, the loops converge to the steady state ones, the maximum bending capacity of which is somewhat smaller than that of the former case, due to the fully plastic state of the web and the compression flange.

Table 1 Types of Members

	Type	σ_{yf}(t/cm^2)	σ_{yw}(t/cm^2)
Homogeneous Member	A	3.0	3.0
	B	5.0	5.0
Hybrid Member	C	5.0	3.0
	D	3.0	5.0

σ_y(t/cm^2)	$\mu=E_{st}/E$	$\zeta=\sigma_y/\sigma_{max}$
3.0	1/110	0.64
5.0	1/150	0.80

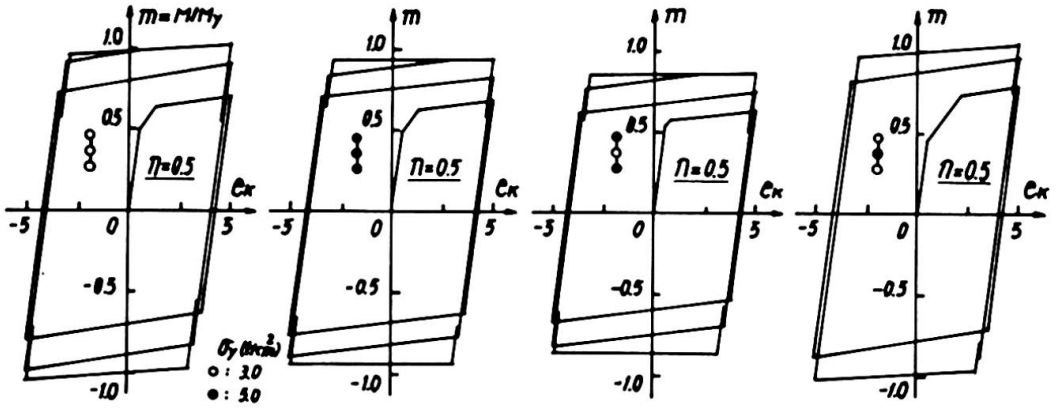

(a) Type A (b) Type B (c) Type C (d) Type D

Fig.6 Bending Moment-Curvature Relationship

2.3. Load-Deformation Relationship

Fig.7 shows the lateral load-deflection relationship of the column, the slendreness ratio of which is 25, under the constant axial load of $N=0.5N_y$. Alternately repeated horizontal force $P=pP_y$ is applied at the constant lateral

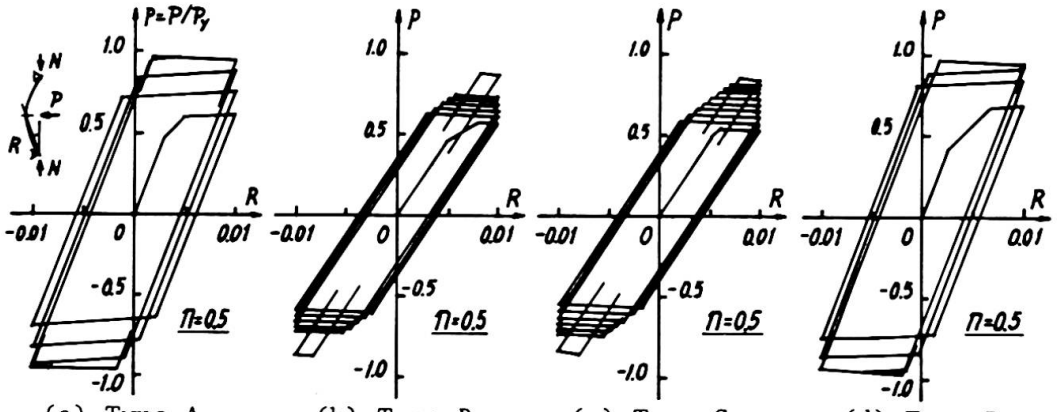

(a) Type A (b) Type B (c) Type C (d) Type D

Fig.7 Load-Deformation Relationship

sway rotation angle of R=±0.01. Figs.(a) and (b) correspond to the homogeneous member and Figs.(c) and (d) correspond to the hybrid one. In the case of the columns having a mild steel flange (type A and D), the load-deflection relationships converge to the steady state loop at the few cycles because of the small yield ratio (ζ=0.64) and of the large strain hardening coefficient (μ=1/110). The relationships of type B and C columns having high strength steel flange converge to the steady state loop at 17 and 13 cycles,respectively.

2.4. Variation of Maximum Strength and Accumulated Plastic Strain

Fig.8 shows the relationship between the maximum strength and the number of cycles. The abscissa W shows the number of half cycles. The maximum strength increases with the number of cycles. The strength of the hybrid member using a high strength steel as the web (type D) is the largest and using a mild steel as the web is the smallest. Convergence to the steady state loop is rapid in the case of the member having mild steel flange. Fig.9 shows the variation of the accumulated plastic strain of the web. The accumulated plastic strain induced is large in the case of a hybrid member using the mild steel web, and small in the case of the member using high strength steel web. In some cases, the plastic strain increases with the number of cycles even after the maximum strength converges to the steady state value.

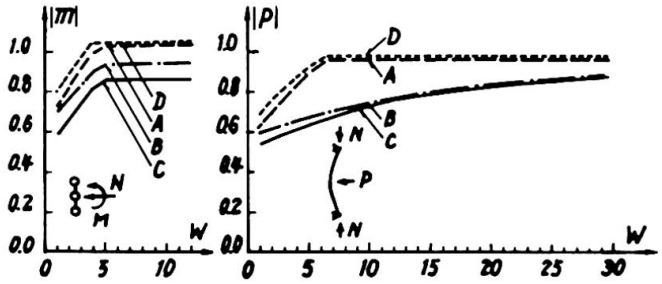

Fig.8 Variation of Maximum Strength

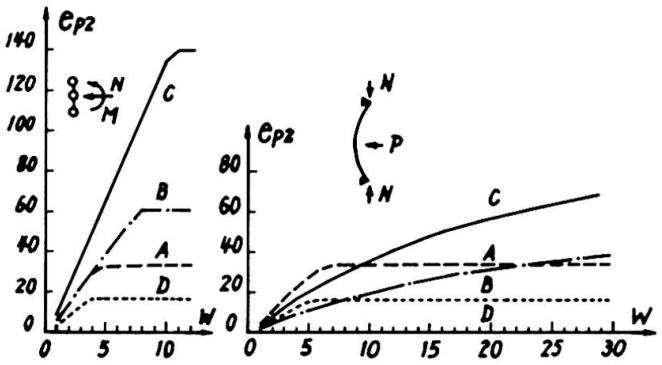

Fig.9 Accumulated Plastic Strain

3.CONCLUDING REMARKES

Elastic plastic behavior of the wide flange columns with homogeneous and hybrid sections was discussed. In the case of the members having high strength steel with large yield ratio and small strain hardening coefficient, the increase in the strength under the cyclic loading is relatively small. The hybrid member having a mild steel web shows a relatively small increment in the strength under the cyclic loading and induces the large amount of accumulated plastic strain in the web even under the small axial force range.

On the other hand, the hybrid member having a high strength steel web shows a relatively large increment in the strength and induces relatively small amount of plastic strain in the web.

BIBLIOGRAPHY

(1) Yamada,M. : Freie Diskussion IIIc, Final Report, 8th. Congr., IABSE, New York, 1968, pp.693-695.
(2) Yamada,M., Shirakawa,K. : Elaso-plastische Biegeformänderungen von Stahlstützen mit I-Querschnitt, Teil II : Wechselseitig wiederholte Biegung unter konstanter Normalkrafteinwirkung, Der Stahlbau, 40. Jahrg., H.3, 1971, S. 65-74 u. H.5, 1971, S.143-151.
(3) Horikawa,K. : Experimental Study on Shape and Size of Tensile Specimen, JSSC, Vol.5, No.48, 1969, pp.52-67, (in Japanese).

SUMMARY

Elasto-plastic cyclic bending deformation behaviour of the hybrid members is discussed assuming a wide flange section as a three points model and stress-strain relationship as tri-linear type. In the case of the hybrid member, the increase in the strength under the cyclic loading are larger and the amount of the accumulated plastic strains are smaller for the member with weaker flange than with weaker web. The limiting axial force level within which the bending resistance of the column asymptotes to that of pure bending is lower for the weaker web member.

RESUME

Les auteurs présentent le comportement élasto-plastique d'éléments hybrides soumis à des flexions cycliques; ils remplacent le profilé à larges ailes étudié par un modèle à trois surfaces et admettent une relation contraintes-allongements du type trilinéaire. Pour des éléments hybrides possédant un âme en acier à haute résistance, l'augmentation de résistance sous charges cycliques est plus élevée et la quantité de déformations plastiques accumulées, plus faible que pour une âme en acier doux. L'effort normal limite permettant asymptotiquement un moment de ruine égal à celui correspondant à la flexion pure est moins élevé lorsque l'âme est en acier doux.

ZUSAMMENFASSUNG

Das elasto-plastische Biegeverformungsverhalten einer zyklisch beanspruchten hybriden Stahlstütze ist unter der Annahme eines drei Punkt-Modelles des Breitflansc Querschnittes und einer tri-linearen Vereinfachung der σ-ε-Beziehung untersucht. Im Fall von hybriden Stahlstützen mit schwächerem Flansch ist der Zuwachs des Widerstandes grösser und die Verzerrungsakkumulation kleiner als für Querschnitte mit schwächerem Steg. Der Grenzwert des Normalkraftniveaus,für das der Biegewiderstand mit demjenigen unter reiner Biegung asymptotisch übereinstimmt, ist niedriger für einen Querschnitt mit schwächerem Steg.

On Structural Behaviour of Hybrid I-Beams

Sur le comportement à la ruine des poutres en I hybrides

Zum Tragverhalten hybrider I-Balken

ZBIGNIEW CYWIŃSKI
Assistant Professor
Technical University of Gdańsk
Gdańsk, Poland

This contribution refers to Theme Va of the Introductory and Preliminary Reports. It represents certain proposal for the plastic analysis of hybrid I-beams assuming combined action of bending and shear.

Author's treatment of mentioned problem bases upon that suggested by Strel'bitskaya for homogeneous beams /1/. Simultaneously Schilling's optimum design criteria are taken into account /2/. Collapse loads determined are compared with those resulting from the ASCE-AASHO regulations /3/.

Plastic bending-shear interaction analysis of homogeneous I-beams bases generally on the yield condition

$$\sigma^2 + 3\tau^2 = \sigma_0^2 , \qquad (1)$$

where σ , τ are the elastic bending and shear stresses, respectively, and σ_0 is the yield stress. According to /1/ the elastic stress patterns are as shown in Fig. 1; both of them are more (σ) or less (τ) inaccurate but fulfil the yield condition (1) at each point of the I-section and develop sufficiently exact (conservative) collapse load values. Similar analysis of hybrid I-beams can be based on stress patterns as given in Fig. 2.

With the specifications of Fig. 2 the fully plastic moment and shear, M_0 and Q_0 respectively, can be expressed as follows:

$$M_0 = \sigma_0 \frac{A_f h}{2} + \alpha \sigma_0 \frac{th^2}{4} = \sigma_0 \frac{th^2}{4}(1+\alpha), \qquad (2)$$

$$Q_0 = \alpha \tau_0 th = \sigma_0 \frac{th}{\sqrt{3}} \alpha , \qquad (3)$$

whereby the following numerical values of α and σ_0 are being considered:

$\alpha = 1.00$, for $\sigma_0 = 36{,}000$ psi (homogeneous beam),
$\alpha = 0.72$, for $\sigma_0 = 50{,}000$ psi
$\alpha = 0.36$, for $\sigma_0 = 100{,}000$ psi (hybrid beams).

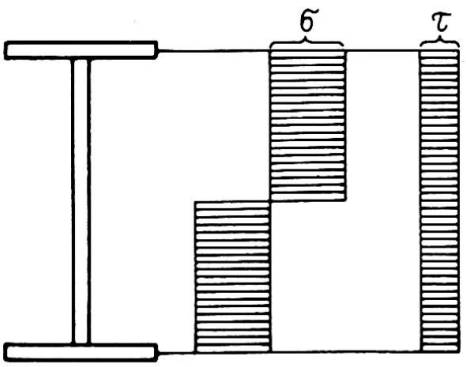

Fig. 1. Elastic stress patterns for homogeneous I-beam; assumed in [1]

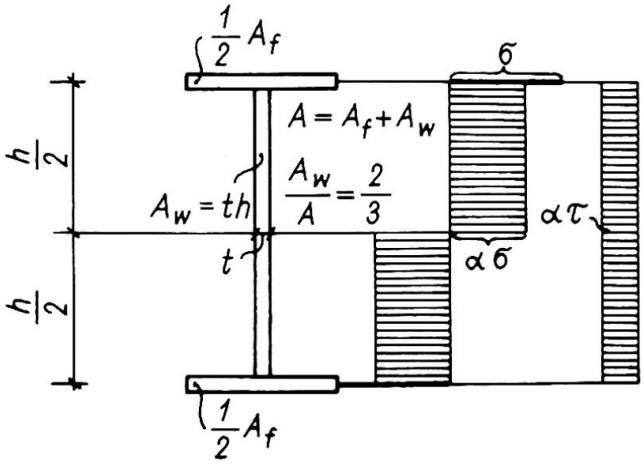

Fig. 2. Elastic stress patterns for hybrid I-beam; Author's assumption

Investigations performed concern in particular the beam fixed at both ends carrying single load P at span-mid or uniform load q all over the span (Fig. 3).

According to Author

$$P = \frac{8\,\frac{M_o}{l}}{\sqrt{\frac{16\,M_o^2}{l^2\,Q_o^2}+1}} = \frac{8\,\frac{M_{ou}}{l}}{\sqrt{12\left(\frac{h}{l}\right)^2+\left(\frac{2\alpha}{1+\alpha}\right)^2}}$$

$$q = \frac{16\,\frac{M_o}{l^2}}{\frac{16\,M_o^2}{l^2\,Q_o^2}+1} = \frac{16\,\frac{M_{ou}}{l^2}}{6\left(\frac{h}{l}\right)^2\frac{1+\alpha}{\alpha}+\frac{2\alpha}{1+\alpha}}$$

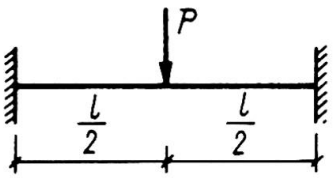

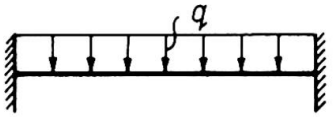

According to ASCE-AASHO

$$P = \frac{16\,\frac{M_o}{l}}{\sqrt{64\,\frac{M_o^2}{l^2\,Q_o^2}\,\frac{\alpha}{1+\alpha}+1}+1} = \frac{8\,\frac{1+\alpha}{\alpha}\,\frac{M_{ou}}{l}}{\sqrt{12\left(\frac{h}{l}\right)^2\frac{1+\alpha}{\alpha}+1}+1}$$

$$q = \frac{32\,\frac{M_o}{l^2}}{\sqrt{128\,\frac{M_o^2}{l^2\,Q_o^2}\,\frac{\alpha}{1+\alpha}+1}+1} = \frac{16\,\frac{1+\alpha}{\alpha}\,\frac{M_{ou}}{l^2}}{\sqrt{24\left(\frac{h}{l}\right)^2\frac{1+\alpha}{\alpha}+1}+1}$$

Fig. 3. General expressions of collapse loads

Extending the interaction formula of /1/

$$\frac{M^2}{M_o^2} + \frac{Q^2}{Q_o^2} = 1 \tag{4}$$

over to hybrid I-beams and taking into account the corresponding equation

$$\frac{M}{M_o} + \frac{Q^2}{Q_o^2}\,\frac{\alpha}{1+\alpha} = 1$$

resulting from ASCE-AASHO regulations /3/ a set of general collapse load expressions can be obtained which is given in Fig. 3; therein

$$M_o = \frac{1+\alpha}{2\alpha}\,M_{ou} \tag{5}$$

where $M_{ou} \equiv M_o(\alpha=1)$ holds for homogeneous (uniform) beam.

On the basis of the expressions derived the corresponding interaction curves, in terms of Pl/M_{ou} and ql^2/M_{ou} respectively, as functions of the span-depth ratio l/h can be found; this is illustrated in Fig. 4 and Fig. 5.

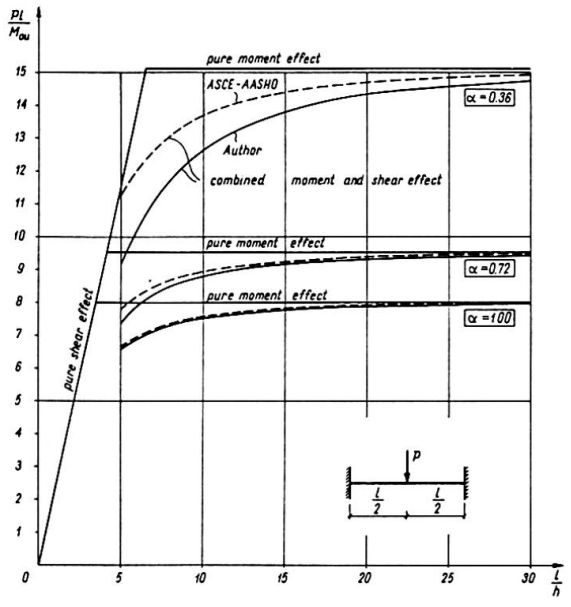

Fig 4 Collapse loads - concentrated

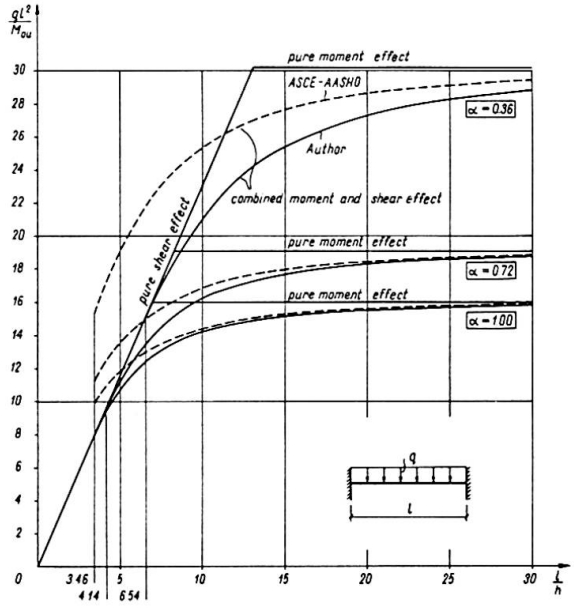

Fig 5 Collapse loads - uniform

In conclusion Author's proposal can be characterized as follows:

1. It yields collapse loads close (conservative) to those of the ASCE-AASHO regulations whereby the relative difference increases with a decrease of the l/h-ratio and the α-value.
2. It visualizes clearly the dominating effect of pure shear for small l/h-ratios.
3. It can be found handy analysing non-uniform plastic torsion problems (bimoment - flexural-torsional moment interaction, St.-Venant torsional moment effect) of hybrid sections, as shown for the homogeneous ones in /1/ and /4/.

References

/1/ Strel'bitskaya, A.I.: A study of strength of thin-walled beams beyond the elastic limit (in Russian). Izdatel'stvo AN USSR, Kiev 1958.

/2/ Schilling, Ch.G.: Optimum properties for I-shaped beams. Journal of the structural Division, ASCE, Vol. 100, No. ST 12, Dec. 1974, pp. 2385-2401.

/3/ Design of hybrid steel beams. Report of the Subcommittee 1 on Hybrid Beams and Girders of the Joint ASCE-AASHO Committee on Flexural Members. Journal of the Structural Division, ASCE, Vol. 94, No. ST 6, June 1968, pp. 1397-1426.

/4/ Strel'bitskaya, A.I.: Limit state of frames out of thin-walled members in bending with torsion (in Russian). Izdatel'stvo AN USSR, Kiev 1964.

SUMMARY

Simplified procedure is used to determine the ultimate load of hybrid I-beams in combined bending with shear. It has been found sufficiently exact and is recommended for analysis of similar problems within the theory of non-uniform torsion.

RESUME

Pour la détermination de la charge ultime de poutres hybrides en I soumises à la flexion et au cisaillement, on applique une méthode simplifiée. Celle-ci a donné des résultats suffisamment précis et est recommandée pour la résolution des problèmes similaires dans la théorie de torsion non uniforme.

ZUSAMMENFASSUNG

Ein vereinfachtes Verfahren wurde benutzt, um die Traglast hybrider I-Balken bei zusammengesetzter Biegung mit Schub zu bestimmen. Dieses wurde ausreichend genau gefunden und wird zur Behandlung benachbarter Probleme innerhalb der Theorie der Wölbkrafttorsion empfohlen.

Comportement à la fatigue des poutres hybrides raidies

Ermüdungsverhalten von ausgesteiften hybriden Trägern

Fatigue Behaviour of Stiffened Hybrid Beams

ANDRÉ PLUMIER
Ingénieur aux Laboratoires d'Essais des Constructions du Génie Civil
Université de Liège
Liège, Belgique

Cette étude, financée par la CECA et le CRIF et réalisée sous la direction du Professeur R. BAUS, concerne des poutres hybrides dont les semelles sont en acier E 70 et dont l'âme et les raidisseurs sont en acier E 27 ; quelques poutres homogènes en acier E 70 ont également été testées. Les poutres comportent des raidisseurs soudés aux deux semelles, à l'exception d'une poutre hybride et d'une poutre homogène dont les raidisseurs ne sont soudés qu'à la semelle comprimée ; par ailleurs, une des poutres hybrides comporte une série de goussets soudés à la semelle tendue. Les dimensions générales des poutres et la mise en charge sont schématisées à la figure 1.

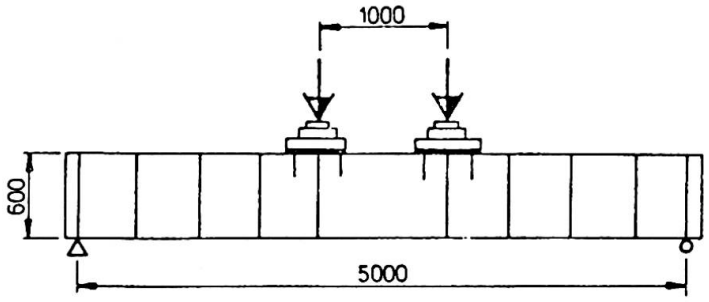

Schéma du montage d'essai

Figure 1

On diffuse les charges appliquées au moyen de plats de forte épaisseur, de plaques de néoprène et de goussets complémentaires. Les types de fissures observés sont présentés à la figure 2.

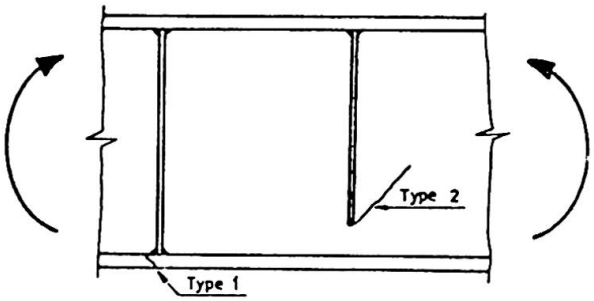

Types de fissure

Figure 2

Les résultats des essais sont donnés à la figure 3, pour les fissures du type 1.

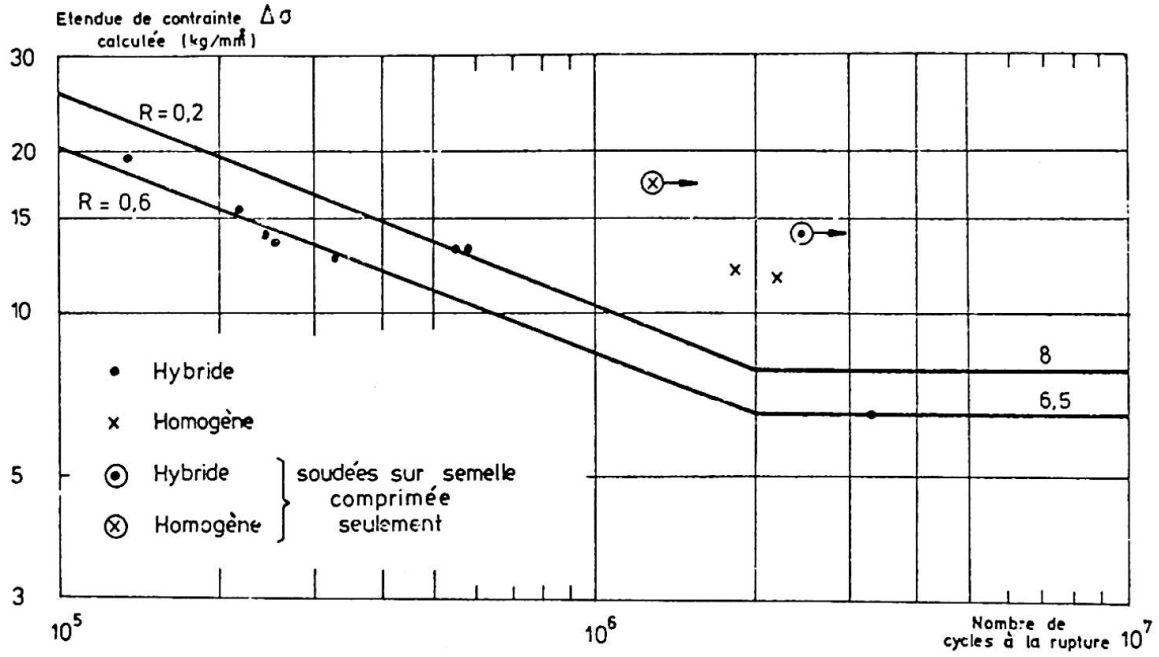

Courbes ΔO - N pour les fissures du type 1

Figure 3

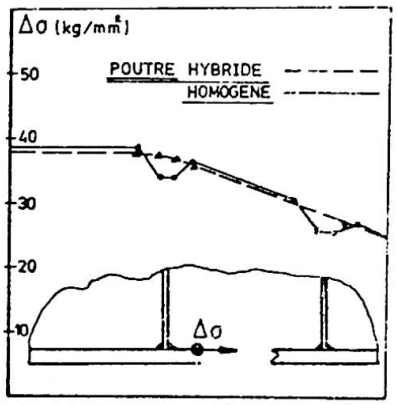

Distribution des ΔO de service

Figure 4

On donne à la figure 4 la distribution des étendues de contraintes Δσ mesurées en service à la fibre intérieure de la semelle tendue entre les charges maximales et minimales. On constate une différence marquée entre la poutre hybride, dans laquelle la plastification initiale égalise les étendues de contrainte en service et la poutre homogène, dans laquelle le raidisseur reste un point dur engendrant une flexion locale.

Des essais effectués, on peut tirer les conclusions suivantes :

1° La résistance en fatigue correspondant à l'assemblage du raidisseur à la semelle est, dans le cas des poutres hybrides, voisine de celle des poutres homogènes classiques ;

2° Dans les poutres hybrides cette résistance ne paraît pas différente selon que le raidisseur est fixé aux deux semelles ou seulement à la semelle tendue, ou selon qu'il se trouve, ou non, sous la charge ; ceci peut être expliqué par l'égalisation des contraintes mentionnée plus haut ;

3° Dans les poutres hybrides, l'étendue des contraintes mesurées en service au niveau du cordon d'assemblage des raidisseurs est égale à la valeur calculée ; dans les poutres homogènes, elle est de 10 % inférieure à la valeur calculée. Ce fait et le meilleur profil des cordons réalisés sur les poutres homogènes expliquent leurs résultats légèrement supérieurs ;

4° De cette constatation, on peut conclure que les résultats des essais sur modèles de grande dimension doivent être étudiés avec circonspection, car les effets locaux du comportement structurel entraînent une différence entre les contraintes réelles et calculées au droit du cordon de soudure.

5° L'hypothèse selon laquelle, par suite de l'existence de contraintes résiduelles, il faut considérer que tout joint soudé d'une pièce soumise à fatigue travaille en traction entre unecontrainte maximale égale à la limite élastique de l'acier et une contrainte inférieure à celle-ci [1] constitue une simplification sécuritaire. Ni dans les essais effectués à Liège, ni en [2], il n'a été observé de fissuration au départ d'un joint de raidisseur à une semelle comprimée, même pour de grandes étendues de contraintes et en dépit de l'existence de contraintes résiduelles de traction particulièrement élevées (70 kg/mm2). On peut penser que la fissuration n'apparaît en zone comprimée qu'en présence d'actions locales de cisaillement ou de flexion [2], souvent ignorées lors du calcul des éléments.

6° Il convient d'éviter la soudure de raidisseurs sur la semelle tendue dans les zones de grands moments de flexion.

BIBLIOGRAPHIE.

[1] T.R. GURNEY et S.J. MADDOX. A re-analysis of fatigue data for welded joints in steel. W.I. Report E/44/72.

[2] Y. MAEDA, MI. ISHIWATA,Y. KAWAI. Structural Behaviour of Hybrid Plate Girders in Bending - Preliminary Report of the 10th Congress of IABSE.

RESUME

La résistance des poutres hybrides raidies aux sollicitations dynamiques est un peu inférieure à celle des poutres homogènes, en raison de certaines particularités du comportement structurel.

ZUSAMMENFASSUNG

Das Ermüdungsverhalten von ausgesteiften hybriden Trägern ist leicht weniger günstig als dasjenige von homogenen Trägern, wegen der besonderen örtlichen Spannungsverteilung in der Umgebung der Steifen.

SUMMARY

The resistance of stiffened hybrid beams to dynamic loads is a little less than that of homogenous beams, because of a particular stress distribution near the stiffener.

Leere Seite
Blank page
Page vide

Additional Tests for "Type 2 Crack" in Hybrid Girders

Essais complémentaires pour les fissures de "type 2" dans les poutres hybrides

Zusätzliche Versuche bezüglich der Risse von "Typ 2" in hybriden Trägern

Y. MAEDA
Professor of Civil Engineering
Osaka University
Suita, Osaka, Japan

M. ISHIWATA
Senior Engineer
Kawasaki Steel Co., Ltd.
Tokyo, Japan

Y. KAWAI
Research Engineer
Kawasaki Steel Co., Ltd
Chiba, Japan

1. Introduction

At the Preliminary Report of the 10th Congress of IABSE[1)], we pointed out that the fatigue failure of thin-walled hybrid girders is generally due to "Type 2 Cracks" initiated at transverse stiffener-to-web fillet weldments. Further, a good correlation between the large-sized girder test results and the small-sized model test results using a steel plate with a transverse fillet welded attachment, was demonstrated. The girder tests, however, were not sufficient in numbers to warrant the fatigue strength, and the model tests did not exactly simulate the structural behavior of the girders because of the difference of strain states.

We are now presenting the results of additional fatigue tests, which have been carried out on axially loaded transverse non-load-carrying fillet welded specimens under strain control to examine the fatigue strength of "Type 2 Cracks" in hybrid girders.

2. Tests

Transverse non-load-carrying fillet welded specimens, as shown in Fig. 1, intended for simulating the boxing parts of the transverse stiffener-to-web fillet welds in hybrid girders, are axially loaded under strain control by fixing the out-put of strain gauges on the specimens to the maximum strain of 1700×10^{-6}, which corresponds to the design working strain of 80 kg/mm^2 high strength steel in a tension flange of girders.

The specimens consist of JIS-SS41 steel with a specified tensile strength of 41 kg/mm^2, and are divided into two series, namely, the ones of which at weld toe are as-welded and the others are lightly ground at the toe to examine the effect of finishing. Such a test simulates the structural behavior proper

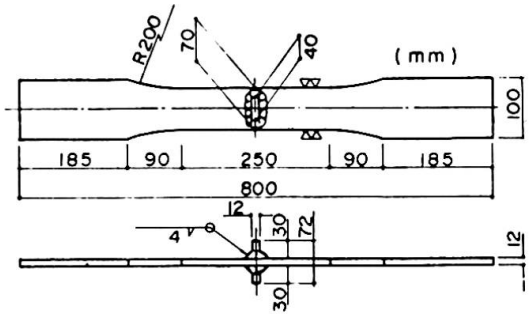

Fig.1 Details of As-Welded Specimen

to hybrid girders that a web reaches a kind of strain-controlled state after yielding due to the contribution of elastic frame action of flanges to the restraining of plastic flow of the web.

3. Results

The test results are graphically shown on the S-N diagram in Fig.2, in terms of equivalent stress range due to the strain range versus number of cycles to failure, neglecting the effect of stress ratios. The fatigue strength at 2×10^6 cycles of the as-welded specimens and of the lightly-ground specimens can be estimated at 9.5 kg/mm^2 and 10.5 kg/mm^2 as the mean value of stress ranges, respectively. The effect of finishing on the fatigue strength is not so remarkable at the present tests. This may be attributed to the fact that the grind operation was not fully performed and consequently some fine notches were not removed.

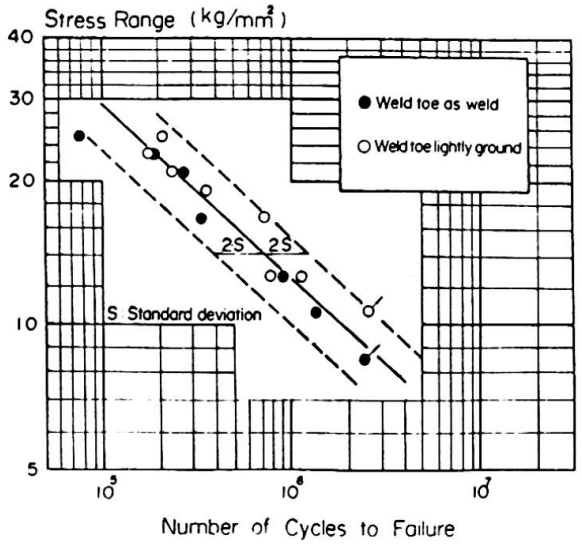

Fig.2 Fatigue Test Results

4. Discussions

(1) To study the influence of load controlling method on fatigue lives, comparison of the present test results with previous fatigue data on model specimens with the same configuration as the present ones, which were given by reanalysis of Gurney et al[2] about numerous tests, is shown in Fig.3.

It can be seen that the present test results, unexpectedly, agree well with the reanalyzed S-N curve by Gurney et al, which took into account the effect of residual stress on fatigue. It may be recognized that such a good agreement was obtained, because the correction of S-N curves was done on the assumption that residual stresses resulting from welding would generally be as high as the yield stress of the parent material as expected in a large as-welded structure, and such an assumption can be applied to the present tests,

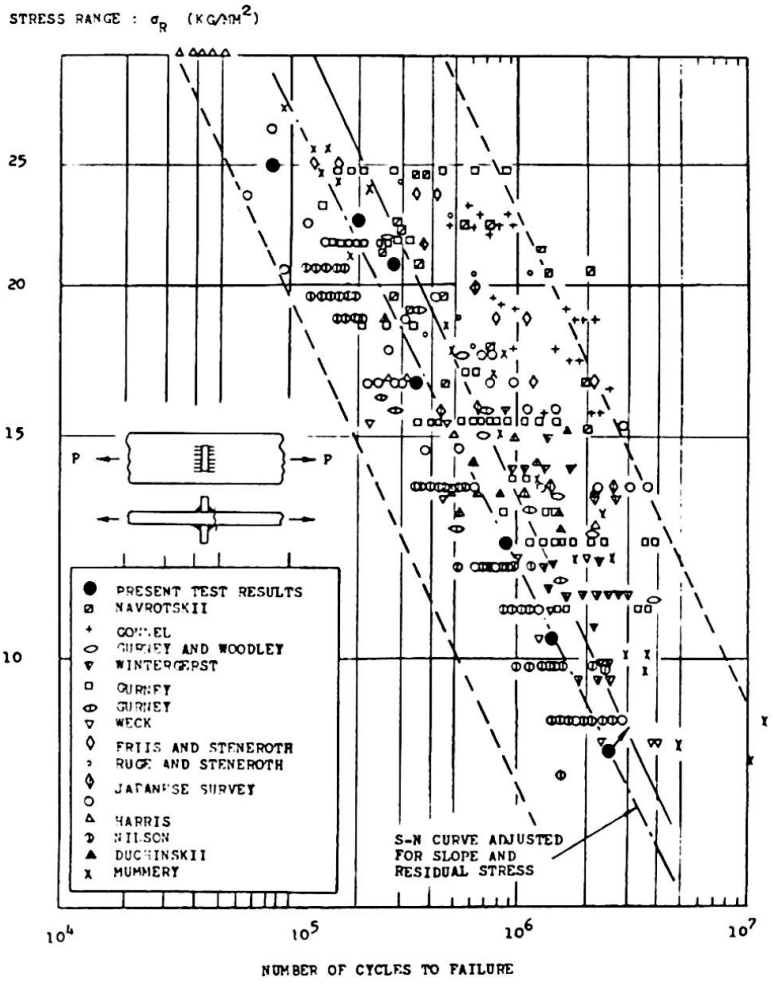

Fig.3 S-N Curves for Transverse Non-Load-Carrying Fillet Welded Joints

in which the specimens could yield at the maximum loading controlled by the strains.

(2) To study on the effect of steel grades on the fatigue strength, another comparison of the present test results for as-welded specimens with other steels[3], is made as shown in Fig. 4. Here, JIS-SM58 and WES-HT80 are high-strength steels with a specified tensile strength of 58 kg/mm^{2}and 80 kg/mm^2, respectively. The latter specimens are provided with the same configuration as the present test specimens, but their loading was controlled by loads from zero to tension.

Since any significant difference among those data cannot be observed, it will be concluded that, at such a welded joint with a large notch effect, the fatigue strength in terms of stress ranges are almost identical one another regardless of steel grades, stress ratios and load-controlling methods.

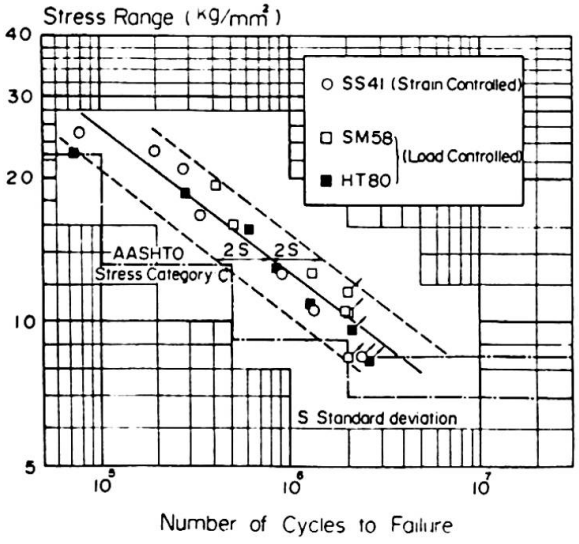

Fig.4 Fatigue Strength of Transverse Non-Load-Carrying Fillet Welded Joints for SS41, SM58 and HT80

(3) Finally, the relation between girder fatigue tests[1),4)] and some model fatigue tests is shown in Fig.5 . The model test results consist of the present test results and the previous ones in Japan [5),6)] on steel plates with transverse fillet welded attachments without boxing. The figure reveals that the present test results under relatively severe loading conditions, can be compared well with the lower 95 % confidence limit line of all the quoted test results except the present test results, and this implies that the present test results give conservative fatigue strengths due to "Type 2 Cracks" in hybrid girders.

It can be also noticed that the allowable fatigue stresses for "Stress Category C" specified at AASHTO Interim Specifications[7)], 1974, are reasonable for "Type 2 Cracks" in hybrid girders as seen in Fig. 4.

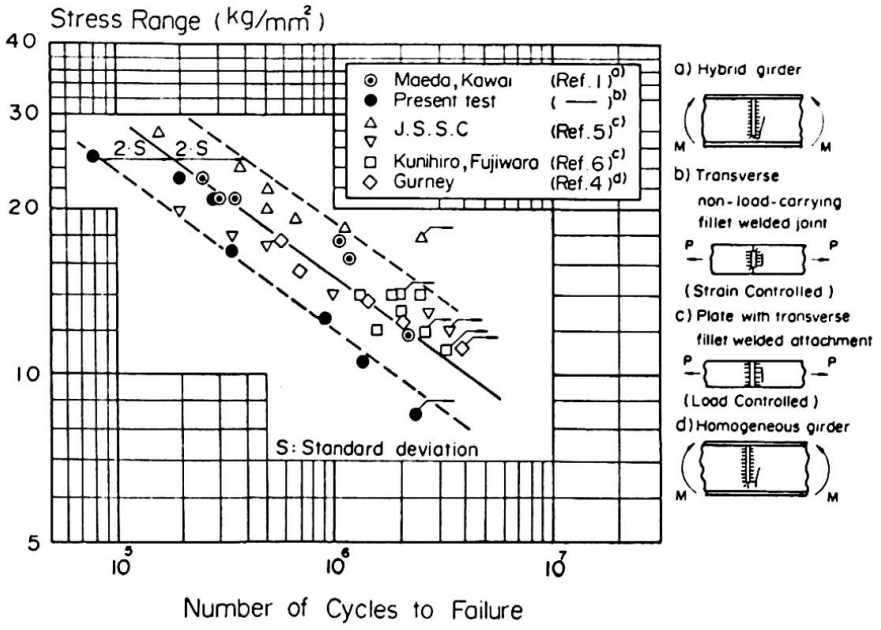

Fig.5 Comparison of Fatigue Strength for Type 2 Cracks in Girder Tests with Model Specimen Tests

References:

1) Y. Maeda, M. Ishiwata and Y. Kawai, Preliminary Report of the 10th Congress of IABSE, 1976.
2) T.R. Gurney and S.J. Maddox, The Welding Institute Research Report, E/44/72, 1972.
3) M. Ishiwata, Y. Tanaba, H. Yukitomo and Y. Kawashima, Preprints of the 26th National Conf. of the Japan Society of Civil Engineers, 1971 (in Japanese).
4) T.R. Gurney and C.C. Woodley, British Welding J., Vol.9, Sept., 1962.
5) J. of the Jpan Society of Steel Construction, Vol.7, No.72, 1971 (in Japanese).
6) T. Kunihiro and M. Fujiwara, Tech. Rept. on Civil Engineering, Vol.14, No.2, Tokyo, 1972 (in Japanese).
7) AASHTO, Interim Specification for Bridges - Interim 8, 1974.

SUMMARY

To supplement the paper presented by the same authors at the Preliminary Report on "Structural Behaviour of Hybrid Girders in Bending and Application to Actual Bridges", additional tests on "Type 2 Cracks" are reported with the results and the discussions. It will be concluded that the fatigue strengths for Type 2 cracking are almost identical one another regardless of steel grades, stress ratios and load-control methods.

RESUME

Pour compléter la contribution présentée par les mêmes auteurs dans le Rapport Préliminaire, "Comportement à la flexion de poutres à âme pleine hybrides. Application aux ponts actuels", des essais complémentaires ont été réalisés pour étudier les fissures de"type 2". Résultats et discussions sont présentés. Il est possible de conclure que les résistances à la fatigue correspondant aux fissures de "type 2" sont pratiquement les mêmes, et indépendantes du type d'acier et de la contrainte moyenne.

ZUSAMMENFASSUNG

Um den von den gleichen Autoren im Vorbericht erschienenen Beitrag zu ergänzen ("Biegeverhalten von hybriden Vollwandträgern. Anwendung im Brückenbau"), wurden zusätzliche Versuche zur Untersuchung von "Typ 2" Rissen durchgeführt. Ergebnisse und Diskussion werden dargestellt. Die Schlussfolgerung lautet, dass die den Rissen "Typ 2" entsprechenden Ermüdungsfestigkeiten praktisch gleich sind, unabhängig von der Stahlfestigkeit und von der mittleren Spannung.

Fatigue Life Prediction of Hybrid Members

Prédiction de la résistance à la fatigue d'éléments hybrides

Vorhersage der Lebensdauer von auf Ermüdung beanspruchten hybriden Elementen

T. YAMASAKI, General Manager
M. HARA, Senior Research Engineer
Y. KAWAI, Research Engineer
Structure Research Center, Kawasaki Steel Co., Ltd.
Chiba, Japan

1. INTRODUCTION

In the Preliminary Report for 10th Congress of the IABSE, 1976, fatigue crack growth rate observations were illustrated on the hybrid tee-shaped specimens to explore a possibility of the estimation of fatigue lives by using fracture mechanics(1).

Additional fatigue crack propagation test was conducted on a center-notched hybrid plate specimen to warrant the fatigue life prediction method for hybrid members.

2. FATIGUE CRACK PROPAGATION TEST

The configuration of the specimen is shown in Fig.1. One specimen consisting of JIS-SS41 (with specified tensile strength of 41 kg/mm^2) and WES-HW70 (with specified tensile strength of 80 kg/mm^2) was longitudinally butt welded along the specimen center line, and an artificial notch was introduced into its center to start a fatigue crack. The chemical analysis and mechanical properties of the materials are shown in Table 1.

The fatigue test was carried out in a 100-ton electro-hydraulic alternating testing machine under stress ranges of 15 kg/mm^2 and 10 kg/mm^2 and at a stress ratio of zero. Fatigue crack growth rate was observed on both the SS41 plate and the HW70 plate by using crack gauges and a 15 power magnifying glass with 1/20 mm micro scales.

The fatigue crack propagation results obtained, fatigue crack growth rate, da/dN, and stress intensity factor ranges, ΔK, were plotted in the conventional manner(2), that is, log-log plots of da/dN as a function of ΔK represented in the form of

$$\frac{da}{dN} = C\,(\Delta K)^m \qquad (1)$$

to evaluate the material constants, C and m, that characterize the fatigue crack propagation behavior of hybrid members.

An effect of a slight difference of crack growth rate between SS41 and HW70 can be considered by using the Ishida's formula for an eccentrical crack in a finite plate (3) in calculating the value of K, based on the fact that the crack center shifted from the plate center as the crack grew. The eccentricity caused by the difference

of the crack growth rate, however, was small compared with the plate width, as was noted in previous report (1), such effect proved to be macroscopically negligible. The exposed fracture surface of the specimen is shown in Fig.2.

Table 1 Chemical Analysis and Mechanical Properties of Materials

Chemical Composition (Wt. %)											
	C	Si	Mn	P	S	Cu	Ni	Cr	Mo	V	B
WES-HW70	0.10	0.30	0.85	0.007	0.010	0.19	0.78	0.46	0.33	0.035	0.004
JIS-SS41	0.18	0.04	0.95	0.014	0.028	--	--	--	--	--	--

Mechanical Properties				
	Y.P.(kg/mm^2)	U.T.S.(kg/mm^2)	Elong.(%)	$_vE_{-5}$(kg·m)
WES-HW70	80	84	27	15.6
JIS-SS41	27	46	30	--

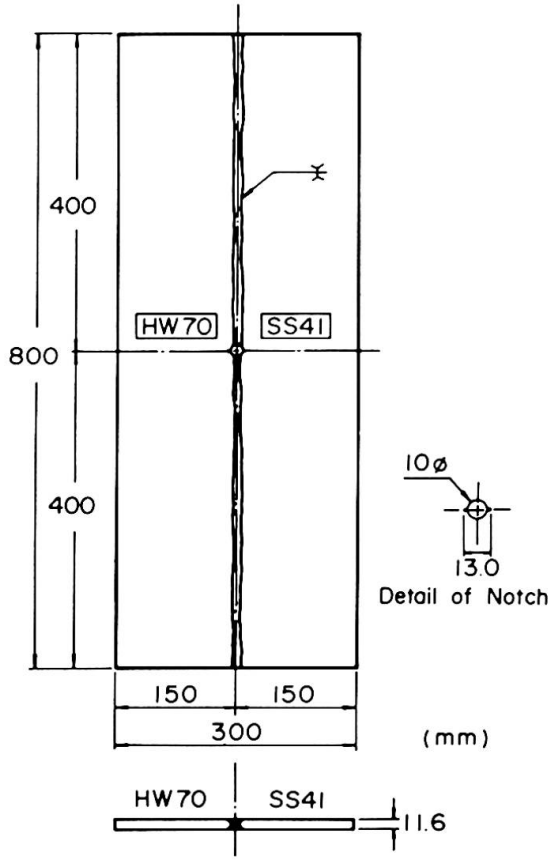

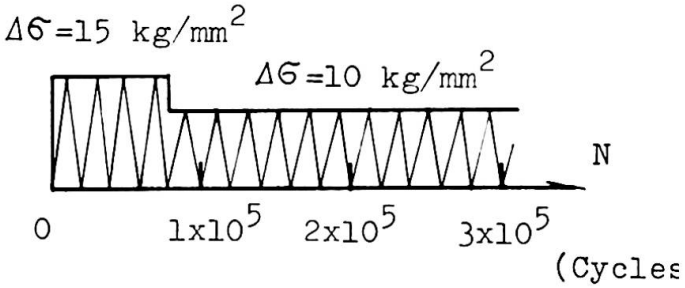

Fig.1 Configuration of Specimen and Stress Sequence

Fig.2 Exposed Fracture Surface

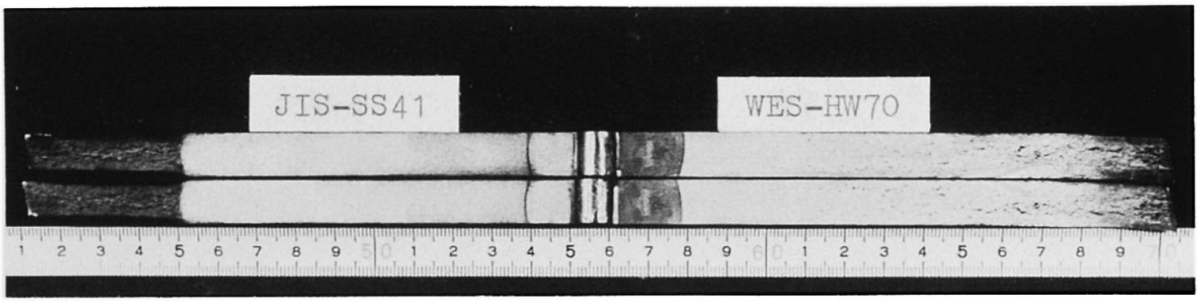

Fatigue crack growth rates, da/dN, in terms of Eq.(1) were shown in Fig.3, and the best fitted line by the method of least squares is also given in comparison with the derived crack-growth relationship given by Fisher et al.(4), a conservative upper bound for growth rates on ferrite-pearlite steels proposed by Barsom(5) and the authors' previous test results(1). The calculated material constants, C and m, were 1.2×10^{-11} and 3.6, respectively, namely the fatigue crack growth rate is numerically represented as

$$\frac{da}{dN} = 1.2\times10^{-11}\times(\Delta K)^{3.6} \qquad (2).$$

3. FATIGUE LIFE PREDICTION

To predict the fatigue lives on the previous hybrid tee-shaped specimens(1), these material constants and the value of K for a disk-like penny shaped crack in infinite body (6),

$$K = \frac{2}{\pi}\sigma\sqrt{\pi a} \quad ,$$

can be used, and the estimated S-N curves are calculated from the integrated version of Eq.(2).

The calculated S-N curves are shown in Fig.4 for various initial crack sizes, a_i, together with the test results on the hybrid tee-shaped specimens. The figure reveals that the predicted S-N curve taking the initial crack size, a_i, as 0.5 mm agrees well with the test results. This crack size of 0.5 mm is the same as the previously assumed one(1).

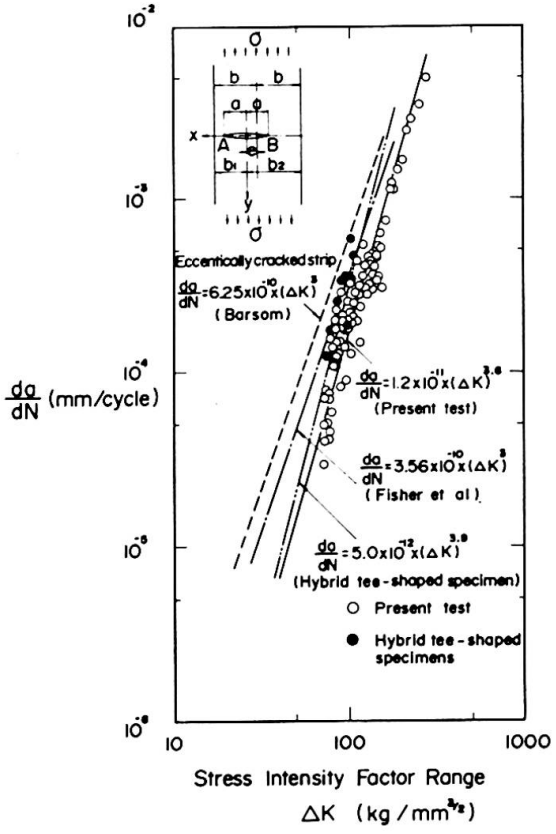

Fig.3 Summary of Fatigue Crack Growth Rate

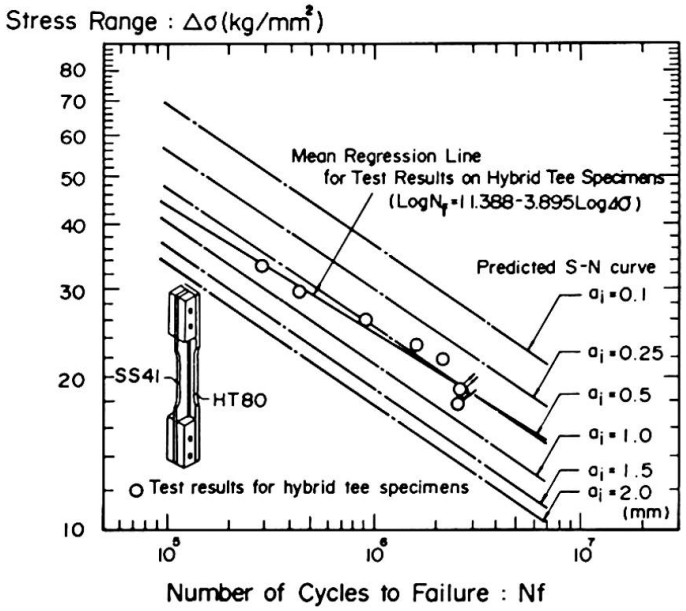

Fig.4 Comparison of Predicted S-N Curves and Previous Fatigue Test Results on Hybrid Tee-shaped Specimen(1)

4. CONCLUDING REMARK

The calculated S-N curve by using fracture mechanics, taking the initial crak size of 0.5 mm, successfully agreed well with the test results. Consequently, the fatigue life prediction method by fracture mechanics approach proved to be an effective tool for also hybrid members, if only a pertinent initial crack size can be evaluated.

REFERENCE

1) T.Yamasaki, M.Hara, Y.Kawai;Preliminary Report, IABSE, 10th Congress, 1976
2) P.C.Paris, F.Erdogan;Trans. of ASME, Series D, Vol.85, No.4, 1963
3) M.Ishida;Trans. of ASME, Series E, Vol.33, No.3, 1966
4) M.A.Hirt, J.W.Fisher;Eng. Frac. Mech., Vol.5, 1973
5) J.M.Barsom;U.S. Steel Corp., Applies Res. Lab. Rpt., 1971
6) I.N.Sneddon;Proc. Royal Soc., London, Vol.A-187, 1946

SUMMARY

A fatigue crack propagation test was conducted on a longitudinally butt welded 'WES-HW70' --'JIS-SS41' hybrid plate specimen to predict fatigue lives of hybrid members. The fatigue crack growth rates obtained were represented as a function of stress intensity factor ranges in the form of the so-called Paris' law. By using the material constants and fracture mechanics approach, the fatigue lives were successfully estimated on the hybrid tee-shaped specimens which were previously tested.

RESUME

La propagation d'une fissure due à la fatigue a été étudiée sur une plaque hybride en WES-HW70/JIS-SS41 soudée bout à bout, afin de prédire la résistance à la fatigue. Le développement de la fissure ainsi obtenue a été représenté en fonction des facteurs de concentration de contraintes, selon la loi dite de Paris. Au moyen des constantes des matériaux et de la mécanique de fissure, on a pu déterminer la résistance à la fatigue d'échantillons en forme de T qui avaient fait auparavant l'objet d'essais.

ZUSAMMENFASSUNG

Die Ausbreitung eines Ermüdungsrisses wurde an einer stumpf geschweissten hybriden Platte aus WES-HW70/JIS-SS41 untersucht, um daraus die Lebensdauer von hybriden Elementen vorhersagen zu können. Die gewonnene Rissausbreitungsgeschwindigkeit wurde in Funktion des Spannungskonzentrationfaktors nach dem sogenannten Paris'schen Gesetz dargestellt. Ausgehend von den Materialkonstanten lieferte die Bruchmechanik eine Vorhersage für die Lebensdauer von T-förmigen hybriden Proben, die vorher experimentell untersucht worden waren.

The Application of J_{IC} Fracture Criterion to the Fracture of Connections in Steel Structures

Application du critère de rupture J_{IC} au comportement à la rupture d'assemblages en construction métallique

Anwendung des Bruchkriterions J_{IC} auf das Bruchverhalten von Verbindungen im Stahlbau

HIROFUMI AOKI
Associate Professor
Yokohama National University
Yokohama, Japan

TADAO NAKAGOMI
Graduate Student
Tokyo Institute of Technology
Tokyo, Japan

1. INTRODUCTION

The criterion based on critical stress intensity factor K_{IC} is applicable to brittle fracture in low stress level, and the design procedure has been satisfactorily established on this account. While, much of our concern is now paid to the fracture in high stress level such as the case of general yielding in the section of members. One of the examples of this kind is the transition fracture of heavy members of framework at room temperature reported by Prof. Ben Kato.[1)]

As one of the nonlinear fracture mechanics, the COD criterion is introduced in the introductory report, and strain around crack tip has been related to crack opening displacement by F.M.Burdekin.[2)] The COD theory, however, reveals to be indefinite in its physical concept when applied to wider yield portion. On the other hand, comprehensible is the physical concept of J_{IC} fracture criterion[3,4)] which is the extension of the concept of energy release rate G to nonlinear region, and because J_{IC} is comparatively insensitive to the scale effect, the specimens to obtain J_{IC} may be made smaller than those for K_{IC}.

In discussing the basic applicability of J_{IC} fracture criterion, J_{IC} value of SM50B(B class) and SM58QT(C class) are obtained from the 3-point bending test at room temperature.

Bending tests are carried out for the specimens of 4 types in various stress distributions,[5)] and the fracture configurations are discussed based on J_{IC} fracture criterion.

2. COMPARISON OF J_{IC} VALUES BETWEEN SM50B AND SM58QT

2.1 Specimens and Experimental Procedure

J_{IC} values are obtained from the 3-point bending test for which specimens are made from steel plates 25mm of SM50B and SM58QT. Chemical composition, mechanical properties and Charpy values of the materials are shown in Table-1~3 respectively.

The shape of the specimens, as shown in Fig.-1, is based on ASTM E399-72 and BS DD-19. All specimens are prepared with

fatigue crack at the tip of the crack. Three kinds of crack length, 23mm, 25mm and 27mm are adopted for the specimens of SM50B. The crack length for the specimen of SM58QT is either 23mm or 25mm.

The bending test is carried out at room temperature(+20°C) and -65°C. Since it is difficult to determine the displacement δ_c experimentally to initiate crack propagation at room temperature, the crack propagation is checked by cutting the specimens in the cource of experiment after J. A. Begley and J. D. Landes.[6]

The value of J integral is obtained approximately from the following equation.

$$J = \frac{2}{Bb}\int_0^{\delta_i} Pd\delta \qquad (1)$$

where, B: Width of the specimen
b: Difference of crack length a from height W
P: Load
δ: Displacement at the loading point

2.2 Test results

Relationships between J value and increment of crack length Δa are shown in Fig.-2 which are lead by P~δ diagrams in the bending test. The results from the experiments on various crack lengths present reasonable J_{IC} values. It is recognized, therefore, that the method proposed by Begley and Landes for determining J_{IC} value should be available.

Fig.-3 shows a comparison of J~Δa relationships between SM50B and SM58QT obtained from the bending test.

In the study by J. R. Rice, et al.[7], J value is calculated for simplified P~δ relationships composed of elastic part and perfectly plastic part beyond general yielding. In this paper, P~δ relations are computed up to the general yield point by applying finite element method. After reaching the general yield point, P~δ relation is assumed as perfectly plastic. Fig.-4 shows the element division of the specimen. Calculated values of J integral are compared with the experimental results in Fig.-5.

It is confirmed that the above method for estimation of J value by calculation should be available.

It is observed in Table-4 that J_{IC} value of SM58QT is considerably smaller than that of SM50B at room temperature. Seeing that J_{IC} value of SM58QT at -65°C is larger than that of SM50B, the difference of J_{IC} values at room temperature should be adequately noted.

3. DISCUSSION CONCERNING THE FRACTURE OF TEE-JOINTS

It is emphasized in the introductory report that the welding condition free of micro cracks and steels possessing enough notch toughness should be substantial to prevent unstable brittle fracture. Further investigation should be focussed on the relations of notch toughness of material and fracture under complex stresses such as connections in steel structure.

Bending tests by using the specimens of 4 types are carried out in various stress states and conditions of test temperature. As shown in Fig.-6, the thickness of the specimens is 25mm and roller span is 280mm.

The specimen of J-type has the ratio of thickness to width 25:35 and this type is a model to expect plane stress. The ratio

Table-1 Chemical Composition (%)

Grade of Steel	C	Si	Mn	P	S	Cu	Cr	Nb	V
SM50B PL25mm	0.16	0.39	1.46	0.014	0.025	0.01	—	—	—
SM50B PL65mm	0.16	0.46	1.45	0.008	0.007	0.31	0.03	0.036	—
SM58QT PL25mm	0.12	0.27	1.11	0.012	0.007	—	0.16	—	0.03

Table-2 Mechanical Properties

Grade of Steel	Y.P.	T.S.	EL.	φ
SM50B PL25mm	41	60		73
SM50B PL65mm	39	56	38	77
SM58QT PL25mm	55	71	30	71

Y.P.: Yield Point (kgf/mm²)
T.S.: Tensile Strength (kg/mm²)
EL.: Elongation (%)
φ: Reduction of Area (%)

Table-3 Charpy Values

Grade of Steel		$_vE_0$	$_vT_{rE}$	$_vT_{rS}$
SM50B PL25mm	Surface	15.1	-6	-7
	(1/2)t	12.5	-12	-10
SM50B PL65mm	Surface	30.0	-67	-65
	(1/2)t	30.0	-52	-54
SM58QT PL25mm		24.0 *		

$_vE_0$: Absorbed energy at 0°C, but * is at -5°C (kgf.m)
$_vE_{rE}$: Energy transition tempetrature (°C)
$_vE_{rS}$: Surface transition temperature (°C)

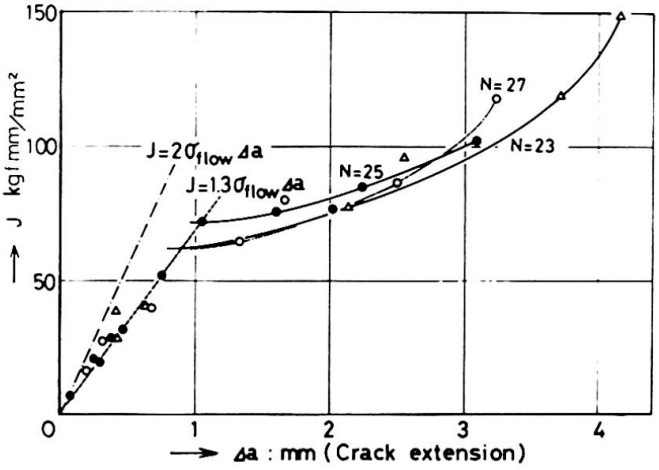

Fig.-2 Relations between J and Δa (SM50B)

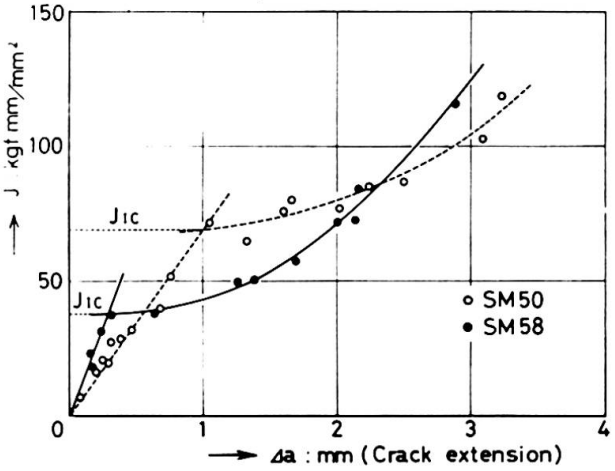

Fig.-3 A comparison of J~Δa relations between SM50B and SM58QT

Table-4 J_{IC} (kgf.mm/mm²) values

Grade of Steel	Test Temperature 15°C	-65°C
SM50B pl25	63	12.8
SM58QT PL25	43	15.1

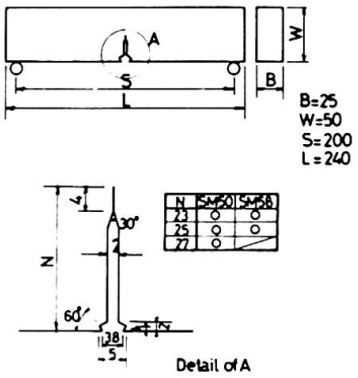

Fig.-1 Specimens for the 3-point bending test

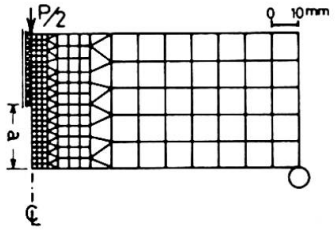

Fig.-4 Element division

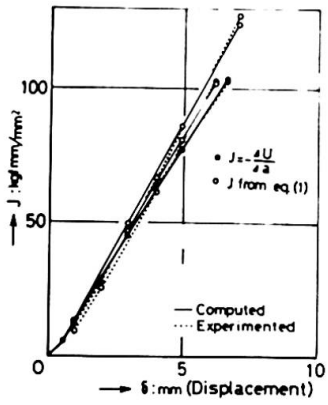

Fig.-5 Relations between J and δ

of M-type is 25:125 to expect plane strain state. B_T-type is made of steel plate 25mm with a Tee-joint where is welded. Tee flange of this type is the same dimension as M-type. The specimen of A_T-type is shaped from steel plate 65mm in order to eliminate the influence of welding. The dimension of A_T-type is same as that of B_T-type except fillet portion. The fillets of A_T and B_T-type are shown in detail in Fig.-7, respectively. The radius r at the toe of fillet in A_T-type specimen is determined to be 2mm in order to approach the same condition as the welded part in B_T-type. B_T specimen is built up by manual welding and stress relief annealing is not treated after welding. A_T and B_T-type are both pull-bend specimens.

The specimens of J-type, M-type and B_T-type are made from the steel plate which is dealt with at the preceding section. The properties of SM50B plate 65mm for A_T-type are also shown in Table-1~3. J_{IC} values for these mother metals and welded portion of the joint are summarized in Table-5.

Fig.-8 shows the relationships between the maximum bending angle θ_{max}(degree) and the test temperature T°C obtained from these bending tests.[4] It is observed in this figure that the more complex the stress state is, the smaller θ_{max} is. Especially, the specimen of B_T-type with welded joint might be the most fragile in these 4 types.

J values of the specimens are estimated by the method described at previous section. Element divisions are shown in Fig.-9.[6] J values are obtained by computing two P~δ relationships of the cases a/W=0 and a/W=2/25. Fig.-10 shows the computed results of P~δ relationships.

J_C value for each specimen which is J value at fracture of the specimen is determined by θ_{max} and P~δ curves. The ratio of J_C to J_{IC} is shown in Table-5.

This result indicates that the more complex the stress distribution of the specimen is, the smaller J_C/J_{IC} is. This ratio comes to almost unit in the case of B_T.

4. Conclusion

J_{IC} values of SM50B and SM58QT both of which are obtained from the 3-point bending test at -65°C are remarkably equal, nevertheless J_{IC} value of SM58QT is approximately 2/3 of that of SM50B at room temperature.

Experimental results from bending tests on various stress states of 4 types specimens indicate that the more complex the stress distribution is, the more fragile the joint of steel structure is. And this phenomenon can be explained by J_{IC} fracture criterion.

Finally, it should be pointed out that the independence of path in J integral is valid only under the deformation theory, and it is not directly applicable to the frames in which stress redistribution may take place significantly. J integral in this paper is introduced beyond limitation in this sence. It is necessary, therefore, to obtain more basic experimental data in order to apply J_{IC} fracture criterion in practice.

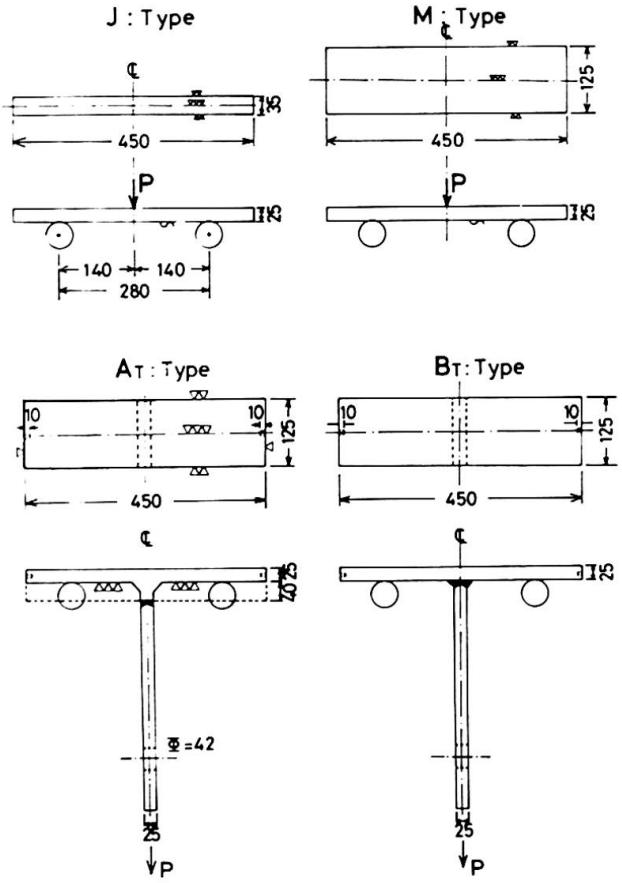

Fig.-6 Specimens of 4-types for bending tests

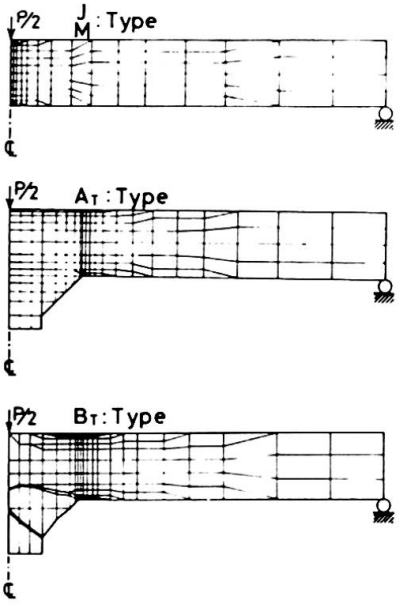

Fig.-9 Element division for 4-type specimens

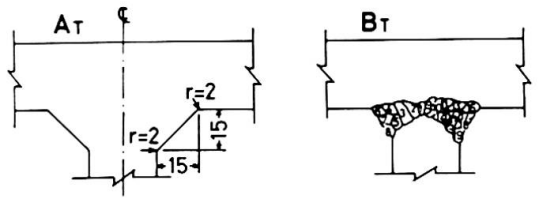

Fig.-7 Details of the fillets

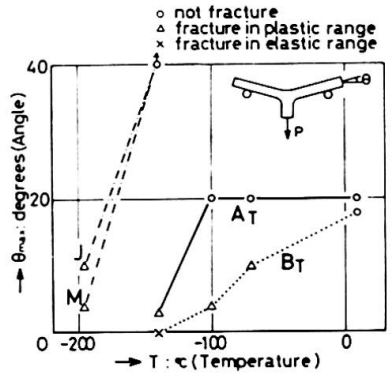

Fig.-8 Test results

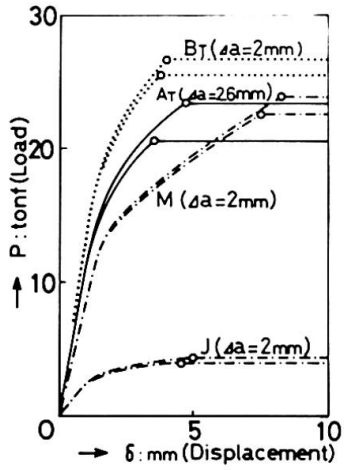

Fig.-10 Computed results

Table-5 J_C Value and the Ratio to J_{IC}

	J-type	M-type	A_T-type	B_T-type
$J_C(\frac{kgf.mm}{mm^2})$	35.46	8.42	143.11	30.38
$J_{IC}(\frac{kgf.mm}{mm^2})$	0.49	0.49	76.24	26.80
J_C/J_{IC}	72.4	17.2	1.88	1.13

5. REFERENCES

1. Kato,B.,Brittle Fracture of Heavy Steel Members,National Conf. on the Planning and Design of Tall Building,Tokyo,August,1973
2. Burdekin,F.M. and Dawes,M.G.,Practical Use of Linear Elastic and Yielding Fracture Mechanics with Particular Reference to Pressure Vessels,Conf. Practical Application of Fracture Mech. to Pressure Vessel Technology,London,May,1971
3. Rice,J.R.,A Path Independence Integral and the Approximate Analysis of Strain Concentration by Notches and Cracks,J.Appl. Mech.June,1968
4. Begley,J.A..and Landes,J.D.,The J Integral as a Fracture Criterion ,ASTM STP 513,1972
5. Fujimoto,M.,Aoki,H.,Nakagomi,T. and Hosozawa,O.,Study on Fracture of Connections in Steel Structure by Nonlinear Fracture Mechanics,Part 1, Trans. of A.I.J.No.238,Dec.1975(in Japanese)
6. Landes,J.D. and Begley,J.A., Test results from J-Integral Studies,an Attempt to Establish a J_{IC} Testing Procedure,ASTM STP 563,1974
7. Bucci,R.J.,Paris,P.C.,Landes,J.D. and Rice,J.R.,J Integral Estimation Procedure,ASTM STP 513,1972
8. Fujimoto,M.,Aoki,H.,Nakagomi,T. and Hosozawa,O.,Study on Fracture of Connections in Steel Structure by Nonlinear Fracture Mechanics,Part 2, Trans. of A.I.J.No.239,Jan.,1976(in Japanese)
9. Aoki,H.,Nakagomi,T. and Ogura,N.,Fracture and Deformation Capacity of Tee Welded Joints by Pull-bend Test,JSSC,Vol.11,No.110, Feb.,1975(in Japanese)

SUMMARY

J_{IC} values are compared between SM50B and SM58QT. Both are remarkably equal at -65° C, nevertheless J_{IC} value of SM58QT is approximately 2/3 of that of SM50B at room temperature. Bending tests on various stress states of 4-types specimens are carried out, and the experimental results indicate that the more complex the stress distribution is, the more fragile the joint of steel structure is. This phenomenon can be explained by J_{IC} fracture criterion.

RESUME

Les valeurs de J_{IC} sont comparées pour les aciers SM50B et SM58QT. Elles sont remarquablement identiques à - 65° C, bien que,à la température ambiante, la valeur J_{IC} du SM58QT ne soit que les 2/3 de celle du SM50B. Des essais de flexion sous différents états de contraintes ont été effectués sur des éprouvettes de 4 types. Les résultats expérimentaux montrent que, plus la distribution de contraintes est complexe, plus les assemblages sont fragiles. Ce phénomène peut être expliqué à l'aide du critère de rupture J_{IC}.

ZUSAMMENFASSUNG

Die J_{IC} Werte werden für die Stähle SM50B und SM58QT verglichen. Beide sind praktisch gleich bei -65° C, obwohl bei Raumtemperatur der J_{IC} Wert des SM58QT nur ungefähr 2/3 des Wertes des SM50B beträgt.Biegeversuche unter verschiedenen Spannungszuständen wurden an Proben mit 4 Ausbildungsformen durchgeführt; die experimentellen Ergebnisse haben gezeigt, dass die Gefahr eines Sprödbruches bei Stahlbauverbindungen mit der Komplexität der Spannungsverteilung zunimmt. Dieses Verhalten wird mit dem Bruchkriterium J_{IC} erklärt.

Further Studies on Composite Beams with Formed Steel Deck

Etudes complémentaires sur des poutres mixtes à platelage métallique

Weitere Untersuchungen über Verbundträger mit Stahlblechdecken

JOHN W. FISHER
Professor of Civil Engineering

JOHN A. GRANT
Research Assistant

Fritz Engineering Laboratory, Lehigh University
Bethlehem, Pennsylvania, U.S.A.

After publication of our paper in the Preliminary Report, Tenth Congress IABSE (1), additional tests were undertaken on composite beams with 3 in. (76 mm) formed steel deck with a w/h ratio equal or greater than 2.0 In addition, it was desirable to provide further experimental data on shear connectors with an increased embedment length above the rib. In the study reported in Ref. 1, most stud shear connectors were embedded 1½ in. (38 mm) above the rib (H - h). In the additional beam tests, all connectors were embedded 2 in. (50.8 mm) above the rib in order to optimize the shear connector resistance. The rib geometry provided w/h ratios of 2 and 2.42.

As a result of the additional beam tests, the shear connector resistance was re-evaluated and a slight modification suggested by Lim (2) was introduced into Eq. 2 of the preliminary report. It was found that replacing the coefficient 0.6 with $0.85/\sqrt{N}$ provided a better fit to the test data with single connectors in a rib, as well as providing for more than two connectors in a rib. This results in the expression:

$$Q_{rib} = \frac{0.85}{\sqrt{N}} \cdot \frac{H - h}{h} \cdot \frac{w}{h} \cdot Q_{sol} \leq Q_{sol} \qquad (1)$$

where N = number of shear connectors placed in a rib. The parameters w, h and H were defined previously (w = average rib width, h = height of rib, H = height of stud shear connector) and Q_{sol} is the connector strength in a solid slab.

Figure 1 shows the 56 beam tests results summarized in Fig. 4 of Ref. 1 as well as 19 additional beam tests including one test with three connectors per rib. The plot shows that Eq. 1 provides a good estimate of flexural capacity for 1, 2 or 3 connectors in a rib. Pushoff tests summarized in Ref. 3 indicate the same type of change in connector capacity with varying numbers of shear connectors in a rib. Equation 1 provides the same connector capacity as Eq. 2 in the preliminary report when two connectors are placed in a rib. For a single connector a higher capacity results which approaches the solid slab value for longer embeddment lengths.

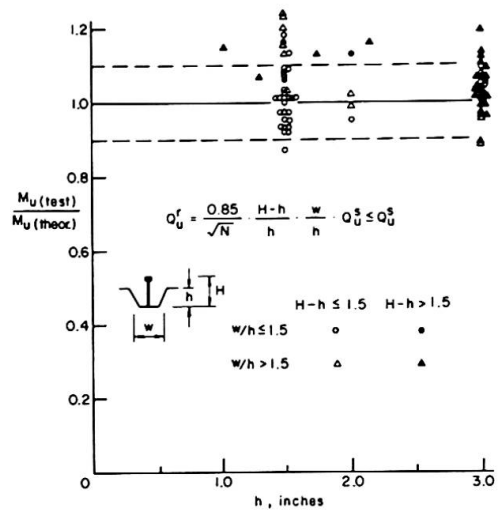

Fig. 1

In the Preliminary Report, Eq. 4 was incorrectly shown. It was intended to be expressed as:

$$I_{eff} = I_s + \sqrt{\frac{V'h}{Vh}} (I_{tr} - I_s) \quad (2)$$

The shear connection ratio was missing its exponent in the Preliminary Report.

All additional tests verified the applicability of Eqs. 1 and 2 to composite beams with formed steel deck, including deck with larger w/h ratios.

REFERENCES

1. Grant, J. A., Fisher, J. W. and Slutter, R. G., High Strength Steel Composite Beams with Formed Steel Deck, Preliminary Report, Tenth Congress, IABSE, Tokyo, 1976.
2. Lim, L. C., Private Correspondence, April 28, 1976.
3. Iyengar, S. H. and Zils, J. J., Composite Floor System for Sears Tower, AISC Engineering Journal, American Institute of Steel Construction, Vol. 10, No. 3, 1973.

SUMMARY

Additional tests on composite beams with formed steel deck verified that the w/h ratio could be extended beyond 2. A modification to the expression developed for shear connection capacity was found to provide for differing numbers of shear connectors installed in a rib.

RESUME

Des essais complémentaires sur des poutres mixtes avec platelage métallique ont montré que le rapport w/h (largeur de la nervure/hauteur de la nervure) peut être étendu au-delà de 2. Une modification de l'expression développée pour la résistance des connecteurs a permis de tenir compte du nombre de connecteurs par nervure.

ZUSAMMENFASSUNG

Zusätzliche Versuche an Verbundträgern mit Stahlblechdecken zeigten, dass das w/h Verhältnis (Rippenbreite/Rippenhöhe) über 2 hinaus vergrössert werden darf. Eine Erweiterung des Ausdruckes für die Dübeltragfähigkeit, die die Anzahl der Dübel pro Rippe berücksichtigt, ist gefunden worden.

The Ultimate Load of Monosymmetric Sections due to Lateral Torsional Buckling

Calcul de la charge ultime de sections monosymétriques en tenant compte du déversement

Traglasten von einfach-symmetrischen Profilen unter Berücksichtigung des Kippens

JOACHIM LINDNER
o. Prof. Dr.-Ing.
Technische Universität Berlin
Berlin, BRD

1. INTRODUCTION

Structural members loaded by transverse loads and moments acting in the plane of greatest stiffness may also twist and deform laterally as shown in fig.1. The most general case includes initial imperfections of a bar or eccentricities of the loads and inelastic material behaviour, fig.2.

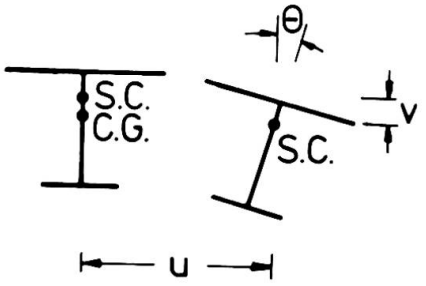

fig.1

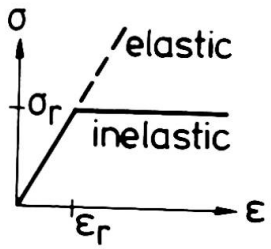

fig.2

Solutions for this problem of lateral torsional buckling are well known for the elastic behaviour, including monosymmetric sections. For inelastic material behaviour solutions are known only recently ([1] - [6]), most of them for double symmetrical sections. For monosymmetric sections only single results are known ([2], [4]).

2. THEORETICAL SOLUTION

The used theoretical solution is an approach for the inelastic material behaviour. It takes into consideration the elastic-plastic stress-strain relationship (fig.2), the spread of the plastic zones in the longitudinal direction of the beam-column, residual stresses and the alteration of the position of the shear centre due to plastification.

At first there is investigated a solution using the theory of elasticity. If the greatest stress in the most unfavourable fibre of the section exceeds the yield stress, this must be taken into account by iteration. Thus the spread of plastification in the section, the alteration of deformations and twist are considered. The ultimate strength is reached when equilibrium between external and internal forces is no longer possible.

This solution is described properly in literature ([2], [3], [4], [7]).

	St 37 σ_y=240 N/mm²	StE 70 σ_y=700 N/mm²
780·8 — 500·20 / 400·15 [mm]	1769	5159
780·8 — 400·20 / 400·20 [mm]	1828	5331

Table 1: Full plastic moments [kNm]

3. RESULTS

For getting numerical results, there are investigated a monosymmetric and a double symmetrical section with equal area and height. The loading is assumed as concentrated load, because the most unfavourable case of constant end moments are seldom given in practical members. The level of application of the load is the upper flange. The end conditions correspond to simple support in the lateral plane. This means that lateral deflection and twist are prevented but no resistence is provided against either lateral bending or warping.

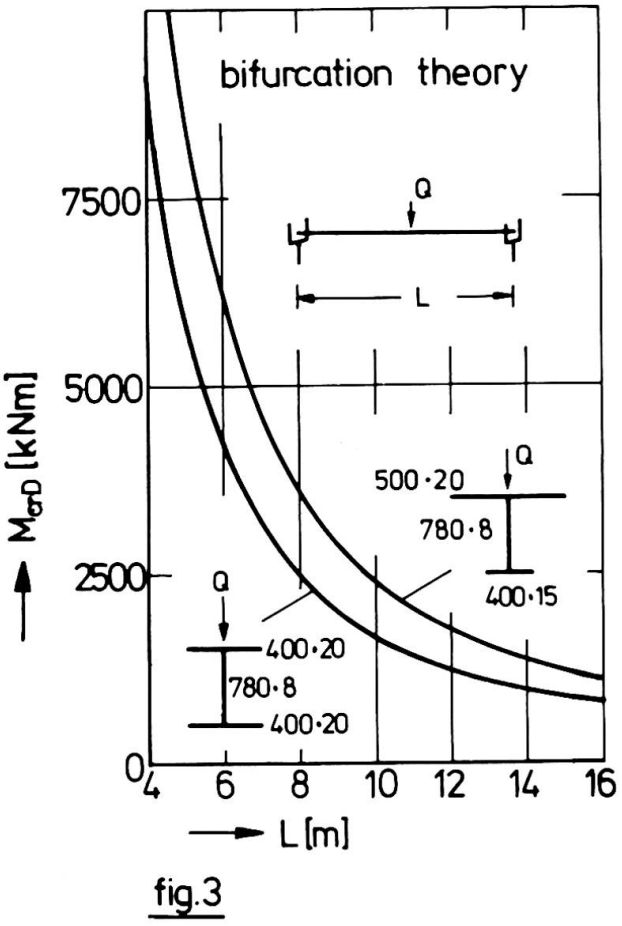

fig.3

The greatest capacity of the section is given by the full plastic moment, [8]. The results are given in table 1. It is seen, that the symmetric section gives the greater maximum capacity, but the difference does not exceed 3%.

The monosymmetric section is the better one, if the bifurcation theory is used (fig.3). The reason is, that the compression flange, which may buckle, get a greater area, the center of gravity and the shear center have a smaller distance to the compression flange and therefore it is clear, that the critical load increases. The differences amount to 45% related to the double symmetrical section.

The ultimate load carrying capacity is seen in fig.4. In addition mild steel St 37 and high strength steel StE 70 are compared. They are drawn in a nondimensional way. The parameters are M/M_{Pl} and $\bar{\lambda}$. M is the given moment of the beam, taking into account the load enhancement factor. M_{Pl} means the full plastic moment (table 1). The value of $\bar{\lambda}$ depends on the yield stress and the critical moment due to lateral torsional buckling. For each length of the beam $\bar{\lambda}$ can be calculated using table 1 and fig.3.

The value of the residual stresses was chosen to a maximum compression value of $\sigma_{rc} \cong 120$ N/mm².

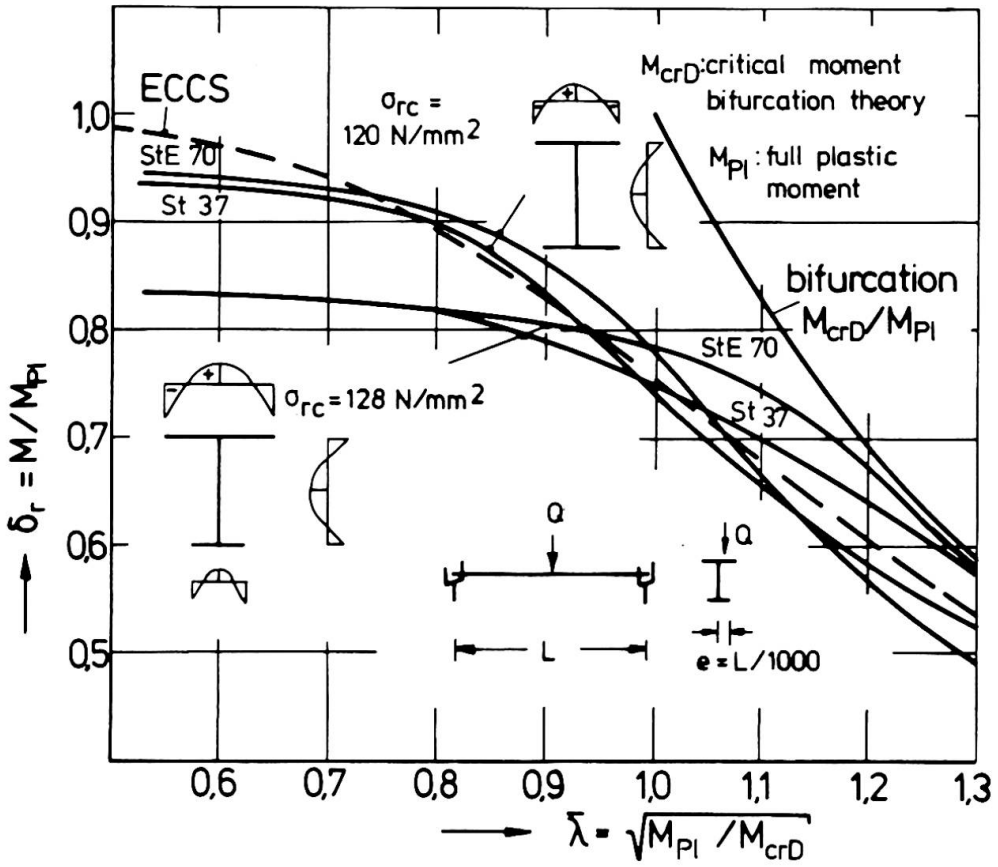

fig.4: Utimate load carrying capacity

That means for steel St 37 50% of the nominal yield stress. Even for the high strength steel StE 70 the same value for the residual stresses was chosen.

Some interesting results are seen in fig.4. It is seen, that for small values $\bar{\lambda} \lesssim 1{,}0$, that means small values L of the length, the ultimate load of the monosymmetric section lies significantly below that of the double symmetrical section. In the region of $\bar{\lambda} \gtrsim 1{,}0$ it is contrary, but the differences are a great deal smaller. The differences between St 37 and StE 70 are small, they exceed not more than 8%.

The curves for the double symmetrical section give a satisfying agreement to the new ECCS-curve [9], which should be valid only for double symmetrical sections. For the monosymmetric section the ECCS-curve may be used for $\bar{\lambda} > 1{,}0$.

In addition a comparison is made to the elastic theory of second order. This theory is usually used if there is no possibility to calculate the real ultimate strength. Using this theory the assumption is made that the load carrying capacity is reached when at the most unfavourable point of the beam the yield stress σ_y is reached.

In the present case there are 3 types of normal stresses taken into account. These stresses are originated from moments about the strong axis, moments about the weak axis and warping moments.

The used calculation method is the energy method. The computer program was kindly given by D.BAMM, it is similar to these discribed in [3], [4].

The results are given in fig.5. It is seen that the shape of the curves is similar using the ultimate strength method or the elastic second order theory.

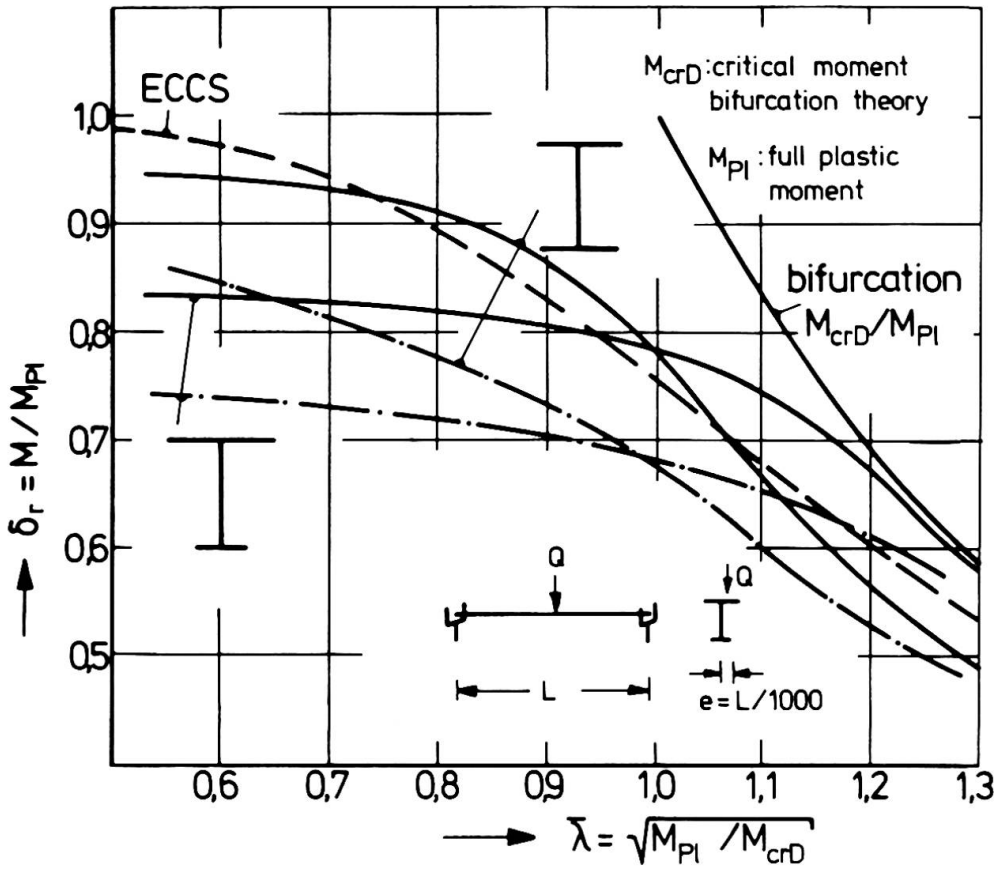

fig.5: load carrying capacity StE 70
—— ultimate strength
—·— second order theory, $\sigma_{cr} = \sigma_y$

But in the whole region of $\bar{\lambda}$ is a great reserve from reaching the yield stress at the most unfavourable point to the load carrying capacity, where the cross section is partly yielded.

Therefore from the economical point of view it is usefull to use the ultimate strength method or as an approximation using the method given in [6].

4. REFERENCES

[1] Galambos,T.V.: Inelastic Lateral Buckling of Beams. Journal of the Struct.Div., Proc. ASCE, Vol.89, No.St 5, Oct. 1963, p.217.

[2] Lindner,J.: Näherungsweise Ermittlung der Traglasten von auf Biegung und Torsion beanspruchten Stäben. Dissertation TU Berlin 1970. Auszug in: Die Bautechnik 48(1971), H.5, S.160-170.

[3] Lindner,J.: Der Einfluß von Eigenspannungen auf die Traglast von I-Trägern. Habilitationsschrift. Berlin 1972. Auszug in: Der Stahlbau 43(1974), H.2, S.39-45, H.3, S.86-91.

[4] Bamm,D.: Näherungsweise Berücksichtigung der Schubspannungen bei der Ermittlung von Traglasten gerader dünnwandiger offener Profile. Diss. TU Berlin, 1974.

[5] Vinnakota,S.: Inelastic stability of laterally unsupported I-beams. Symposium on structural analysis, Washington D.C., 1976.

[6] Unger,B.: Einige Überlegungen zur Zuschärfung der Traglastberechnung... Der Stahlbau 44(1975), H.11, S.330-335, H.12, S.367-373.

[7] Lindner,J.: Theoretical Investigations of Columns under Biaxial Loading. Proc. Joint CRE-ECCS-IABSE Colloquium on Column Strength, Paris 1972, p.182.

[8] Roik,K., Lindner,J.: Einführung in die Berechnung nach dem Traglastverfahren. Stahlbau Verlags GmbH, 1972, Neudruck 1976.

[9] ECCS Manual on Stability. Chapter 5 Lateral Supported and Unsupported Beams. Paris 1976.

SUMMARY

The paper deals with the load carrying capacity of monosymmetric sections taking into account lateral torsional buckling. Numerical results are calculated for a double symmetrical and a mono symmetrical cross section with equal height and area. From the results is seen, that the ultimate load of the monosymmetric cross section is smaller than that of the doublesymmetric cross section. The ECCS recommendation curve should only be used for monosymmetric cross-sections, if the length of the bar is great.

RESUME

L'article traite de la résistance ultime de sections monosymétriques en tenant compte du déversement. Des résultats numériques sont calculés pour des profils à symétrie double ou simple ayant des hauteurs et des surfaces égales. Les résultats montrent que la résistance ultime du profil monosymétrique dans le domaine plastique est inférieure à celle du profil à symétrie double. Pour des sections monosymétriques, les courbes des recommendations CECM ne doivent être appliquées que lorsque l'élancement est grand.

ZUSAMMENFASSUNG

Der Beitrag beschäftigt sich mit der Traglast von einfach-symmetrischen Profilen im Hinblick auf das Stabilitätsproblem des Kippens. Zahlenmässige Ergebnisse werden für ein doppelt-symmetrisches Profil und ein einfach-symmetrisches Profil mit gleicher Höhe und Fläche angegeben. Aus den Ergebnissen ist zu ersehen, dass im plastischen Bereich die Traglast des einfach-symmetrischen Profils unter der des doppelt-symmetrischen liegt. Die Bemessungskurve der EKS-Empfehlungen darf für einfach-symmetrische Profile nur benutzt werden, wenn die Stablänge gross ist.

Leere Seite
Blank page
Page vide

Utilisation d'aciers à haute résistance dans quelques ponts mixtes suisses

Verwendung hochfester Stähle im schweizerischen Verbundbrückenbau

Application of High-Strength Steels in some Swiss Composite Bridges

PIERRE DUBAS
Professeur à l'Ecole Polytechnique Fédérale
Zurich, Suisse

1. Introduction

La réalisation du réseau des routes nationales suisses a entraîné, ces dernières années, la construction de nombreux ponts mixtes acier-béton. Une vingtaine d'entre eux comportent des tronçons en acier à haute résistance, la plus grande partie de l'ouvrage étant cependant exécutée en acier E 36[1)], c'est-à-dire dans la nuance la plus répandue pour les ponts-routes européens. Dans le cadre du septième congrès de l'AIPC [1] nous avions eu l'occasion de présenter deux des premières applications des aciers spéciaux. Entretemps, cette technique s'est largement répandue et il nous a paru utile d'exposer brièvement les réflexions faites dans le cadre des études et les conclusions principales découlant des expériences acquises lors de la fabrication et du montage des ouvrages.

2. Caractéristiques des aciers à haute résistance utilisés

Comme l'illustre (Fig. 1) la répartition des matières du pont sur la Veveyse, avec une travée latérale de 111 m imposée par les conditions géotechniques et une travée centrale atteignant 129 m, c'est uniquement le tronçon sur la pile située à la jonction des deux portées précitées, tronçon hautement sollicité à la flexion et au cisaillement, qui est prévu en acier à haute résistance.

Cette région est de plus caractérisée par un rapport assez faible entre les contraintes dues aux surcharges, pratiquement déterminantes pour la fatigue, et celles dues au poids mort et aux charges permanentes. On sait en effet [2] que la résistance à la

---

1) Le sigle E 36 désigne un acier à 36 kg/mm^2 de limite élastique, avec une résistance à la rupture d'au moins 52 kg/mm^2. Cette notation est utilisée par exemple dans les recommandations allemandes "Stahl-Eisen-Werkstoffblatt 089 - 70; Schweissbare Feinkornbaustähle; Gütevorschriften" ainsi que "DASt-Richtlinie 011; Anwendung der hochfesten schweissgeeigneten Feinkornbaustähle St E 47 und St E 70 für Stahlbauten mit vorwiegend ruhender Belastung (Ausgabe 1.74)"

fatigue des constructions soudées dépend principalement de la variation des contraintes $\Delta\sigma$ et que celle des éléments en acier à haute résistance est en première approximation la même que pour l'acier doux. Les micro-fissures inévitables ainsi que les effets d'entaille même modérés empêchent en effet de réaliser le gain de résistance que montrent les essais d'endurance sur barreaux polis. Dans les régions à valeurs $\Delta\sigma$ faibles, cette caractéristique en soi défavorable des aciers à haute résistance ne pose pas de problèmes, la limite élastique - et non la résistance à la fatigue - étant le facteur déterminant pour le dimensionnement. Dans les ponts-rails par contre, où la fatigue joue le premier rôle même dans la région des piles, l'acier à haute résistance n'offrira en général pas d'avantages par rapport à l'acier E 36.

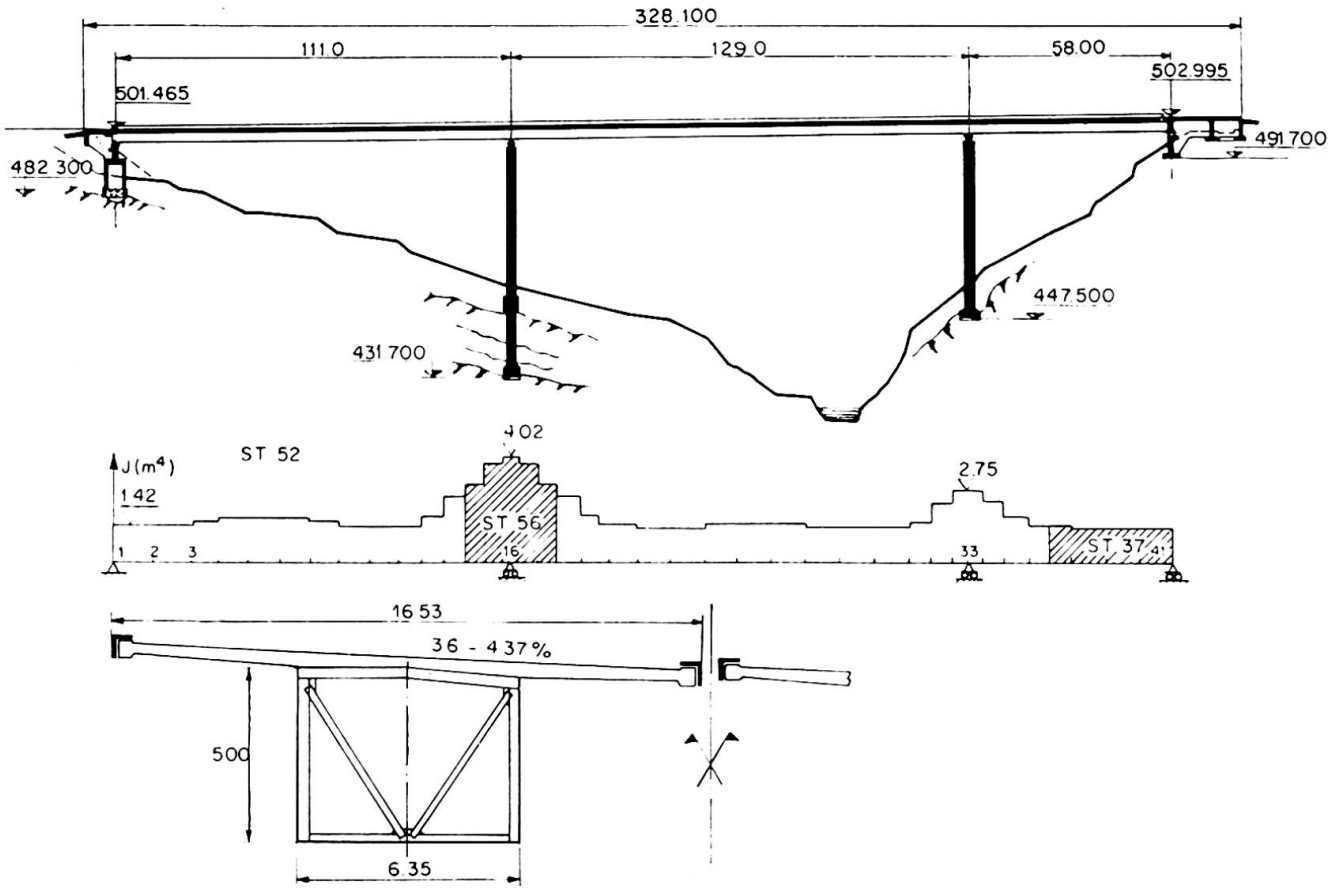

FIGURE 1
Ensemble et section de principe du pont sur la Veveyse

Les aciers à haute résistance utilisés dans les ponts-routes suisses sont généralement du type à résistance naturelle, obtenue comme l'indique le tableau I par des éléments d'alliage appropriés, spécialement des liaisons azotées de nickel ou de vanadium sous forme de dispersoïdes bloquant les glissements cristallins. Ces aciers sont livrés à l'état normalisé grains fins et possèdent une excellente ductilité, contrôlée tant par des essais de résilience que par des pliages Kommerell pour les fortes épaisseurs.

TABLEAU I
Acier à haute résistance E 43 utilisé au viaduc de Bergbach (SG)

Aciérie: AG der Dillinger Hüttenwerke, nuance Dillinal 55/43

COMPOSITION CHIMIQUE (analyse des coulées, en %)

C	Si	Mn	P	S	Ni	V
≤ 0,18	0,10÷0,50	1,0÷1,7	≤ 0,035	≤ 0,035	≤ 0,7	0,10÷0,18

CARACTERISTIQUES MECANIQUES

Limite élastique garantie	≥ 43 kg/mm^2 (≤ 16 mm)
Limite élastique effective	43,6 ÷ 51,7 (t = 16 mm)
(réception en aciérie)	40,7 ÷ 49,2 (t = 62 mm)
Résilience ISO-V, état de livraison (en long)	≥ 5 kg·m/cm^2 à -20° C

La mise en oeuvre de ces aciers en atelier requiert bien entendu les précautions d'usage pour les matériaux à carbone équivalent élevé, en particulier un préchauffage à 80° ÷ 200°, selon l'épaisseur, pour éviter la trempe que provoquerait un refroidissement trop rapide après le soudage ou même après l'oxycoupage. Les procédés opératoires et l'ampleur des contrôles doivent de plus être adaptés à la nuance d'acier choisie, généralement E 43 ou même E 47 à l'heure actuelle, ainsi qu'aux épaisseurs à mettre en oeuvre.

Nous ne saurions ici entrer dans les détails des spécifications adoptées: celles-ci dépendent en partie de l'équipement des ateliers et de l'appareillage de soudage utilisé. On indiquera cependant que les difficultés de fabrication sont légèrement supérieures à celles des ouvrages en acier classique E 36 mais bien inférieures à celles rencontrées pour la mise en oeuvre des aciers trempés et revenus du genre E 70, souvent utilisés en chaudronnerie lourde.

3. Avantages et inconvénients des aciers à haute résistance

On peut se demander quelles raisons parlent en faveur des aciers à haute résistance mentionnés. Nous pouvons éliminer immédiatement le gain de poids puisqu'il s'agit, d'une part, de portées modérées et, d'autre part, des tronçons sur piles dont le poids passe pratiquement directement dans les appuis. Des comparaisons faites sur des ouvrages réalisés ou simplement projetés montrent de plus que le tonnage d'un pont mixte dépend avant tout des choix constructifs et en particulier de l'espacement transversal des poutres[2]; le poids propre de l'ossa-

2) Pour des ponts-routes mixtes comportant deux poutres sous une chaussée large de 15 m au maximum, l'auteur a proposé [3] la formule linéaire $g = 10 + 2\,\ell_m$ pour une première approximation du kilotage d'acier g par m^2 de chaussée en fonction de la portée moyenne $\ell_m = \Sigma\ell_i^2/\Sigma\ell_i$ d'une poutre continue. Une extension de cette relation à des ponts mixtes très larges, mais ne possédant toujours que deux poutres maîtresses a montré [4] que l'on pouvait réduire à 1,5 le multiplicateur de ℓ_m.

ture est de toutes façons faible par rapport à celui de la dalle de couverture et de son tapis bitumineux, de sorte qu'une réduction du poids mort reste pratiquement sans influence sur les sollicitations totales.

L'économie sur le prix des matériaux n'est pas déterminante non plus: le prix relatif des aciers à haute résistance considérés, E 39 ou E 43, c'est-à-dire le prix unitaire rapporté à la limite élastique avec une valeur prise arbitrairement à 100 % pour l'acier doux, est en effet pratiquement égal à celui de l'acier classique E 36 (Fig. 2). Seul l'acier E 70 serait plus avantageux de ce point de vue; il requiert toutefois, comme indiqué plus haut, des précautions coûteuses lors de la fabrication.

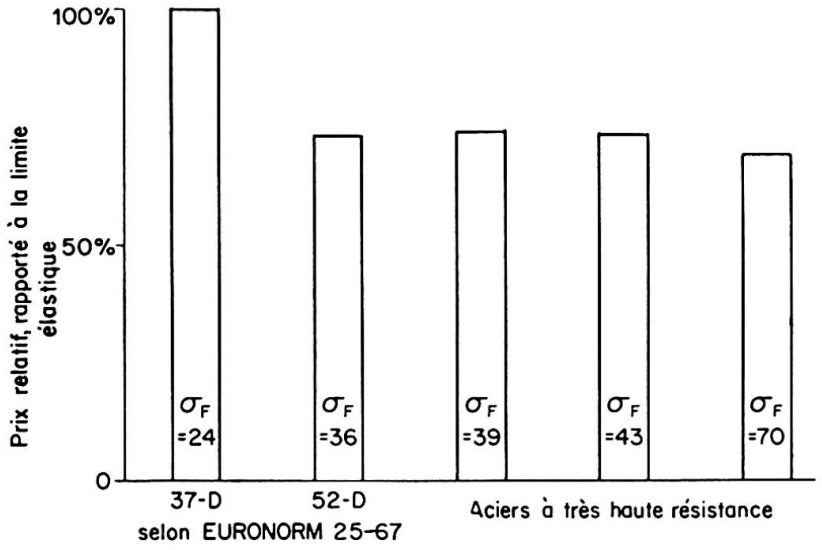

FIGURE 2 - Comparaison du prix relatif de divers aciers

La limite élastique ou, si l'on préfère, les contraintes admissibles sont plus élevées et permettent dès lors de réduire la section des semelles, par exemple de 20 % lorsque l'on passe de l'acier E 36 à E 43. Même dans les régions très sollicitées, une semelle unique est ainsi possible (Fig. 3), de largeur et d'épaisseur permettant une fabrication à la fois aisée et économique (réduction du nombre de cordons longitudinaux) sans poser de problèmes de stabilité en service. L'épaisseur des âmes sera réduite en proportion, ceci au moins dans la région des piles où se limite, comme indiqué précédemment, l'emploi d'aciers à haute résistance; dans cette zone, en effet, l'âme doit être assez épaisse pour reprendre les efforts tranchants très élevés et la stabilité au voilement n'est pas déterminante comme cela serait le cas en travée.

Pour une poutre mixte, la réduction de l'aire des sections diminue de plus les tractions parasites dans le béton dues au retrait empêché. De même, lorsque la dalle est mise en précontrainte par dénivellation d'appuis ou par des câbles pour diminuer le risque de fissuration sur piles, les pertes de précompression seront plus faibles, c'est-à-dire que le rendement sera plus élevé.

On ne dispose pas encore en Europe d'aciers patinables à haute résistance, c'est-à-dire avec des limites élastiques supérieures à

celle de l'acier E 36. Ce fait est regrettable puisque les aciers patinables offrent des avantages certains dans l'entretien des ponts. Espérons que les progrès de la métallurgie permettront sous peu de remédier à cet inconvénient qui risquerait de freiner l'extension de l'utilisation des aciers à haute résistance.

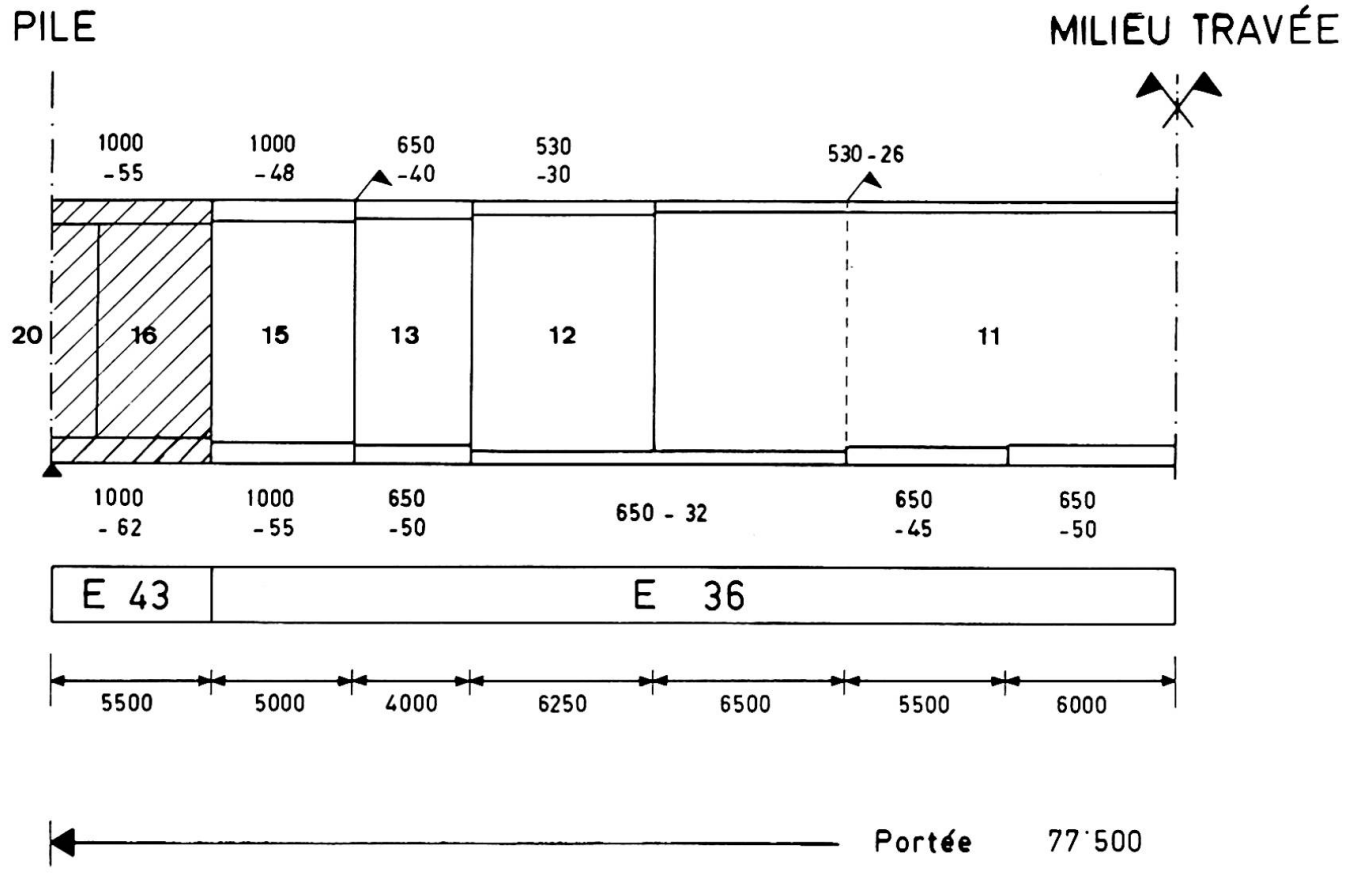

FIGURE 3 - Viaduc de Bergbach (SG): répartition des matières dans les travées centrales

4. Particularités de la mise en oeuvre

On mentionnera pour conclure certaines particularités de la mise en oeuvre en atelier et au montage. L'utilisation de l'acier à haute résistance étant réservée aux tronçons sur piles, les semelles correspondantes ne comportent généralement pas de joints intermédiaires et les cordons de soudure transversaux à leurs extrémités concernent des épaisseurs déjà plus faibles (voir Fig. 3 plus haut).

Les ponts dont nous nous occupons ont été montés par lancement; l'assemblage se fait dès lors au sol dans des conditions favorables. On soudera même durant l'hiver (Fig. 4) en prenant les précautions d'usage comme cabines de protection, etc. Pour l'ouvrage visible sur la figure, on a utilisé le soudage sous CO_2 avec fil fourré de flux aggloméré basique.

Le lancement sur la travée latérale de 111 m (Fig. 5) a tout au moins prouvé que les soudures présentent une excellente résistance à des sollicitations statiques très élevées!

FIGURE 4
Pont sur la Veveyse. Assemblage au sol avant lancement.

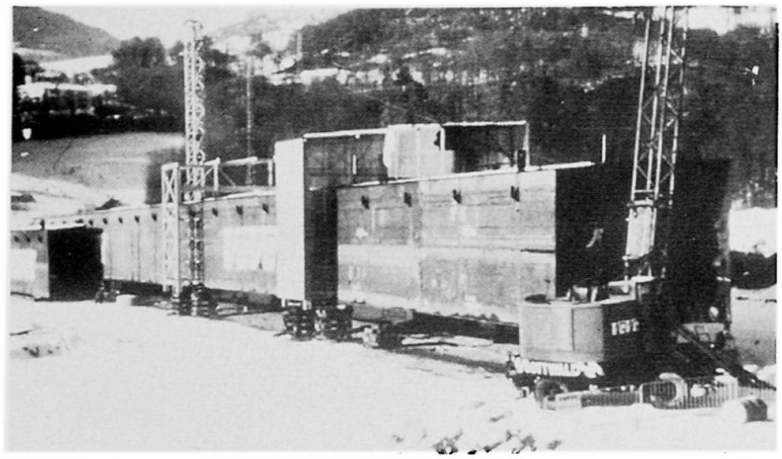

FIGURE 5 →
Pont sur la Veveyse. Ouvrage à la fin du lancement; rayon de courbure en plan 907 m.

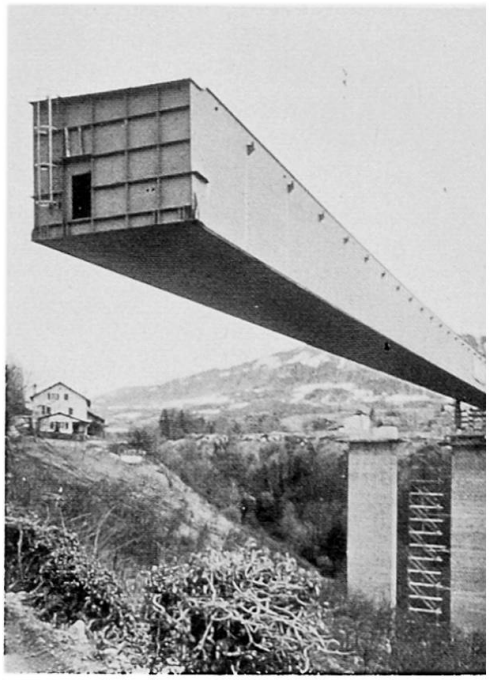

Références bibliographiques

[1] P. Dubas: Utilisation d'aciers à haute résistance dans deux ouvrages suisses. Rapport Final du septième congrès de l'AIPC, Rio de Janeiro 1964, p. 161.

[2] J.W. Fisher, K.H. Frank, M.A. Hirt, B.M. McNamee: Effect of Weldments on the Fatigue Strength of Steel Beams, NCHRP Report No. 102, Highway Research Board, Washington D.C., 1970.

[3] P. Dubas: Développements suisses récents en matière de ponts mixtes acier-béton. Costruzioni metalliche, 1969, p. 11.

[4] J. Pétignat, H.G. Dauner: Evolution dans la conception et la construction des ponts mixtes acier-béton en Suisse. Schweiz. Bauzeitung, 1974, S. 89.

RESUME

On présente quelques exemples d'utilisation d'aciers à haute résistance dans la région des piles de ponts-routes mixtes continus. On expose les avantages résultant de l'emploi de ces aciers et les particularités de mise en oeuvre.

ZUSAMMENFASSUNG

Es werden einige Beispiele der Verwendung hochfester Stähle im Stützenbereich durchlaufender Verbundstrassenbrücken dargestellt. Neben einer Beschreibung der Besonderheiten der Verarbeitungsverfahren erwähnt man auch die Vorteile, die sich aus der Anwendung dieser Stähle ergeben.

SUMMARY

Some examples are given of the use of high strength steels in the support regions of continuous composite highway bridges. The advantages resulting from the use of those steels are outlined and the particularities of the fabrication methods described.

Steel Bridge Decks Realized with Corrugated Plates and Plane Sheets Connected by High Strength Bolts

Tabliers de pont métallique réalisés au moyen de tôles pliées et planes reliées par des boulons à haute résistance

Stählerne Fahrbahntafeln aus mit hochfesten Schrauben verbundenen kaltgeformten und ebenen Blechen

GIULIO CERADINI
Professor of Strength of Materials
University of Rome
Rome, Italy

MARIO P. PETRANGELI
Assoc. Professor of Bridge Construction
University of L'Aquila
L'Aquila, Italy

Introduction

The results of an experimental research on a model of steel orthotropic bridge deck are here briefly summarized.

Tests were performed in the University of Rome in collaboration with the Italsider society during the years 1973-75.

The model, scale 1:2, was made by an upper plane sheet connected by high strength bolts to a botton folded sheet, the resulting deck being similar to an orthotropic plate with closed ribs (fig. 1 2 and 3).

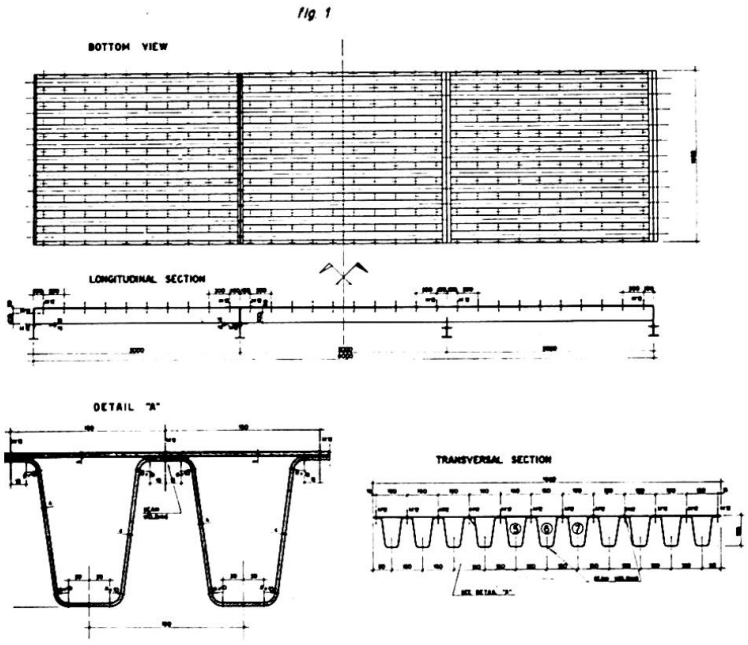

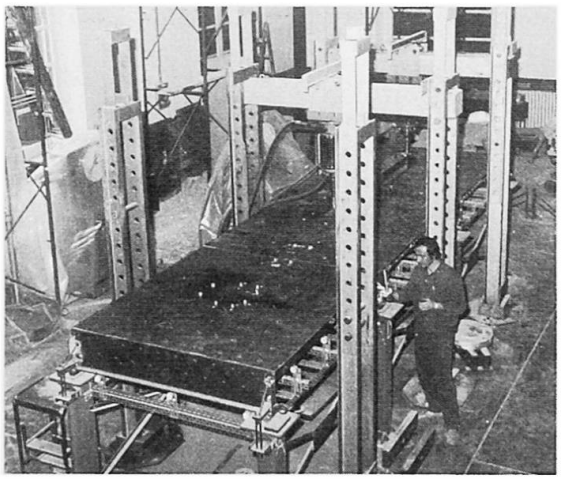

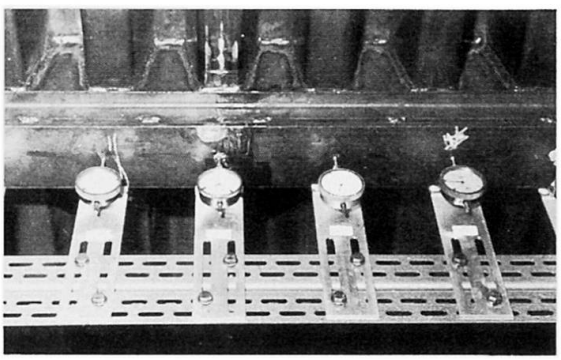

In such a type of deck weldings are almost completely eliminated, with reduction of costs expecially when highyield strength steels are employed.

This type of deck could be adopted also in civil or industrial buildings where heavy liwe loads must be carried with limitation on permanent loads.

Tests in the elastic range

Static tests in the elastic range have been performed by loading the plate in a number of points with two types of load. One acting on a small area simulated the action of a truck wheel; load acting on a large area represented the action of coupled wheels.

By making use of mechanical devices, the absolute displacements of the plate and tre relative displacement between bolts and sheet have been meastured. Strains have been measured by means of electrical strain gages.

From the several tests performed the following conclusions can be drawn:

a) the connection of flat sheet and corrugated sheet by means of high strength bolts is reliable due to the fact thet relative displacements have not been noticed and the behaviour exhibited by the model has been nearly linear.

b) the torsional rigidity of this deck type is small and similar to the one of orthotropic plates with open ribs. Fig. 4 compares the values of stresses meaured at midspan of ribs and the corresponding theoretical values furnished by the Pelikan-Esslinger method for several values of the relative stiffness. A good agreement is achieved for values of x as little as 0.2. This effect is seemingly due to the shape loss of the bottom corrugated sheet.

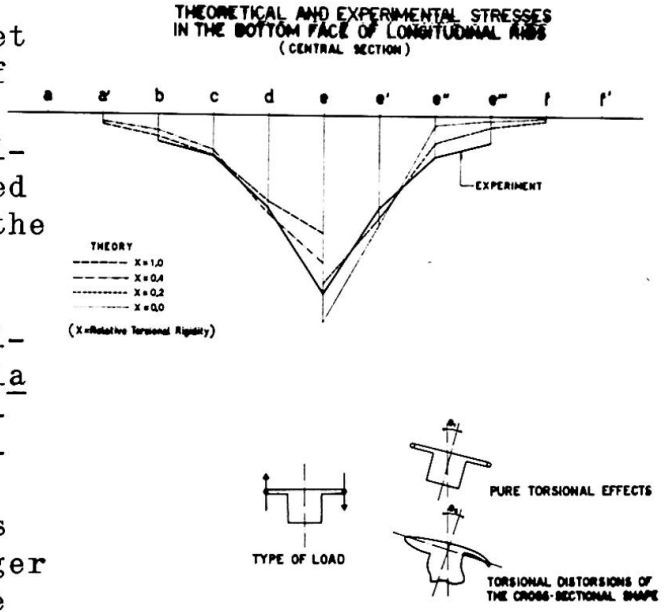

fig. 4

c) local stresses within the loaded area are rather high due to the fact that the deflection length of the top flat sheet is of the order of the bolts distance (fig.5).

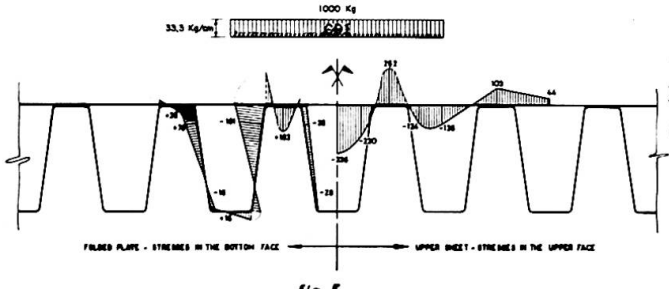

fig. 5

With regard to points b) and c) a better behaviour of the model could be obtained with a double row bolts, possibly in a "quinconces" setting.

Fatigue tests

Tests under pulsating loads have been performed to get information on the predominant types of fractures and on the importance of fatigue in comparison with the static behaviour.

The minimum value of the pulsating load was about 1/20 of the maximum and therefore it can be assumed, for all practical purposes, as equal to zero.

The load has been applied at seven different spots and it has been increased after a suitable number of cycles.

Displacement have been recorded by means of trasducers. Penetrating liquid of the Spotcheck type has been employed in order to spot fractures.

The result of tests are here summarized:

a) local fractures occur in the top flat plate within the loaded area and are of the type shown in fig. 6.

b) stresses which cause fracture are nearly the same as those associated with fatigue fracture in a flat sheet under pure bending, i.e. no reduction in strength has been noticed because of the presence of bolts.

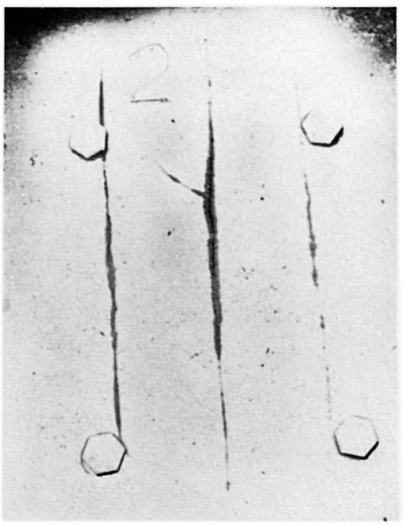

Collapse test

A section of the model has been tested under proportional loading up to collapse after the fatigue fractures have been repaired.

The load has been increased stepwise, each step being 1/10 of the theoretical collapse load. At each level a numer of loading cycles has been performed until a steady situation has been reached (differences between deformations of two subsequent cycles smaller than 5/100 mm).

In the central loaded area stress coat paint has been used to spot yielded regions.

The test confirmed that the model presents a very high load-carrying capacity, collapse load being about ten times the service load. This is due to a progressive load transfer from the loaded area to the adjacent areas caused by the membrane behaviour of the top flat sheet. This effect can be clearly seen in fig. 7 where plots of loads vs displacements are shown, as well as in fig. 8 which shows stresscoat paint fracture on the top sheet near the load.

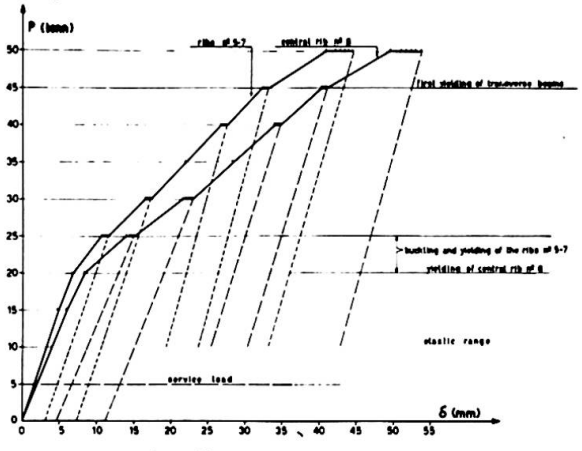

fig. 7

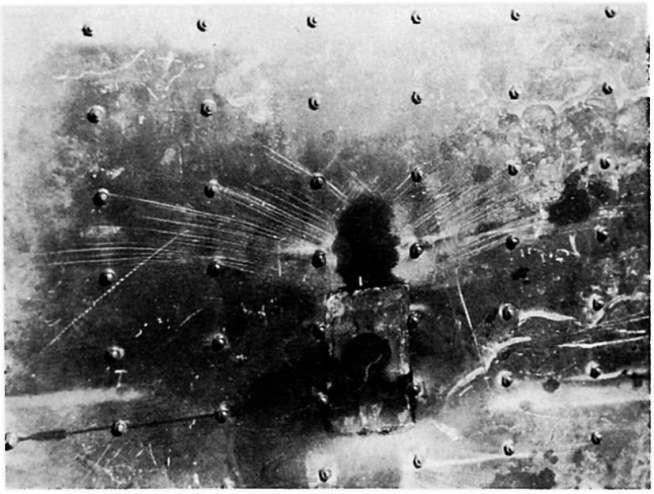

The continuation of the research with forces acting in the plane of the plate is in future scheduled. These forces will probably emphasize local instability with subsequent reduction of the load-carrying capacity of the model.

References

1. Ceradini,G., Pedicini,A., and Petrangeli,M.P., "Ricerca su impalcati da ponte in acciaio realizzati con lamiera sagomata a freddo e giunzioni ad attrito. Le prove in fase elastica" Technical Reports n. 168-169, Istituto di Scienza delle Costruzioni, Facoltà di Ingegneria, Università di Roma, Rome, Italy, 1974 - 1975.
2. Kloppel, K., and Roos,E., "Statische Versuche und Dauerversuche zur Frage der Bemessung von Flachblechen in orthotropen Platten," Der Stahlbau, Vol. 29, 1960.
3. Design Manual for Orthotropic Steel Plate Deck Bridges, American Institute of Steel Construction, New York, N.Y., 1963.
4. Croci,G., and Petrangeli,M.P., "Indagine Teorico-Sperimentale su un Modello di Impalcato da Ponte in Acciaio a Piastra Ortotropa," Costruzioni Metalliche, No.6, 1968.
5. Ceradini,G., Gavarini,C., and Petrangeli,M.P., "Steel Orthotropic Plates under Alternate Loads" Journal of the Structural Division, ASCE, Vol. 101, No ST 10, October 1975.

SUMMARY

The results of an experimental research on a model of steel bridge deck are briefly summarized. The model was made by an upper plane sheet connected by high strength bolts to a bottom folded sheet to form a deck similar to an orthotropic plate with closed ribs. Static tests in the elastic range as well as tests under pulsating loads and under proportional loading up to collapse have been performed.

RESUME

On présente les résultats d'une recherche expérimentale sur un modèle de tablier de pont métallique. Le modèle était constitué par une tôle supérieure plane reliée au moyen de boulons à haute résistance à une tôle pliée inférieure de façon à former un tablier du type plaque orthotrope avec nervures fermées. On a effectué des essais statiques dans le domaine élastique, des essais sous charges variables et enfin des essais de chargement proportionnel jusqu'à la rupture.

ZUSAMMENFASSUNG

Die Ergebnisse von Versuchen an einem Modell einer stählernen Leichtfahrbahntafel werden kurz erörtet. Das Modell wurde mit einem oberen ebenen Blech hergestellt, das durch hochfeste Schrauben mit einem unteren kaltgeformten Blech verbunden war, so dass eine Art orthotroper Platte mit Hohllängsrippen entstand. Die Versuche wurden statisch im elastischen Bereich, auf Ermüdung mit Ursprungsbelastung sowie bei Proportionalbelastung bis zur Traglast durchgeführt.

Welding of High-Strength Steels

Soudage des aciers à haute résistance

Schweissen von hochfesten Stählen

ICHIRO KONISHI
Professor Emeritus
Kyoto University
Kyoto, Japan

TOSHIE OKUMURA
Professor
Saitama University
Tokyo, Japan

SHUNJI MINAMI
Adviser
Nissho-Iwai Co. Ltd.
Osaka, Japan

MATSUJI SASADO
Manager
Hanshin Expressway Public Corporation
Osaka, Japan

1. INTRODUCTION

It should be taken great pains with not only the characteristics of materials but also the welding methods from a viewpoint of risk of failure of long-span bridge made of high-strength steels. In the preliminary report, the outline of way to build-up of long-span truss bridge, i.e., design, materials, fabrication and erection were discussed. In this report, the conditions and methods of welding and the quality control of welding during the fabrication course may be presented.

2. CONDITIONS OF WELDING

As a procedure test to determine welding conditions of high-strength steels 70 kg/mm^2 and 80 kg/mm^2 classes, the following tests were conducted prior to fabrication;

(1) lamellar tear test,
(2) restrained cracking test,
(3) tests on the performance of corner weld joints,
(4) tests to check residual stresses due to welding, and
(5) tests to investigate the various characteristics of the actual members using full scale models.

The maximum heat input of less than 50 KJoule/cm during welding was preset based on the results of such tests to avoid "bond" embrittlement of weld joint. Welding conditions including minimum preheat temperature, maximum preheat temperature, interpass temperature, and preheat temperature for tack welds were determined from the condition mentioned above. (Table 1)

The three factors of kind of materials, restraining and hydrogen are said to be main ones causing weld cracking. The first was settled by employing the steels passing the new specification. The second was thought not to be serious problem because of no steel plate having great restraining with neighbour plate in the Osaka Port Bridge. Therefore, the final factor was remained as the most considerable one which brought so called transverse cracking, i.e., the cracking along weld line. The suitable control method with which hydrogen entry could be minimized as much as possible was settled for fabrication in order to avoid such possible cracking.

Table 1 Preheat Temperature

Minimum Preheat Temparature (°C)

High-Strength Steels of 70 kg/mm² and 80 kg/mm² Classes				
Welding Method / Thickness (mm) \ Kind of Joint	Covered Arc Welding	M I G ※ Welding	Submerged Arc Welding	
	Butt , Fillet , Corner		Butt ,	Fillet
t ≦ 50	100	80	100	80
t > 50	120	100	150	100

※ M I G Welding.....Inert Gas Shielded Metal Arc Welding.

Maximum Preheat Temparature and Interpass Temparature

Thickness (mm)	Temparature
t ≦ 50	200°C and under
t > 50	230°C and under

3. WELDING METHOD

The automatic welding technique was made every effort to use in order to uniformalize the fabrication conditions. Among the automatic methods, two techniques of submerged arc welding and MIG welding were selected. The latter has an advantage to avoid the possible occurrence of cracking because of small heat input, but involves the serious problems of ill efficiency of work and of increased hardness in weld joint. Therefore, the first was used as the butt and fillet welding and the latter as the corner one. Also the following three types of preheating methods were used;

(1) electric preheating type with automatic control, (Photo 1)
(2) fixed burner type, and
(3) manual burner type.

The separate preheating method was specified for each type of weld joints. In welding major members, symmetrical preheating and symmetrical welding methods were employed to secure higher fabrication accuracy and minimize residual stresses. (Photo 2)

The preheating prior tack welding of small heat input and rapid cooling was carried out with careful concern, and its temperature was set higher by 20-40°C than that of primary weld.

4. QUALITY CONTROL OF WELDING

The close quality control system is necessary for the use of high-strength steels 70 kg/mm^2 and 80 kg/mm^2 classes to long span bridge. Although the detail explanation of such system is omitted in this report, the non-destructive inspections involves serious and many problems. Especially at the ultrasonic examination of corner joint shown in Fig.1, as the ultrasonic flaw detector possessed by the fabricators were different in the kind and the material and dimension of probe, the inspection was quite different each other, and the correlation between flaw and echo from discontinuity captured on the Braun tube could not be obtained. Therefore, the inspection standard was rechecked from the measurements with various test material.

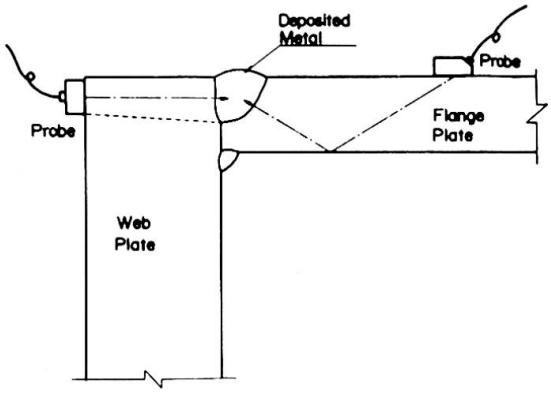

Fig. 1 Corner Joint

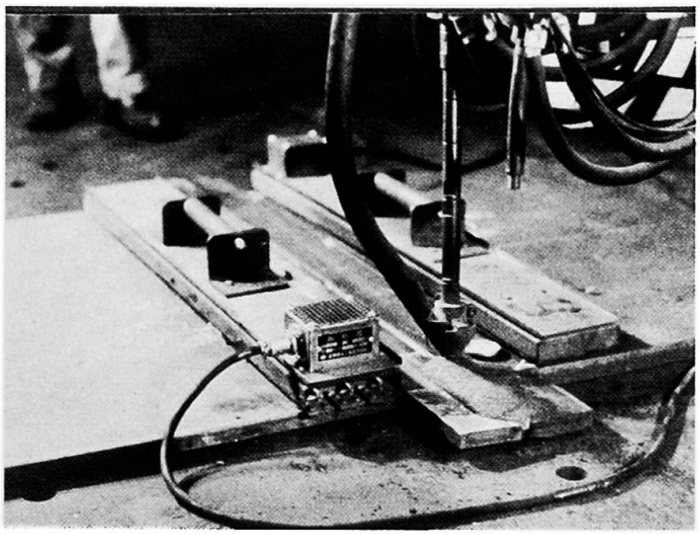

Photo 1

This photograph shows preheat performance with electric preheating equipments.

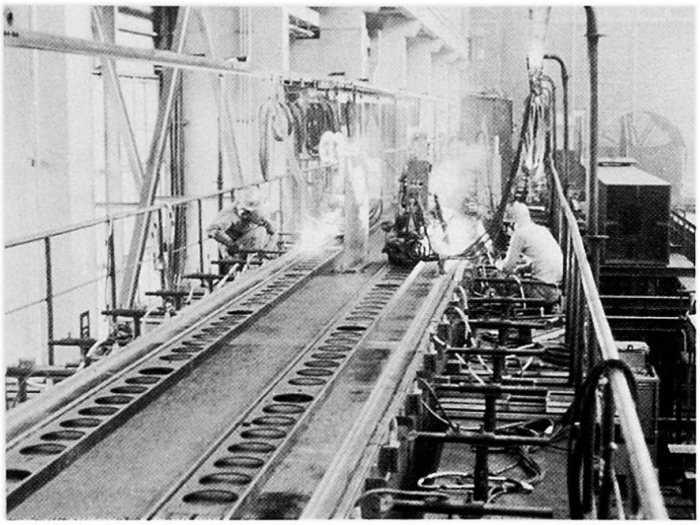

Photo 2

This photograph shows the appearance of symmetrical welding.

SUMMARY

Due attention was paid to the problem of cracking and embrittlement of weld joints of high-strength steels. The maximum heat input of less than 50 K Joule/cm during welding was preset and the preheat temperature was determined. The suitable control method with which hydrogen entry could be minimized was settled for fabrication. Among the automatic welding methods, two techniques of submerged arc welding and MIG welding were selected.

RESUME

On a prêté une attention particulière au problème des fissures et des ruptures fragiles dans les joints soudés en acier à haute résistance. L'apport de chaleur durant le soudage a été limité à 50 K Joule/cm et la température de préchauffage, déterminée. On a fixé la méthode de contrôle permettant de réduire au minimum la teneur en hydrogène. Parmi les méthodes de soudage automatiques, on a retenu le soudage sous flux et le procédé MIG.

ZUSAMMENFASSUNG

Der Vermeidung von Rissen und Sprödbrüchen in Schweissnähten an hochfesten Stählen wurde besondere Beachtung geschenkt. Das Wärmeeinbringen während der Schweissung wurde auf 50 K Joule/cm begrenzt und die Vorwärmetemperatur bestimmt. Man verwendete eine geeignete Kontrollmethode, um die Wasserstoffaufnahme möglichst niedrig zu halten. Unter den automatischen Schweissmethoden wurden das Unterpulverschweissen und das MIG-Verfahren ausgewählt.

V

Synthesis and Conclusions

Synthèse et conclusions

Synthese und Schlussfolgerungen

BEN KATO
Prof. Dr.-Eng.
University of Tokyo
Tokyo, Japan

Prepared Discussion

The numbers of papers presented at the prepared discussion are seven for theme Va,two for theme Vb and two for theme Vc. The following is a short summary of these contributions.

Theme Va. Starting with theme Va."Structural Behavior Including Hybrid Construction", P.Ferjencik reported on the structural behavior of prestressed steel beams. A wide flange beam is prestressed by means of high-strength tension wires installed just beneath the lower flange. Test results showed that elastic limit capacity of this system increases remarkably compared with that of non-prestressed regular steel beam. Due to the effect of prestressing and of plastic reserve strength,the ultimate strength of this system can attain as high as twice the computed ultimate strength of non-prestressed beam if the premature lateral and local buckling is carefully prevented.

M.Yamada and B.Tsuji carried out an elastic-plastic analysis of hybrid beam-columns subjected to repeated and reversed bending under constant axial force. It was demonstrated that in hybrid beam-columns,the expansion of hysteresis loops for each additional cycle can not be expected so much when the magnitude of the axial force is large.

Z.Cywinski carried out a plastic analysis of hybrid beams on the basis of lower bound criterion,and pointed out that for short span beams,the effect of shear stress becomes more severe than that assumed in the present ASCE-AASHO regulation.

A.Plumier investigated the fatigue strength of plate girders with rather unique details.Main series of test girders had transverse stiffeners both ends of which were welded to upper and lower flanges. A girder in which only one end of stiffener is welded to tension flange was also tested as a supplement. Both hybrid girders and homogeneous girders made entirely of C-class steel were tested. Obtained results are that the fatigue strength of these girders are inferior than that of regular girders in which stiffener is welded at compression flange only, and that there are no difference in fatigue strength between these two types of girders tested and fatigue strength of homogeneous girders is a bit superior than that of hybrid girders. J.Janss has reported this in lieu of Plumier.

Y.Maeda reported an additional study on type 2 cracks in hybrid girders which supplements his previous paper presented in Preliminary Report. He checked the

effect of finishing of weld toes,and showed that fatigue strength will increase about 1 kg/mm^2 by this finishing. However this effect will be covered up by other fluctuating factors such as residual stress,quality of weldment and misalignment of loading system.

Also as a supplement of his investigation presented in the Preliminary Report, T.Yamasaki discussed on the possibility of estimating fatigue lives by means of fracture mechanics approach. He showed that fatigue lives can be predicted by using material constants obtained from a simple test,and thus the fracture mechanics approach is useful for fatigue problem also,if the size of initial crack could be estimated in advance.

The COD criterion is widely used in the field of non-linear fracture mechanics However,when the yield region is spreaded widely enough,the physical meaning of COD theory becomes not so clear compared with the concept of J_{1c} fracture criterion. Furthermore,since the J_{1c} value is rather insensitive to the scale effect,one can determine the J_{1c} value using the smaller test specimens. H.Aoki had evaluated J_{1c} values for B and C-class steels,and showed that J_{1c} value of C-class steel is about 2/3 of that of B-class steel. He also pointed out that critical J-value will decrease with the increase of multi-axiality of the stress field.

Theme Vb. First discussion on theme Vb "Design Problems" was contributed by J.Lindner. He discussed on the lateral buckling strength of beams with mono-symmetric cross sections. It is well known that a mono-symmetric cross section of which the upper flange is larger than the lower flange is more advantageous than a doubly symmetric section of equal sectional area as far as elastic bifurcation is concerned. In plastic region,however,he pointed out that the buckling strength of a beam having mono-symmetric cross section will become lower than that having doubly symmetric cross section,and the merit of high-strength steel becomes very small.

P.Dubas talked about the utilization of high-strength steels in the design of composite girder highway bridges in Switzerland refering to the Veveyse bridge and others designed by himself. High strength steel currently used in Switzerland is almost limited to B-class steel. He remarked that though the weight saving and the reduction of material cost expected from the use of high-strength steel is not substantial, some merit can be obtained by performing a good design. A merit will be brought by using high-strength steel at the end portions of each span of a continuous girder where negative moment and shear force are very high. Sectional area at this portion will decrease by this selection and thus the almost uniform cross section will be obtained throughout the span which makes the fabrication very simple. Since the shrinkage of concrete is restrained by shear connectors,tensile stress will arise in the concrete slab. This tensile stress will be reduced by the use of high-strength steel since the sectional area and thus the rigidity of the steel beam is reduced. This is another advantage. He also encouraged the development of the weathering high-strength steel which will offer a merit with respect to the maintenance.

Theme Vc. In theme Vc "Fabrication and Election Problems", a new type of steel orthotropic bridge deck was introduced by M.P.Petrangeli. The upper plane sheet and corrugated metal deck were connected by means of high strength bolts. This fabrication method was adopted by considering the fact that the welding becomes very difficult and expensive when these decks are made of high-strength steel. The structural performance of this deck was investigated by model tests. Elastic behavior,ultimate strength under static loading and fatigue strength were investigated to obtain the satisfactory results.

As a supplement to his contribution to the Preliminary Report,M.Sasado discussed on the welding procedure of high-strength steels used in the construction of Osaka-port bridge. C-class steels up to 75mm in thickness were used in this bridge. The condition of welding,welding methods and quality controll adopted in this construction to avoid the possible cracking and embrittlement at welded joints were reported.

Free Discussion

Nine topics were contributed in the form of free discussion; they are three for theme Va,five for theme Vb and one for theme Vc.

Theme Va. As the results of additional tests on composite beams with formed steel deck undertaken after the publication of their paper in the Preliminary Report, I.M.Viest and J.W.Fisher proposed some modifications of eq.(2) and eq.(4) presented in the Preliminary Report as follows;

$$Q_{rib} = \frac{0.85}{\sqrt{n}} \left(\frac{H-h}{h}\right)\left(\frac{w}{h}\right) Q_{sol.} \leq Q_{sol.} \qquad (2a)$$

where n=number of shear connectors placed in a rib.

$$I_{eff.} = I_s + \sqrt{\frac{V'_h}{V_h}} \left(I_{tr} - I_s \right) \qquad (4a)$$

O.Jungbluth conducted a series of load carrying tests on portal frames made of various grades of steel,and demonstrated that the simple plastic theory may be applicable even for the rigid frame made of C-class high-strength steel (σ_y=685 N/mm^2).

A.C.Wallace discussed on the structural behavior of connection details of the tied bowstring arch bridge made of high-strength steel refering to an actual example.

Theme Vb. N.Streletzky talked about the application of high-strength steels to building and bridge structures in UdSSR. High-strength steels newly developed in UdSSR are 16Г2Aф(σ_y=440 N/mm^2, C'-class) and 14Х2ГМР(σ_y=590 N/mm^2,C-class). Brief comments on the allowable stress and the method of analysis were also given.

The effect of exposure on corrosion of weathering high-strength steel was discussed by W.I.J.Price. He examined the difference between the formation of the protective coating achieved in open exposure and that obtained in a sheltered environment which is the case of composite bridge where the concrete deck shelters the steel beam from direct rain and sun. He demonstrated that the sheltered corrosion rate is higher for marine and saline situations,and also pointed out that severe pitting observed in these environments will cause the adverse effect against fatigue and brittle fracture.

W.Hoyer evaluated the limit of adaptability of weathering high-strength steel for various environmental and service conditions based on a extensive research work.

The reduced modulus of a stayed cable was discussed in both the Introductory Report Vb and the Preliminary Report by Hajdin both of which are based on the formula proposed by Ernst in 1965. M.Ito derived a revised formula which is theoretically more reasonable. It was revealed,however,that Ernst's formula could give practically satisfactory results except for the case where a very long cable is subject to relatively low tensile stress.

K.Horikawa calculated the stress intensity factor which may arise in a welded joint of C-class steel(HW80) containing a possible crack which might be overlooked through the regular nondestructive inspection,and pointed out that the critical toughness of such a joint material must be larger than that calculated value.

Theme Vc. As one of the means to obtain column-to-beam rigid connections,high strength bolted T-stub flange-to-column connections are widely used. K.Sato talked about the utilization of high-strength cast steel T-stubs for this connection system. When beam ends are subjected to very large bending moment due to earthquake or wind force,these attachments can be utilized effectively.

Appendix.

The list of high-strength steels attached at the end of theme Va. of the Introductory Report should be supplemented by the following two high-strength steels. One is of United States,and this steel has been already introduced at the beginning of this session by the author. The other is of F.R.G.(West Germany) which is quite similar to A514 steel of United States,and to HW 70 steel of Japan in quality. This steel was used by J.Lindner and by A.Plumier in their research and reported in this prepared discussion. With respect to 16Г2Aφ and 14X2ГМР steels of UdSSR refered by Streletzky,detailed information is not available.

New High-strength Steels to be Added to Appendix of Introductory Report

Country	Standards	Designation	Min.Yield Stress N/mm^2	Tens. Strength N/mm^2	Class	Y
U.S.A	ASTM	A572,Gr 65	448	552	C'	0.812
F.R.G (West Germany)	DASt. Ri.011	St.E 70	686	785 ~ 932	C	0.875

$Y = \frac{\text{Yield Stress}}{\text{Tensile strength}}$ = Yield ratio of material(maximum)